

TECHNIQUES OF VOLATILE ANALYSIS IN VOLCANIC GLASS
BY QUADRUPOLE MASS SPECTROMETRY
AND APPLICATION TO MOUNT EREBUS, ANTARCTICA

by

Eric A. Bigelow

NOT TO BE TAKEN
FROM LIBRARY

Submitted in Partial Fulfillment
of the Requirements for the Degree of
Master of Science in Geology

New Mexico Institute of Mining and Technology
Socorro, New Mexico

May, 1985

N.M.I.M.T.
LIBRARY
SOCORRO, N.M.

This thesis is accepted on behalf of the faculty of
New Mexico Institute of Mining and Technology
by the following committee:

Philip R. Kyle

Adiser

David L. Norman

Lynn A. Brandwald

24 April 1985

Date

TECHNIQUES OF VOLATILE ANALYSIS IN VOLCANIC GLASS
BY QUADRUPOLE MASS SPECTROMETRY
AND APPLICATION TO MOUNT EREBUS, ANTARCTICA

Eric A. Bigelow
May, 1985

ABSTRACT

A high vacuum extraction line and a computer-controlled quadrupole mass spectrometer were used to extract, identify and measure volatiles in volcanic glass. Matrix and inclusion glasses from recent volcanic ejecta, collected at Mount Erebus, Antarctica from 1972 to 1982, were analyzed.

A persistent convecting lava lake, which has existed for the last ten years, and a nearby adjacent vent periodically throw anorthoclase phonolite bombs over 230 meters to the crater rim of Mount Erebus. The glasses from these bombs were analyzed for their volatile concentrations because difficult access to and the frequent activity of the lava lake and Active Vent made the conventional method of direct gas sampling impractical. Pre-eruptive and post-eruptive volatile concentrations were measured by analyzing glass (melt) inclusions trapped in anorthoclase phenocrysts and matrix glasses (groundmass glass).

Average gas compositions of matrix glasses expressed as approximate mole percents are; H₂O (87%), CO₂ (4%), CO (5%), H₂ (1%), SO₂ (1%), H₂S (1%), with trace amounts of CS₂, COS,

CH₄, C₂H₄, HCl, He, Ar and N₂. Average gas compositions of inclusion glasses expressed as approximate mole percents are; H₂O (83%), CO₂ (6%), CO (4%), H₂ (1%), SO₂ (3%), H₂S (2%), with trace amounts of CS₂, COS, CH₄, C₂H₄, HCl, He, Ar and N₂. The gases account for 0.37 wt.% and 0.44 wt.% of matrix and inclusion glasses respectively. Whole rock and inclusion glass S concentrations are 260 and 440 ppm respectively. Whole rock and inclusion glass Cl concentrations are 1110 and 1600 ppm respectively.

Gas measurements reported in published reports and measurements obtained using traditional analytical techniques indicate that the quadrupole mass spectrometric measurements of H₂O, CO₂, CO, H₂S and SO₂ in volcanic glass are reproducible and probably accurate whereas Cl and F gas measurements are significantly low.

The concentration of structurally bound volatiles in matrix glasses, from bombs erupted between 1972 to 1982, decreased by 0.1 wt.%. Matrix glass gas concentrations probably represent the solubility of residual volatiles in the magma at 1 atm and 1000°C. Volatiles in glass inclusions within anorthoclase phenocrysts are both structurally bound and present as vapor phase gases and seem to accurately reflect pre-eruptive magmatic compositions.

The Mount Erebus magma system has been a closed convecting body of homogeneous magma driven by a large hot heat source since 1972. The magma chamber is approximately 3 to 4 km deep and has a minimum volume of 2 km³. Calculations of the magma convection rate suggest that the calculated magma volume of 2 km³ has cycled through the feeder pipe 6 times since 1972.

ACKNOWLEDGEMENT

I would like to express my appreciation and gratitude to Dr. P. R. Kyle, Dr. D. I. Norman and Ms. L. Brandvold for their advice and participation as committee members. My thanks to Mr. D. Geddert for building the computer interface box and writing the data reduction programs. Significant contributions to this study and my education were made by Dr. J. L. Smith and Dr. J. Robertson.

Funding for this study was provided by the National Science Foundation Grants DPP 8020002 and DPP 8218493 to Dr. P. R. Kyle and the State Mining and Mineral Resources Research Institute grant G1115351 to Dr. D. I. Norman.

TABLE OF CONTENTS

	Page
ABSTRACT	ii
ACKNOWLEDGEMENT	v
TABLE OF CONTENTS	viii vi
LIST OF FIGURES	xi vii
LIST OF TABLES	xii vii
INTRODUCTION	1
Volcanic Gases and Volatile Elements	1
Statement of the Problem	2
Terms and Definitions	3
PART A: TECHNIQUES OF VOLATILE ANALYSIS IN VOLCANIC GLASS BY QUADRUPOLE MASS SPECTROMETRY	5
Introduction	5
Sample Selection and Preparation	5
Analytical Techniques	10
Calibration Techniques	16
Water	16
Volume	19
Sensitivity and Fractionation Patterns ...	20
Gas Analysis Problems	23
Precision and Accuracy	26
Conclusions	29
PART B: MAGMATIC VOLATILES IN VOLCANIC GLASSES FROM MOUNT EREBUS, ANTARCTICA	30
Introduction	30
Results of Volatile Analyses	31
Gases	31
<u>Matrix Glass</u>	31
<u>Inclusion Glass</u>	39
Volatile Elements	45
<u>Whole Rock</u>	45
<u>Matrix Glass</u>	46
<u>Inclusion Glass</u>	48
Major Elements	49
Discussion	57
Assumptions	57
Gases	59
Volatile Elements	62
Major Elements	66
Comparative Results	68
Magma Chamber Volume	77
Depth of Magma Chamber	82
Convection Models	83
Conclusions	87

Table of Contents (Continued)

	Page
APPENDIX A	88
Equipment and Manufacturers	88
APPENDIX B	89
Mount Erebus	89
Geologic Setting	89
Previous Activity	91
Present Activity	93
Field Work	98
APPENDIX C	101
Previous Studies of Volcanic Volatiles	101
Volatile Solution Mechanisms	106
Introduction	106
H ₂ O	107
H ₂ S, HCl and HF	108
CO ₂	108
Others	109
APPENDIX D	110
List of Samples and Analyses	110
Gas Data	111
Volatile Element Data	119
Major Element Data	122
APPENDIX E	130
Statistical Methods used to Test for Trend	130
APPENDIX F	134
Introduction	134
Mass Balance Models	135
REFERENCES	139

LIST OF FIGURES

Figure	Page
1. Gas extraction line and quadrupole	11
2. The calibration line and equation used to estimate water concentrations	18
3. Matrix Glass gas (H_2O , CO_2 , CO , SO_2 , H_2S) concentrations from 1972 to 1982	33
4. Matrix Glass element (O, H, C, S) concentrations, derived from gas concentrations, 1972 to 1982	34
5. Matrix Glass gas (H_2O , CO_2 , CO , SO_2 , H_2S) compositions from 1972 to 1982	37
6. Matrix Glass element (O, H, C, S) compositions, derived from gas compositions, 1972 to 1982	38
7. Whole Rock (WR), Matrix Glass (MG) and Inclusion Glass volatile element (S, Cl, F) concentrations from 1972 to 1982	47
8. Whole Rock (WR), Matrix Glass (MG) and Inclusion Glass (IG) oxide (SiO_2 , Al_2O_3 , FeO_T , CaO , Na_2O , K_2O) concentrations from lava flows and recent bombs	56
9. A comparison of total O, H and (C+S) and C, S and H_2O from gas measurements taken from Mount Erebus and 12 other volcanoes. Ternary diagrams are from Giggenbach (1974a), plus averages from this report .	76
B1. Maps of Antarctica, Ross Island and Mount Erebus ...	90
B2. Topographic map of Mount Erebus, 5 meter contours ..	92
B3. Aerial photograph of Mount Erebus taken in December, 1983	94

LIST OF TABLES

TABLE	Page
1. Sample cleaning methods	8
2. S determinations (ppm), showing the effect of temperature on the extraction results	14
3. Calibration data for water analyses based on pressure in the extraction line	17
4. Fractionation patterns and sensitivities	22
5. Gas concentrations (ppm) of matrix glass from recent bombs, Mount Erebus	32
6. Gas compositions (mole %) of matrix glass from recent bombs, Mount Erebus	36
7. Gas concentrations (ppm) of inclusion glass in anorthoclase phenocrysts from recent bombs, Mount Erebus	41
8. Average H ₂ O, CO ₂ , CO, SO ₂ and H ₂ S concentrations (ppm) of matrix and inclusion glasses from recent bombs, Mount Erebus	42
9. Gas compositions (mole %) of inclusion glass in anorthoclase phenocrysts from recent bombs, Mount Erebus	43
10. Average H ₂ O, CO ₂ , CO, SO ₂ and H ₂ S compositions (mole %) of matrix and inclusion glasses from recent bombs, Mount Erebus	44
11. Whole rock S and Cl analyses (ppm) of recent bombs, Mount Erebus	45
12. S, Cl and F analyses (ppm) of matrix glass from recent bombs, Mount Erebus	48
13. Average S, Cl and F concentrations (ppm) of matrix and inclusion glass and whole rock samples from recent bombs, Mount Erebus	49
14. Whole rock major element analyses of recent anorthoclase phonolite bombs, Mount Erebus	50

LIST OF TABLES (Continued)

TABLE	Page
15. Major element analyses of matrix and inclusion glass from recent anorthoclase phonolite bombs, Mount Erebus	52
16. Trace and rare earth element analyses of matrix glass from recent bombs, Mount Erebus	54
17. Estimated whole rock gas concentrations (ppm) in matrix glass from recent bombs, Mount Erebus	62
18. Selected gas and volatile element concentration analyses (ppm) of volcanic glasses	70
19. Selected gas analyses of rocks and fumarole emissions (mole %)	72
20. Selected gas and volatile element concentration analyses (ppm) of inclusion glasses	75
21. Magma chamber volume calculations	79
22. Total volume of magma convected through a 50m feeder pipe	81
D1. Individual gas concentration analyses (ppm)	111
D2. Individual gas composition analyses (mole %)	115
D3. Whole rock volatile element analyses (ppm) of recent bombs, Mount Erebus	119
D4. Volatile element analyses (ppm) of matrix glass from recent bombs, Mount Erebus	120
D5. S and Cl analyses (ppm) of glass inclusions in anorthoclase phenocrysts, Mount Erebus	121
D6. Individual whole rock major element analyses	122
D7. Individual major element analyses of matrix glass ..	124
D8. Individual trace and rare earth element analyses of matrix glass	127

LIST OF TABLES (Continued)

TABLE	Page
E1. Major element D values, Volatile element D values ..	132
E2. Gas and element D values	133
F1. Mass balance calculation of inclusion glass content in anorthoclase, sample 2E2	135
F2. Mass balance calculation of inclusion glass content in anorthoclase, sample 25723	136
F3. Mass balance calculation of inclusion glass content in anorthoclase, sample 77015	137
F4. Mass balance calculation of inclusion glass content in anorthoclase, sample 81003	138

INTRODUCTION

Volcanic Gases and Volatile Elements

Magmatic volatiles are integral components of magmatic systems because they influence the physical properties of magmas. Volatiles affect density, viscosity, rheology, liquidus and solidus temperatures, thermal and electrical conductivity, and heat flow. Volatiles are important in the transport and deposition of ore-forming components and the prediction and monitoring of volcanic eruptions. Volcanic volatile emissions may also contribute to atmospheric aerosol levels (Berresheim and Jaeschke, 1983) and affect global climate.

Despite the importance of magmatic volatiles, little data on the solubility, composition and concentration of volatiles in magmas is available. In addition, most of the data has been obtained by sampling fumarolic gases from active basaltic volcanoes. In contrast, there are few analyses of gases from silicic volcanoes. Magmatic gas species, in approximate order of decreasing abundances, which have been reported are; H_2O , CO_2 , SO_2 , H_2S , CO , CH_4 , COS , CS_2 , HCl , HF , N_2 , He , Ar , N_2O , NO and NH_3 .

Statement of Problem

Mount Erebus is an active volcano which contains a persistent convecting lava lake which is continuously emitting gases. Little is known about these emissions because observations of the lava lake degassing behavior are limited. In addition, access to the lava lake is difficult because of frequent eruptions. Thus no high temperature gas samples have been obtained because direct collection is impractical.

Recently developed quadrupole mass spectrometry techniques provide an alternative means to measure magmatic volatiles. Concentrations of volatiles in pre-eruptive and post-eruptive magmas may be estimated by analyzing glass inclusions, in phenocrysts, and matrix glasses.

The major objective of this study was to develop techniques to extract and measure volatiles in volcanic glasses. The second objective of this study was to use the volatile data to model the Mount Erebus magma system. Glass samples from volcanic bombs collected between 1972 and 1982, were also analyzed to determine if volatile concentrations and compositions changed with time.

Terms and Definitions

The following terms are used in this thesis.

Condensable Gases - Gases which are below the critical vapor pressure at or below -190°C (H_2O , CO_2 , SO_2 , H_2S , COS , CS_2 , C_2H_4 , CH_4).

Dissociated Volatile Form - Volatiles which are normally molecular gases but which dissociate to form complexes; for example water may dissociate to hydroxyl groups.

Gas - Any chemical substance in a vapor phase form, as opposed to a liquid or solid form.

Gas Composition - The mole % of each gas relative to the total moles of gas.

Gas Concentration - The amount of each gas relative to the mass of the sample, reported in ppm.

Inclusion Glass - Small discrete quantities of glass contained within anorthoclase phenocrysts. The glass inclusions are thought to be melt trapped in the anorthoclase phenocrysts and are assumed to be representative of the magma composition prior to eruption.

Matrix Glass - The exposed and scoriaceous glass which makes up the groundmass of the bombs.

Molecular Volatile Form - Volatiles which are present in glass or the silicious melt as molecules of gas.
(eg. CO_2)

Noncondensable Gases - Gases which do not freeze at -190°C (CO , H_2 , CH_4 , Ar , He , N_2).

Pre-eruptive Volatiles - Volatiles which represent relatively undegassed magma. The pre-eruptive volatiles are those present in the magma at the time of anorthoclase phenocryst crystallization and were measured from inclusion glasses.

Post-eruptive Volatiles - Volatiles which represent degassed magma. The post-eruptive volatiles were measured from matrix glasses.

Residual Volatiles - Volatiles in glass which represents degassed magma. The residual volatiles are those which remain in the melt after equilibration at 1 atm and may be an accurate measure of solubility at 1000°C and 1 atm.

Strombolian Eruption - Relatively small discrete eruptions characterized by liquid lava being thrown into the air. The explosive force of the eruptions is caused by the bursting of large gas bubbles as they approach the surface.

Volatile Elements - The halogens F and Cl plus elemental S.

Volatiles - This term is used to refer to the total gas and volatile element concentrations, regardless of form.

Volcanic Gases - The gases H₂O, H₂, CO₂, CO, SO₂, H₂S, COS, CS₂, C₂H₄, CH₄, Ar, He, N₂ and HCl.

PART A: TECHNIQUES OF VOLATILE ANALYSIS
IN VOLCANIC GLASS
BY QUADRUPOLE MASS SPECTROMETRY

Introduction

The use of quadrupole mass spectrometry to measure volatiles in glass is a relatively new and rapidly evolving science. Thus, detailed descriptions of high vacuum extraction and mass spectrometric analysis of volatiles in glass are rare and incomplete. The following descriptions and discussion of the methods used in this study and the problems which were encountered is an attempt to fill this void.

Sample Selection and Preparation

Fresh samples of recently ejected anorthoclase phonolite bombs were collected from 1972 to 1982. Fresh bombs, bombs which were collected within a week of being thrown to the crater rim, were identified by their dark black to green color and their resinous luster. Bombs that were more than a week old were distinguishable because they had been altered by reaction with gases in the volcanic plume. The acidic vapors in the plume caused the fresh glass to be altered to a light gray color and dull luster. Extended exposure to the summit environment eventually turns the bombs yellow due to sublimation of salts (Keys, 1980).

Samples of the scoriaceous glass were crushed to a fine consistency using a porcelain mortar and pestle.

Phenocrysts were hand picked from the samples before the glass was completely crushed. Sample grain sizes of 0.25 to 0.5 mm and 0.125 to 0.25 mm were obtained by sieving with U.S. Standard sieves.

Killingley and Muenow (1975) and Price et al. (1977) have reported that crushing samples of obsidian causes the loss of H_2O . A direct comparison of obsidians and the scoriaceous glass from Mount Erebus, however, is not totally valid. Water concentrations measured in Mount Erebus matrix glasses with grain sizes of 0.25 mm and 0.125 mm were not significantly different. Therefore, the affect of crushing was assumed to be minimal. The reasoning behind this assumption is that the crushing of scoriaceous glass probably ruptures an insignificant number of microvesicles causing a small H_2O loss whereas the crushing of obsidian ruptures a large number of microvesicles causing a significant H_2O loss, as proposed by Price et al. (1977). Fewer microvesicles are ruptured upon crushing of scoriaceous glass because less crushing is required to obtain the desired grain size. However, future analyses of scoriaceous or pumiceous glasses should resolve this problem by measuring volatile concentrations in crushed and uncrushed samples.

A Frantz Isodynamic Separator (Model 1-1) was used to separate magnetite, pyroxene and feldspar from the matrix glass. A forward tilt 20 degrees and a tilt of 15 degrees, to the nonmagnetic side, was used. Magnetite-pyroxene and feldspar-glass separates were obtained using a setting of 0.6 amps. Pure glass and almost pure feldspar separates were obtained by rerunning the feldspar-glass separate at a magnet setting of 0.8 amps. Glass separates were 99 percent pure after they were hand-picked to remove any remaining contaminants.

Glass samples were cleaned using two methods (Table 1). The major difference between the two methods was in the use of acids. Method 2 did not use the 10 percent hydrochloric acid and concentrated nitric acid, to remove carbonates and oxides. After cleaning, samples were dried and then stored in air-tight glass capsules. There were no significant differences between analyses of samples prepared by the two methods.

Inclusion glass plus feldspar samples were obtained from anorthoclase phenocrysts which had been separated from scoriaceous bombs. Matrix glass was removed from the surfaces of the phenocrysts using a diamond grit grinding wheel. A jaw crusher with ceramic jaws and a pulverizer with 99.6 percent alumina plates were used to crush the

TABLE 1

Sample cleaning methods

METHOD 1

1. Samples were rinsed in doubly deionized water (DDW) until all murkiness was gone.
2. Samples were washed in reagent grade alcohol for 5 minutes.
3. Samples were rinsed in DDW twice.
4. Samples were washed in reagent grade acetone for 5 minutes.
5. Samples were rinsed in DDW three times.
6. Samples were washed in 10% reagent grade hydrochloric acid at 50 degrees C for 15 minutes.
7. Samples were rinsed in DDW three times.
8. Samples were washed in concentrated reagent grade nitric acid for 30 seconds.
9. The above procedures were repeated in the following order; 7,6,5,2,3,4.
10. Samples were rinsed in DDW twice then soaked in DDW at 50 degrees C for 2 hours.
11. Samples were rinsed in DDW twice then dried in an oven at 100 degrees.

METHOD 2

1. Samples were rinsed in DDW until murkiness was gone.
2. Samples were washed in reagent grade alcohol for 30 minutes.
3. Samples were rinsed twice in DDW, then soaked in DDW for 4 hours.
4. Samples were rinsed twice in DDW and dried in an oven at 100 degrees C.

phenocrysts. An inclusion glass plus feldspar grain size fraction of 1.0 to 3.0 mm was sieved and separated in the same manner as previously described . A 0.125 mm glass contaminated feldspar separate was also obtained in the same manner. Separates of feldspar and inclusion glass plus feldspar were cleaned using Procedure Two (Table 1) and stored in air-tight glass capsules. An effective method of separating inclusion glass from anorthoclase was not developed. This is the reason why inclusion glass plus feldspar samples were used instead of pure inclusion glass samples.

Whole rock samples were prepared by crushing a representative 10 cm sized piece of bomb. A jaw crusher, pulverizer and mechanical agate mortar and pestle were used to obtain homogeneous samples less than 0.064 mm in size. Samples were soaked in doubly deionized water for 4 hours, dried in an oven for 4 hours at 50°C, then stored in air-tight glass capsules.

Clean samples of matrix glass, feldspar, and feldspar plus inclusion glass were weighed and placed into sample vials after they had been dried in an oven at 120°C for 12 hours. The vials were sealed with clean dry glass wool, to prevent sample spillage during storage. The vials were placed in clean dry air-tight glass capsules for storage.

Analytical Techniques

The gas analysis system is composed of; a high temperature resistance furnace monitored with a chromel-alumel thermocouple (accurate within 2%), a high vacuum pyrex gas extraction and separation line with high vacuum teflon valves, a Baratron 220 BHS Absolute Pressure Transducer, a Hewlett Packard 85 computer, an Inficon IQ200 quadrupole with an electron multiplier, two high vacuum oil diffusion pumps, and three Welch Duo-Seal Vacuum Pumps (Figure 1).

The quadrupole mass spectrometer is sensitive to 1×10^{-13} torr and measures masses 1 to 200. The pressure transducer has an accuracy of 0.2% and a resolution of 0.0001 torr. A detailed description of how a quadrupole works has been presented by Graham (1978). Standard operating conditions which were used are as follows; an electron multiplier voltage of 1500 volts, a starting quadrupole vacuum of 2×10^{-9} torr, a starting extraction line vacuum of 3×10^{-6} torr, and a room temperature of 25°C.

Preparations made for each run include; baking the extraction line at 200°C while under vacuum, baking a clean furnace tube at 1000°C while under vacuum, and degassing the quadrupole. Once the system had been prepared in this

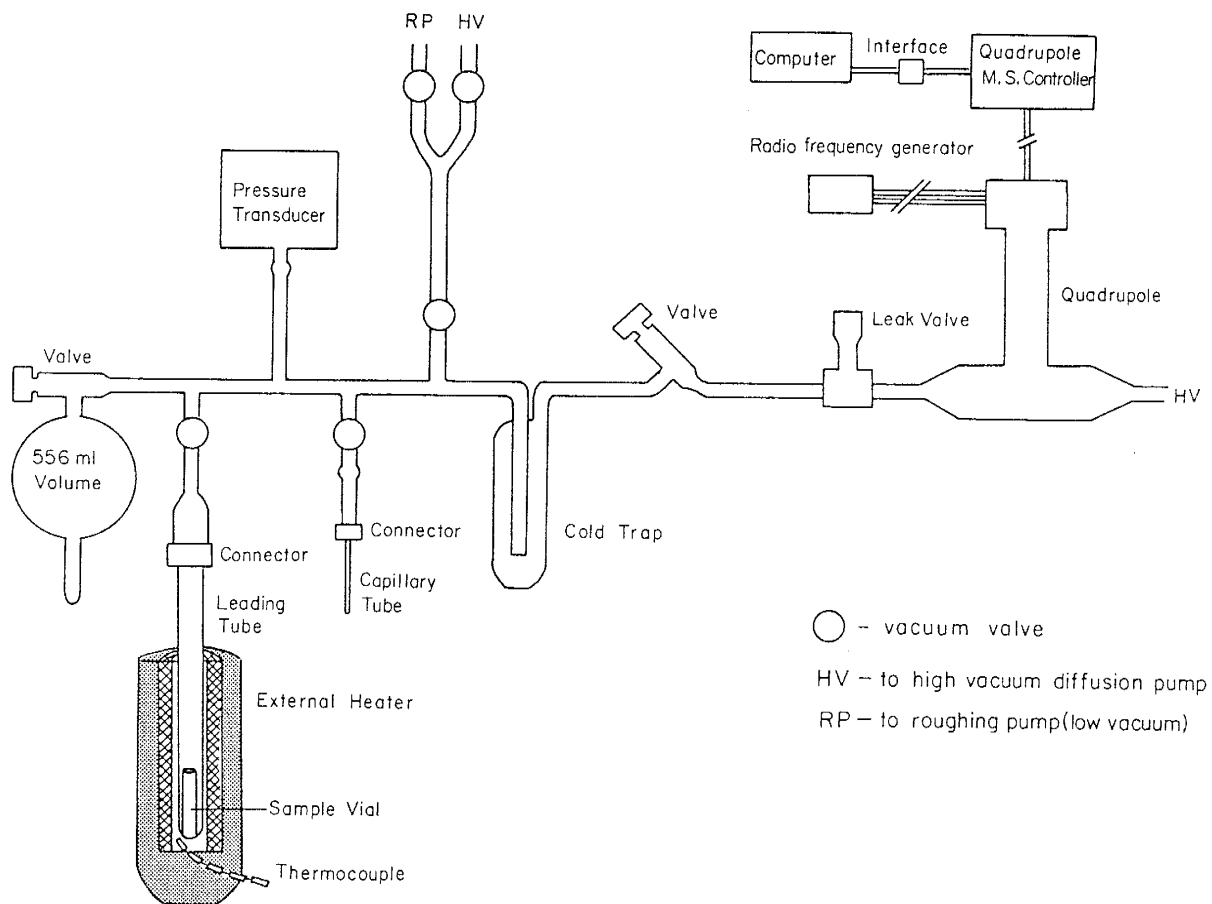


Fig. 1. Gas extraction line and quadrupole.

manner a sample was introduced into the extraction line by placing the sample vial in the clean degassed furnace tube and reconnecting the furnace tube to the extraction line. Absorbed gases were degassed by heating the sample at 150°C for 12 hours while under high vacuum. A pressure of 3×10^{-6} torr in the extraction line (including furnace tube with sample) was usually obtained after the 12 hour degassing period. During the 12 hour sample degassing period the quadrupole was kept isolated and in a vacuum of less than 1×10^{-8} torr, using a Varian Vac Ion Pump. Two hours before an analyses the ion pump was turned off and the quadrupole was opened to high vacuum pumping and turned on. A vacuum of 2×10^{-9} torr was normally obtained before an analysis was initiated.

An analysis was initiated by placing a liquid nitrogen bath (-190°C) around the cold trap and closing off all valves to the vacuum pumps. A background analysis was made by analyzing the gases which remained in the quadrupole, in the extraction line, or on the sample. Once the background gases had been analyzed the appropriate valves were closed so that gases liberated from the sample would expand into a portion of the extraction line for which the volume was known. The sample was then slowly heated to 1250°C and held at 1250°C for 1 hour. Initially samples were heated to 1025°C, but total extraction of sulfur gases was not

obtained (Table 2). Condensable gases were held in a liquid N_2 cold trap while noncondensable gases expanded into the known glass volume (see Terms and Definitions for a list of condensable and noncondensable gases). After 1 hour of heating at $1250^{\circ}C$ the furnace was turned down to $1100^{\circ}C$ and the pressure in the extraction line was allowed to stabilize. Stabilization of the system at sample temperatures less than $1100^{\circ}C$ was not practical because the loading tube and sample had to be cooled at a rate of approximately $5^{\circ}C$ per minute to avoid cracking the loading tube and contaminating the sample. The loading tube cracked at approximately $1000^{\circ}C$ when cooled too quickly. Once the pressure in the extraction line stabilized a noncondensable gas pressure reading was recorded. The noncondensable gas sample was then leaked into the quadrupole and analyzed. Analyses were begun shortly after the leak valve was opened because light gases such as H_2 and He tend to be preferentially depleted. Noncondensable gases which remained in the line after the analysis were pumped away.

TABLE 2

S determinations (ppm), showing the effect of temperature on the extraction results

Sample	1025°C	1250°C
2E2	47	103
77015	24	136
78015	24	140
79301	20	89
81003	28	148

AVE.	29	123

A condensable gas background analysis was taken after a vacuum of 2×10^{-5} torr had been obtained. Evacuating the extraction line for an extended period of time, which would be required to obtain a better vacuum, caused the loss of gases from the cold trap. The condensable gas analysis was made in the same manner as the noncondensable gas analysis except that a CO_2 -Alcohol bath replaced the liquid N_2 bath. Water remained frozen in the cold trap while all remaining gases expanded into the known volume of glass line. A pressure reading was taken for condensable gases after the pressure stabilized. After the analysis the remaining gases in the extraction line were pumped down. Next, the

H₂O held in the cold trap was expand into a known volume by removing the CO₂-Alcohol bath. A pressure reading was taken 2 hours (see Calibration Techniques, Water) after the bath was removed.

A sensitivity calibration of the quadrupole was made once a week. The sensitivities were adjusted, using freon gas as a standard, to the setting at which gas fractionation patterns and sensitivities were measured (see Sensitivity and Fractionation Patterns). These calibration analyses were conducted in the same manner as the gas analyses just described.

Noncondensable and condensable gases were analyzed by scanning masses 1 through 50 and 2 through 90, respectively. Background concentrations were subtracted from sample measurements before the relative abundance of each gas was calculated. The gas compositions (relative abundances) were computed using a least-squares matrix which utilized spectra fractionation outlines and sensitivities determined from standard gases. The total moles of noncondensable and condensable gases were calculated using relative gas abundances, extraction line pressure measurements and extraction line volume estimates. Gas pressures, extraction line volumes and the equation $PV=nRT$ were used to calculate the total moles of noncondensable and condensable gases.

The moles of each gas were calculated by multiplying the total moles of gas by the relative abundances. The H₂O composition was calculated volumetrically. A calibration equation, derived using a standard with a known H₂O concentration, and a pressure reading from the known volume of the extraction line were used to make the calculation (See Calibration Techniques). The total gas composition of the sample was calculated by combining the noncondensable gas, condensable gas and water compositions.

Calibration Techniques

Water

A powdered rock standard was used to calculate the calibration equation used to estimate H₂O concentrations in the glasses. The gabbro standard, MRG, which has a H₂O content of 0.98 wt.%, a low Cl and F concentrations, and a S concentration (Abbey, 1981) similar to that of the Mount Erebus glass samples was used. Samples of MRG were prepared for analysis in the same manner as the Erebus glass samples. Sample weights ranging from 0.05 to 0.005 g were used to give a range of pressure readings in the extraction line (Table 3). Samples were heated and all gases other than H₂O were removed. The CO₂-Alcohol cold trap was removed and the H₂O expanded into the known volume of the extraction line. A pressure reading was recorded after 2 hours. Two hours

was used because water absorption onto the glass line slowed to a rate which allowed accurate and reproducible pressure readings to be taken. Water contents in the standard samples were calculated using the sample weights and the known H₂O concentration. The calibration equation was calculated by linear regression and has a correlation coefficient (r) of 0.996. Water concentrations in the Mount Erebus glasses were estimated using the equation in Fig. 2.

Ion chromatography analyses of the H₂O obtained in the extraction procedure, indicate that dissolved gases account for less than 5% of the H₂O by weight. Carbonate, sulfate, chloride, fluoride and nitrate contaminants have been tentatively identified.

Table 3

Calibration data for water analyses based on pressure in the extraction line.

Sample Weight (Grams)	Calc. H ₂ O (mg)	Pressure (Torr)
0.0505	0.4949	1.716
0.0400	0.3920	1.205
0.0277	0.2715	0.876
0.0197	0.1931	0.650
0.0103	0.1009	0.288
0.0054	0.0529	0.080

A gabbro sample (MRG), with an accepted water content of 0.98 wt.% (Abbey, 1981), was used for the calibration.

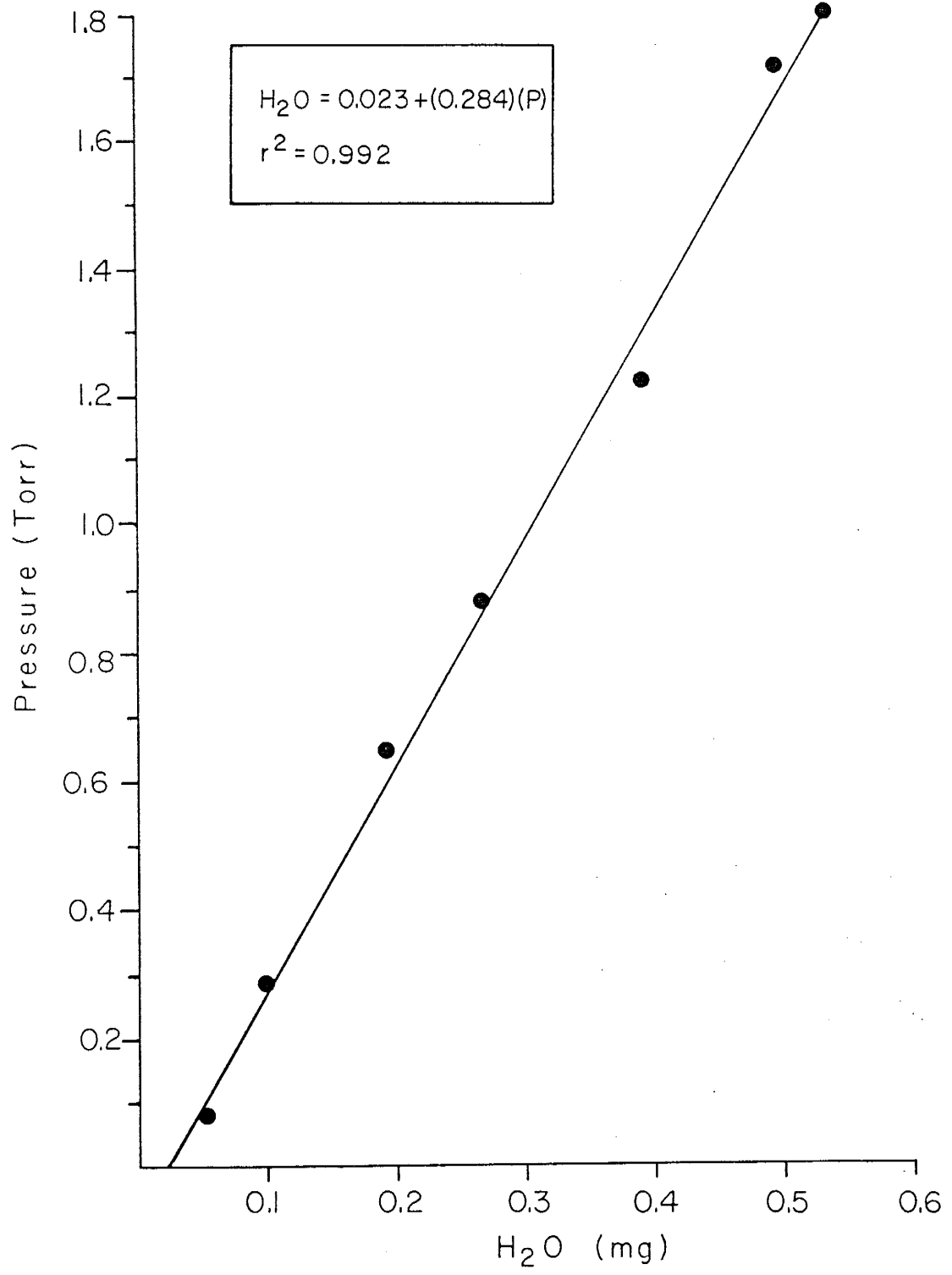


Fig. 2. The calibration line and equation used to estimate water concentrations

Volume

The volumes of the extraction line were estimated by expanding a measured quantity of N_2 into the extraction line. The total moles of N_2 was calculated using $PV=nRT$ and a measured pressure of N_2 in a known volume (556 ml flask). The N_2 in the flask was expanded into the unknown volume of the extraction line so that the pressure, $P(\text{unknown})$, could be measured. Because n , R and T are constants and $P(\text{unknown})$ was measured, the equation $PV(\text{flask}) = PV(\text{unknown})$ may be solved for $V(\text{unknown})$. $V(\text{unknown})$ is the volume of the flask and the extraction line and $P(\text{unknown})$ is the pressure of N_2 in both volumes. Once $V(\text{unknown})$ was calculated the volume of the extraction line was calculated by taking the difference between $V(\text{unknown})$ and flask volumes. Noncondensable gases were measured in a 140 ± 5 ml volume which included the extraction line with a liquid N_2 bath around the cold trap and the furnace tube at 1100°C . Condensable gases were measured in a 78 ± 2 ml volume which included the extraction line with a CO_2 -alcohol bath around the cold trap. The 68 ± 1 ml volume used for water calculations included the extraction line at 25°C .

The following procedure was used to make volume calculations. Both the flask and extraction line were evacuated to 2×10^{-6} torr. Nitrogen gas was then introduced

into both volumes and an initial N_2 pressure, $P(\text{flask})$, was recorded after it had stabilized. The flask was isolated by closing the appropriate valve (Figure 1), and the N_2 in the extraction line was pumped away until a vacuum of 2×10^{-6} torr was attained. $P(\text{unknown})$ was measured by releasing the N_2 from the flask into the extraction line. This procedure was repeated several times to maximize the accuracy of the volume estimate.

Sensitivity and Fractionation Patterns

The sensitivity of the quadrupole was adjusted to a standard setting using a freon gas standard. Mass peaks 12, 35, 47, 50, 66, 69, 85, 101 and 135 were scanned and relative peak intensities were measured. A calibration program was used to ratio the peak intensities and compare the standard ratios to those obtained from the weekly sensitivity checks. The drift of the sensitivities from the standard ratios were expressed as percent deviations of the actual from the standard values. Large deviations were decreased by adjusting the quadrupole sensitivities until the percent deviations were minimized.

The sensitivities of gases, relative to N_2 , and their fractionation patterns were determined using high purity standard gases. Gas sensitivities and fractionation

patterns, normalized to the freon gas standard, are listed in Table 4. Sensitivity and fractionation measurements were made by connecting bottled gases to the extraction line and then evacuating the system to a vacuum of 1×10^{-5} torr or less. Gases were individually leaked into the extraction line and analyzed. The noncondensable and condensable gases were purified by placing liquid N_2 and CO_2 -alcohol baths on the cold trap to remove contaminants. Analyses of each gas were conducted several times to insure accuracy. The sensitivities of each gas were determined relative to N_2 by mixing a known number of moles of each gas with a predetermined number of moles of N_2 . The mixture of the two gases were analyzed and the sensitivity of the quadrupole for each gas was determined from the total peak intensities of each gas relative to the total peak intensities of N_2 .

Table 4

Fractionation patterns and sensitivities

Gas	Fractionation Patter (Mass Number-Intensity Fraction,)	Sensitivity (Gas/N ₂)
H ₂ O	18-0.6382, 17-0.1701, 2-0.1544, 16-0.0229, 28-0.0145.....	(1.00)
CO ₂	44-0.6154, 16-0.1753, 28-0.0942, 12-0.0820, 43-0.0067, 22-0.0152, 45-0.0069, 42-0.0020, 46-0.0023.....	(0.64)
CO	28-0.8898, 12-0.0584, 16-0.0275, 27-0.0063, 29-0.0088, 14-0.0053, 26-0.0022, 30-0.0017.....	(1.48)
H ₂	2-0.9992, 3-0.0008.....	(6.85)
SO ₂	64-0.3995, 48-0.3877, 32-0.1014, 16-0.0650, 66-0.0184, 50-0.0147, 24-0.0132.....	(0.62)
H ₂ S	34-0.4705, 32-0.2476, 33-0.2022, 18-0.0161, 17-0.0112, 16-0.0065, 28-0.0069, 31-0.0040, 30-0.0012.....	(0.96)
CS ₂	76-0.4800, 32-0.2200, 44-0.1800, 78-0.0900, 77-0.0300.....	(1.42)
COS	32-0.3992, 60-0.3116, 28-0.1381, 12-0.0834, 44-0.0675.....	(1.12)
Ar	40-0.8565, 20-0.1435.....	(1.20)
N ₂	28-0.8563, 14-0.1245, 29-0.0089, 27-0.0064, 26-0.0021, 13-0.0010, 25-0.0004, 12-0.0003.....	(1.00)
He	4-0.9845, 3-0.0155.....	(3.06)
HCl	36-0.6712, 38-0.2215, 35-0.0805, 37-0.0268.....	(0.73)
C ₂ H ₄	28-0.3991, 27-0.2483, 26-0.2043, 25-0.0591, 14-0.0344, 24-0.0201, 13-0.0176, 12-0.0171.....	(10.26)
CH ₄	16-0.4728, 15-0.4020, 14-0.0655, 13-0.0325, 17-0.0164, 12-0.0108.....	(2.15)

Fractionation patterns are presented in descending order of intensity. Intensity ratios for each mass are relative to the total intensity of the gas. Sensitivities are relative to N₂.

Gas Analysis Problems

A major obstacle to obtaining reliable gas analyses is the absence of standards. The credibility of gas analyses presented in this or any other report will always be suspect until there are standards with known gas compositions and concentrations.

In the absence of standards of this type, the best solution for verifying results is the use of high purity premixed gases. The use of a mixed gas standard, with a similar gas composition as the samples being analyzed, should be used in the future. This type of a standard would insure the accuracy of the quadrupole. Measured gas compositions could be normalized to the standard or the data reduction program could be adjusted to eliminate discrepancies observed between the analysis results and the known composition of the mixed gas standard.

Several other problems, inherent to the analytical procedures, were not satisfactorily dealt with. One of these problems was the inability to accurately measure total S, Cl and F. Sulfur, Cl and F were probably retained in the fused degassed samples due to their high solubilities in the sample at the low oxygen fugacity in the extraction line.

Sulfur, Cl and F were also absorbed, to an unknown degree, onto the glass surfaces of the extraction line.

The S, Cl and F retained in degassed samples should be measured so that the absorption problem can be addressed. An accurate measure of the S, Cl and F retained in the samples would provide the data needed to calculate the affect of absorption and would allow a calibration adjustment to be made. If the problem is large, absorption of gases onto the glass line can be minimized by creating a stable environment, of approximately 150°C, around the extraction line.

The problem of preferential flow of light gases into the quadrupole generally affects the analysis of H₂. This problem was enhanced, in this study, by decreasing the volume of the extraction line in an attempt to minimize the absorption problem. The preferential flow problem was minimized by analyzing the samples as quickly as possible. The rate of preferential flow was not determined and no data corrections were made. Use of the previously mentioned mixed gas standard would help resolve this problem.

Reactions between gases in the extraction line altered gas concentration and composition results. Gases were extracted from glass samples by heating them to 1025, 1100

and 1250°C. The two lower temperatures were found to be inadequate for maximum extraction of S gases. However, the use of 1250°C may have increased reaction problems. Gas compositions seem to be more reduced as the extraction temperature was increased. This is the main reason why elemental concentrations and compositions, derived from gas data, were used to look for changes in the data. The reaction problem was not quantified but was minimized by using the lowest temperature for the shortest period of time which allowed maximum gas extraction.

Background measurements had several unresolved problems. The background measurements were made at a pressure of 5×10^{-6} torr and therefore did not represent the contamination which occurred at the sample pressures. This problem could have been solved by using a carrier gas, such as He, at an equivalent analysis pressure. Measurement of the background for noncondensable gases were also inaccurate because they were made approximately 2 hours before the sample measurements. Passive degassing of the quadrupole during the time between background and sample measurements resulted in the measured background being greater than that which actually existed at the time of sample measurement. These problems and resulting errors, however, are relatively insignificant when compared to analytical errors produced by pressure measurement limitations.

The H₂O calibration of the extraction line can be improved by using a greater number of data points and a standard with a chemical composition and grain size similar to that of the samples. The largest grain size which allows maximum gas extraction should be used. A comparison of calibration results from standards of different compositions should to be made to determine the affect of sample composition on the calibration.

Precision and Accuracy

The precision of gas measurements made by quadrupole mass spectrometric analyses is presented as coefficients of variation for seven analyses of sample 81003 (Table 10). The repeatability of these measurements (the precision) is based upon analyses performed over a period of one year. The coefficients of variation for the gases measured from sample 81003 in Table 10 indicate that the measurements of the major gases (H₂O, CO₂, CO, SO₂ and H₂S) are reproducible. The minor gases, however, can be identified, but not accurately measured because concentration levels are below those needed to obtain reproducible measurements.

One of the problems which affects the precision is the accuracy of the pressure measurements. If the pressure transducer is controlling the precision the, pressure

measurements should have a variability of less than 1%. Instead, the precision indicates that the reproducibility of the gas measurements is limited mainly by sample variability. Thus, an increase in sample size should increase measurement precision.

The precision for measurements of an individual gas, in contrast, is limited by the judgment of the program operator and the accuracy of the data reduction programs. The accuracy of these data reduction programs is in turn dependent upon fractionation pattern and sensitivity measurements. This is further complicated by the fact that the precision of the fractionation pattern and sensitivity measurements is different for each gas. Some gases, such as CO_2 and H_2S , are amenable to calibration whereas other gases, such as CO and H_2 , are not. These individual differences between gases cause inaccuracies which result in imperfect solutions for the raw data. This, of course, limits the precision of the concentration measurement of each gas.

The accuracy of gas measurements made by quadrupole mass spectrometric analysis is difficult to quantify. Instrumental accuracy has been presented in the Analytical Techniques section. However, it is very unlikely that analytical accuracy is the same as instrumental accuracy. Analytical accuracy is unknown because completeness of gas

extraction and the accuracy of the quadrupole mass spectrometric measurements are unknown. The problem of completeness of gas extraction may be resolved for measurements of total S, Cl and F by analyzing degassed samples using wet chemistry methods. The accuracy of the quadrupole gas measurements may also be quantified by the use of a mixed gas standard. Although both of these problems may be addressed the accuracy of the measurements will not be satisfactorily known until rock and glass standards are available.

The best method to access the accuracy of the gas measurements, in the absence of the methods described above, is to compare the results with measurements presented by other researchers. A comparison of results, presented in Comparative Results and Figure 9, indicates that the measurements made in this study are consistent with previously reported measurements. Although this comparison implies that the measurements are accurate, the level of accuracy is unknown.

Conclusions

- 1) The affect of crushing on the gas analyses of Mount Erebus matrix glasses was not measured but is believed to be minimal. Future work should address this potential problem.
- 2) Total S, Cl and F measurements were not accurate because of incomplete extraction and absorption of S, Cl and F onto the glass line. The amount of S, Cl and F absorption onto the glass line is not known because the completeness of extraction is also unknown. In the future it is recommended that degassed samples be analyzed by wet chemistry methods to determine the concentrations of S, Cl and F which remain in the samples after degassing. Sulfur, Cl and F concentration measurements of the samples made before and after degassing would provide the data needed to estimate the amounts of these elements which are absorbed onto the extraction line.
- 3) The quadruple mass spectrometric technique of analyzing gases in volcanic glass is satisfactory for H_2O , CO_2 and CO . Coefficients of variation for H_2O , CO_2 and CO determined from 7 analyses of sample 81003 indicate that the precision of repeatability for these gases are 13%, 28% and 31% respectively. Sulfur dioxide and H_2S concentrations are not as reproducible, having coefficients of variation of 56% and 35%. All other gases have coefficients of variation equal to or greater than 50%.

PART B: MAGMATIC VOLATILES IN VOLCANIC GLASSES
FROM MOUNT EREBUS, ANTARCTICA

Introduction

Measurements of gas compositions and concentrations in matrix and inclusion glasses were made to determine post-eruptive and pre-eruptive volatile concentrations in the magma. Concentration is used to describe absolute volatile quantities relative to sample mass and is expressed in ppm. Composition is used to describe volatile abundances relative to the total volatiles and is expressed as mole% or atomic%.

Previous studies of volatiles from fumaroles and in volcanic glasses and rocks are presented in Appendix C. The mechanisms of volatile solution in magmas are also discussed in Appendix C. In addition, appendixes B and C provide background information which is very helpful to the understanding of gas analysis results. Kyle (1977a) describes the glasses and anorthoclase.

Results of Volatile Analyses

Gases

Matrix Glass

Analyses of gas concentrations in matrix glass were made to determine the effects of degassing on the magma volatile content. Water concentrations in matrix glass (Table 5) decrease by approximately 1000 ppm from 1972 to 1982. This difference is greater than the estimated analytical precision, and statistical analysis indicates that the data has a significant trend, with a 10% confidence level, from 1972 to 1982 (Figure 3). The only other gas which has a statistically significant trend, with concentrations decreasing with time, is CO₂. All the other gas concentrations remain constant with time.

Total element concentrations, derived from the gas concentrations, were calculated to determine if the observed gas trends are real or due to reaction problems caused by the analytical procedures (Part A). Oxygen, H, C and S are the major elements and their abundances have been recalculated to 100% (Table 5). Oxygen, H and C concentrations have significant trends with time (Figure 4) whereas S remains constant. The average S concentration of 130 ppm determined by mass spectrometry is significantly less than the average S concentration of 330 ppm determined

TABLE 5

Gas concentrations (ppm) of matrix glass from recent bombs, Mount Erebus	Year									
	1972	1974	1975	1977	1978	1979	1980	1981	1982	AVE
n	2	2	1	2	2	2	7	2	2	22
Gas	5380	3700	4780	4290	3320	4080	3130(380)*	3540	3360	3730(710)
H ₂ O	4340	2690	3820	3230	2710	3320	2480(320)	2750	2470	2920(590)
H ₂	2	6	3	5	7	5	4(4)	7	4	5(2)
CO ₂	470	614	423	560	199	233	191(54)	410	402	343(158)
CO	326	238	218	236	151	382	222(69)	210	212	240(61)
SO ₂	133	52	207	165	138	42	156(87)	71	155	128(48)
H ₂ S	49	74	50	39	77	69	49(17)	43	66	56(13)
CO _S	22	13	40	41	20	7	9(10)	19	33	19(12)
CS ₂	2	7	n.d.	6	8	3	7(9)	4	3	5(2)
C ₂ H ₄	3	4	5	4	2	1	2(1)	3	5	3(1)
CH ₄	24	5	11	14	6	10	11(6)	9	6	11(5)
HCl	1	2	2	3	2	5	1(1)	2	2	2(1)
N ₂	10	n.d.	4	3	9	3	1(3)	9	7	4(4)
Ar	tr	tr	tr	tr	tr	tr	tr	tr	tr	tr
He	tr	tr	tr	tr	tr	tr	tr	tr	tr	tr
Element concentrations (ppm) recalculated to 100%.										
O	4460	3000	3940	3680	2710	3360	2550(307)	2910	2700	3065(618)
H	490	310	430	360	310	380	286(39)	320	280	333(63)
C	290	280	230	280	130	240	155(42)	220	220	211(57)
S	125	108	172	144	158	91	135(56)	90	159	130(25)

* = 1 Standard deviation
n = Number of analyses used to determine the listed average.
n.d. = not detected
tr = trace
Individual analyses are given in Table D†

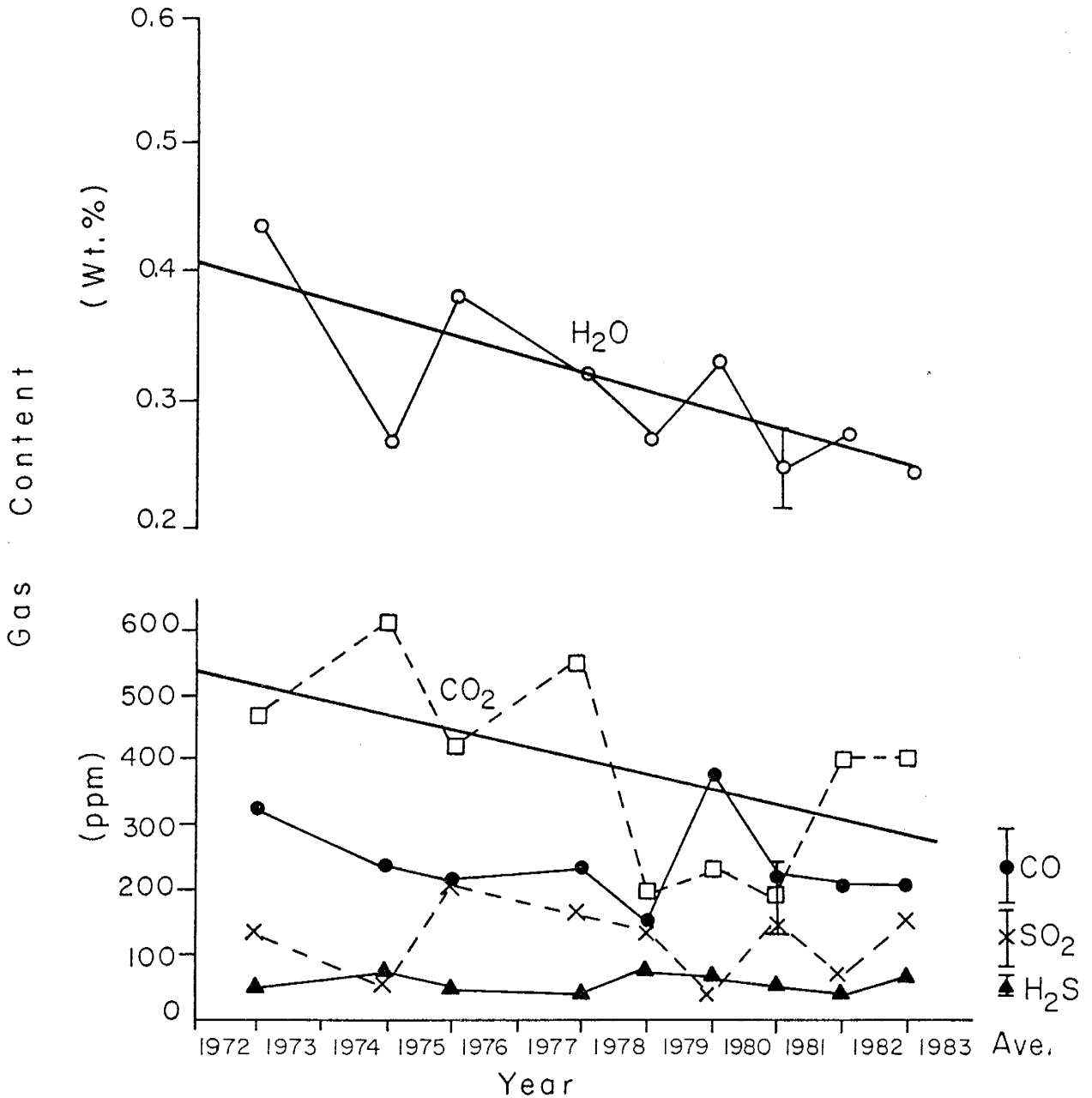


Fig. 3. Matrix Glass gas (H₂O, CO₂, CO, SO₂, H₂S) concentrations from 1972 to 1982.

H₂O, —○—; CO₂, ---□---; CO, —●—; SO₂, ---x---; H₂S, —▲—. The heavy lines through the H₂O and CO₂ points are trend lines determined by linear regressions.

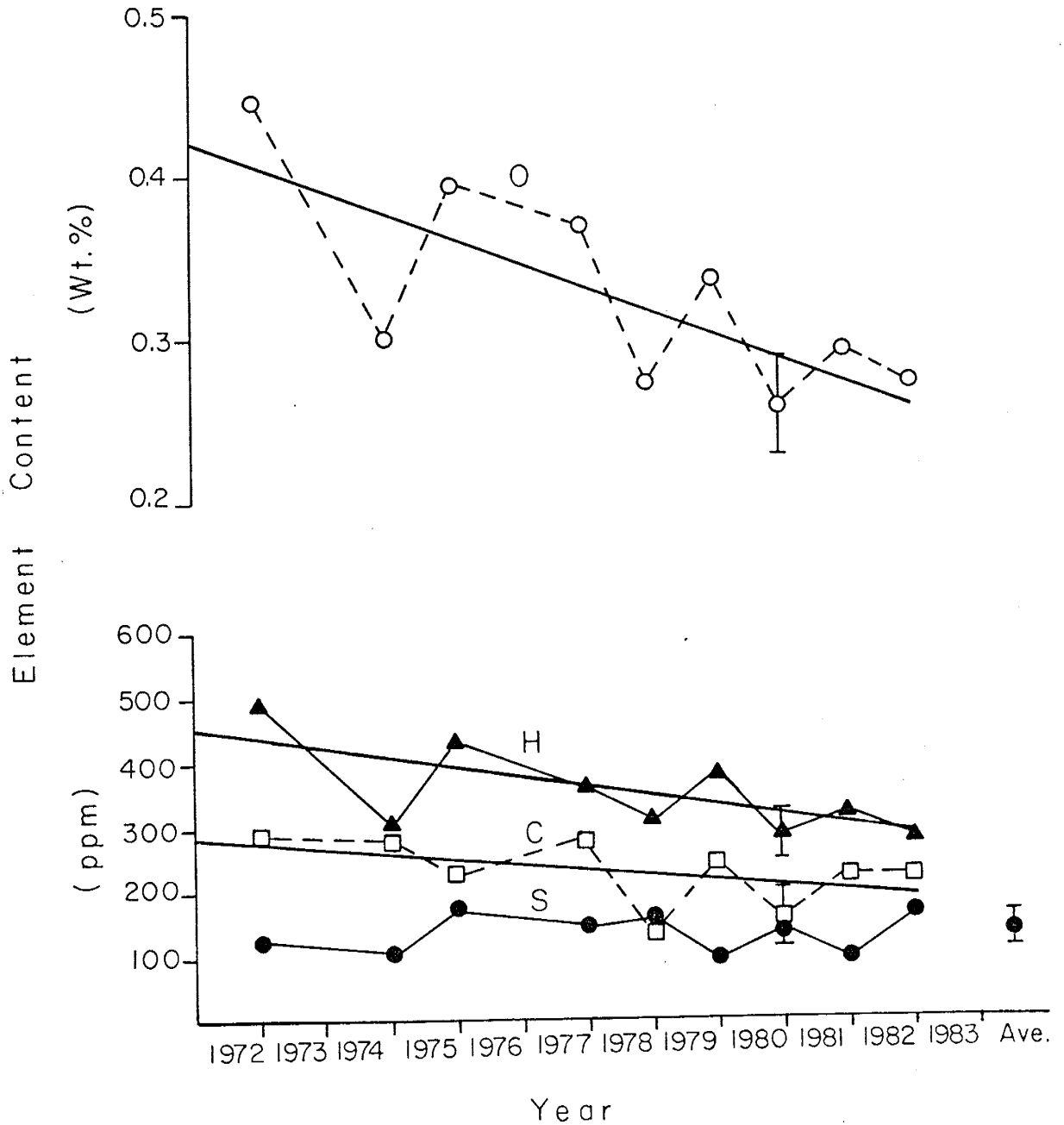


Fig. 4. Matrix Glass element (O, H, C, S) concentrations, derived from gas concentrations, 1972 to 1982.

Oxygen (O), --- \circ ---; Hydrogen (H), — \blacktriangle —;
 Carbon (C), --- \square ---; Sulfur (S), — \bullet —. The heavy
 lines through the O, H and C points are trend lines
 determined by linear regressions.

by wet chemistry. Matrix glass Cl concentrations, determined by mass spectrometry and wet chemistry, of 2 ppm and 1560 ppm, respectively, are also significantly different. Mass spectrometry did not detect F gases whereas specific ion electrode analyses indicate F has an average concentration of 2140 ppm in matrix glass.

Gas compositions in matrix glasses were determined because they may reflect degassed phonolitic melt compositions. Gas composition data is also presented because most volcanic gas measurements are reported in this manner, thus allowing the data in this report to be directly compared to published gas analyses.

The H_2O , CO_2 , CO , SO_2 , H_2S and the minor gases all have constant compositions from 1972 to 1982 (Table 6), within estimated analytical error. Statistical analyses (Appendix E) indicate that gas compositions do not have significant trends with time. However, H_2O and CO_2 do have slight complementary variations which are worth noting even though they are within analytical error (Figure 5). Elemental compositions of O, H, C and S recalculated to 100% (Table 6) indicate that no composition changes or trends occurred from 1972 to 1982. The variations observed in H_2O and CO_2 compositions are not reflected in the O, H or C compositions (Figure 6), which suggests that the H_2O and CO_2 composition variations are due to analytical problems.

TABLE 6

Gas compositions (mole%) of matrix glass from recent bombs, Mount Erebus	1972		1974		1975		1977		1978		1979		1980		1981		1982		AVE	
	n	2	2	2	1	1	2	2	2	2	2	2	7	2	2	2	2	2	22	22
H ₂ O	89.0	83.7	89.3	86.0	86.0	88.8	87.6	87.9(1.4)*	86.5	85.0	87.2(1.6)									
H ₂	0.30	1.55	0.65	1.08	1.08	1.98	1.78	1.25(1.09)	2.42	1.09	1.35(0.56)									
CO ₂	4.0	7.9	4.0	6.1	6.1	2.6	2.7	2.7(0.9)	4.8	5.7	4.1(1.7)									
CO	4.6	4.7	3.3	4.1	4.1	3.2	6.1	5.1(1.6)	4.1	4.6	4.6(0.8)									
SO ₂	0.73	0.45	1.36	1.24	1.24	1.34	0.46	1.53(0.67)	0.63	1.51	1.13(0.44)									
H ₂ S	0.57	1.24	0.62	0.54	0.54	1.30	0.92	0.90(0.29)	0.67	1.20	0.90(0.26)									
COs	0.12	0.56	0.28	0.33	0.33	0.19	0.08	0.10(0.12)	0.17	0.33	0.21(0.16)									
CS ₂	0.01	0.05	n.d.	0.04	0.04	0.06	0.03	0.06(0.08)	0.03	0.03	0.04(0.02)									
C ₂ H ₄	0.05	0.08	0.07	0.06	0.06	0.04	0.03	0.04(0.03)	0.06	0.09	0.05(0.02)									
CH ₄	0.60	0.17	0.28	0.43	0.43	0.21	0.33	0.43(0.24)	0.36	0.24	0.36(0.19)									
HCl	0.01	0.03	0.02	0.04	0.04	0.03	0.05	0.02(0.01)	0.04	0.03	0.03(0.01)									
N ₂	0.15	n.d.	0.05	0.05	0.05	0.18	0.08	n.d.	0.22	0.14	0.08(0.07)									
Ar	tr	tr	n.d.	tr	tr	tr	tr	tr	tr	tr	tr									
He	tr	tr	tr	tr	tr	tr	tr	tr	tr	tr	tr									

Element compositions (atomic%) recalculated to 100%.

O	34.8	35.9	35.3	35.7	34.1	34.1	34.1	34.6(0.4)	34.9	35.9	34.9(0.6)
H	61.6	59.0	61.2	59.7	62.8	62.8	62.3	61.7(2.0)	61.1	59.1	61.1(1.2)
C	3.1	4.5	2.7	3.8	2.1	2.1	3.1	2.8(1.2)	3.5	3.9	3.2(0.7)
S	0.5	0.6	0.8	0.8	1.0	1.0	0.5	0.9(0.3)	0.5	1.1	0.8(0.2)

* = 1 Standard deviation

n = Number of analyses used to determine the listed average.

n.d. = not detected

tr = trace

Individual analyses are given in Table D2

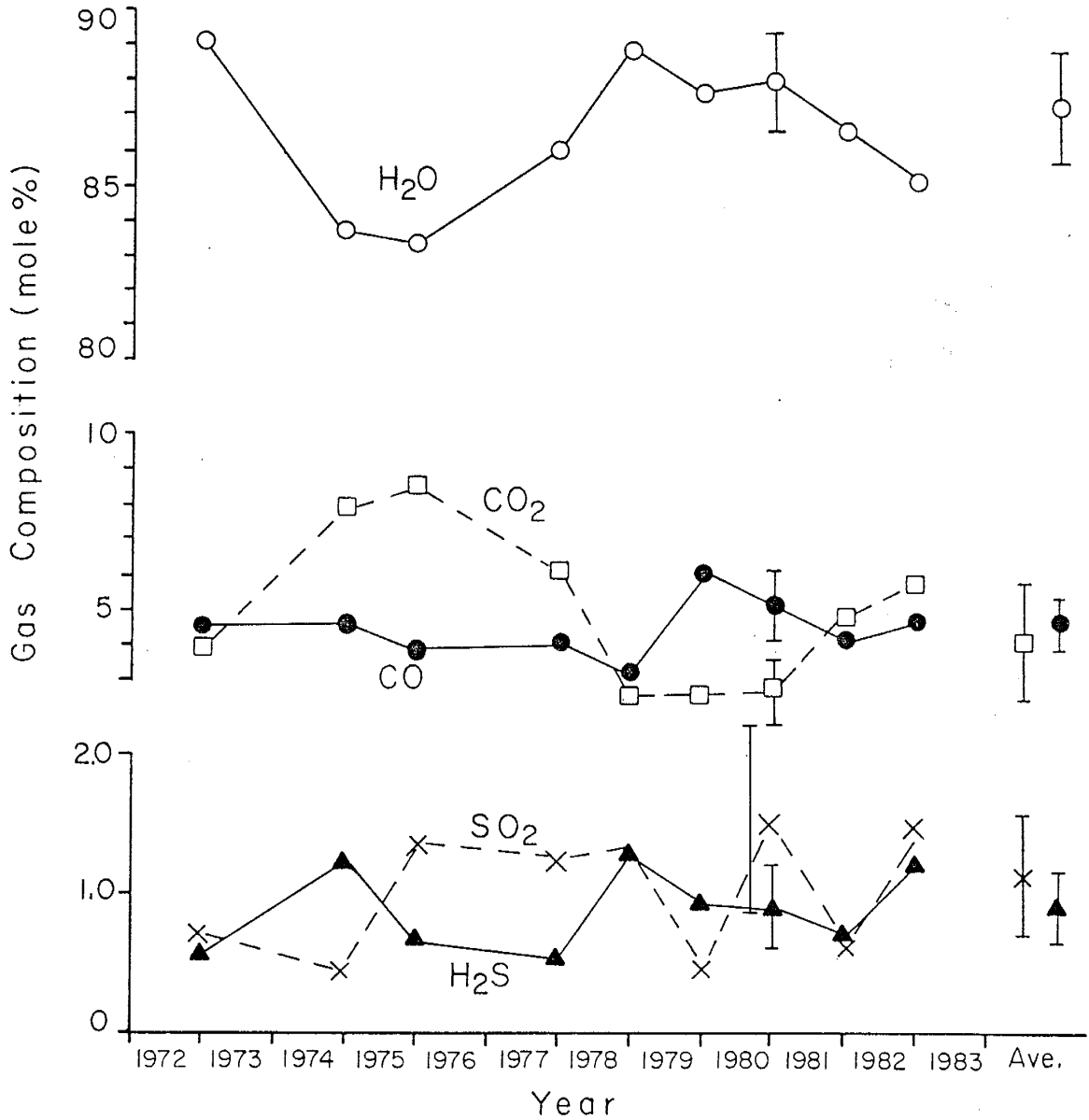


Fig. 5. Matrix Glass gas (H₂O, CO₂, CO, SO₂, H₂S) compositions from 1972 to 1982.

H₂O, —○—; CO₂, ---□---; CO, —●—; SO₂, ---x---; H₂S, —▲—. All gases reported in mole %.

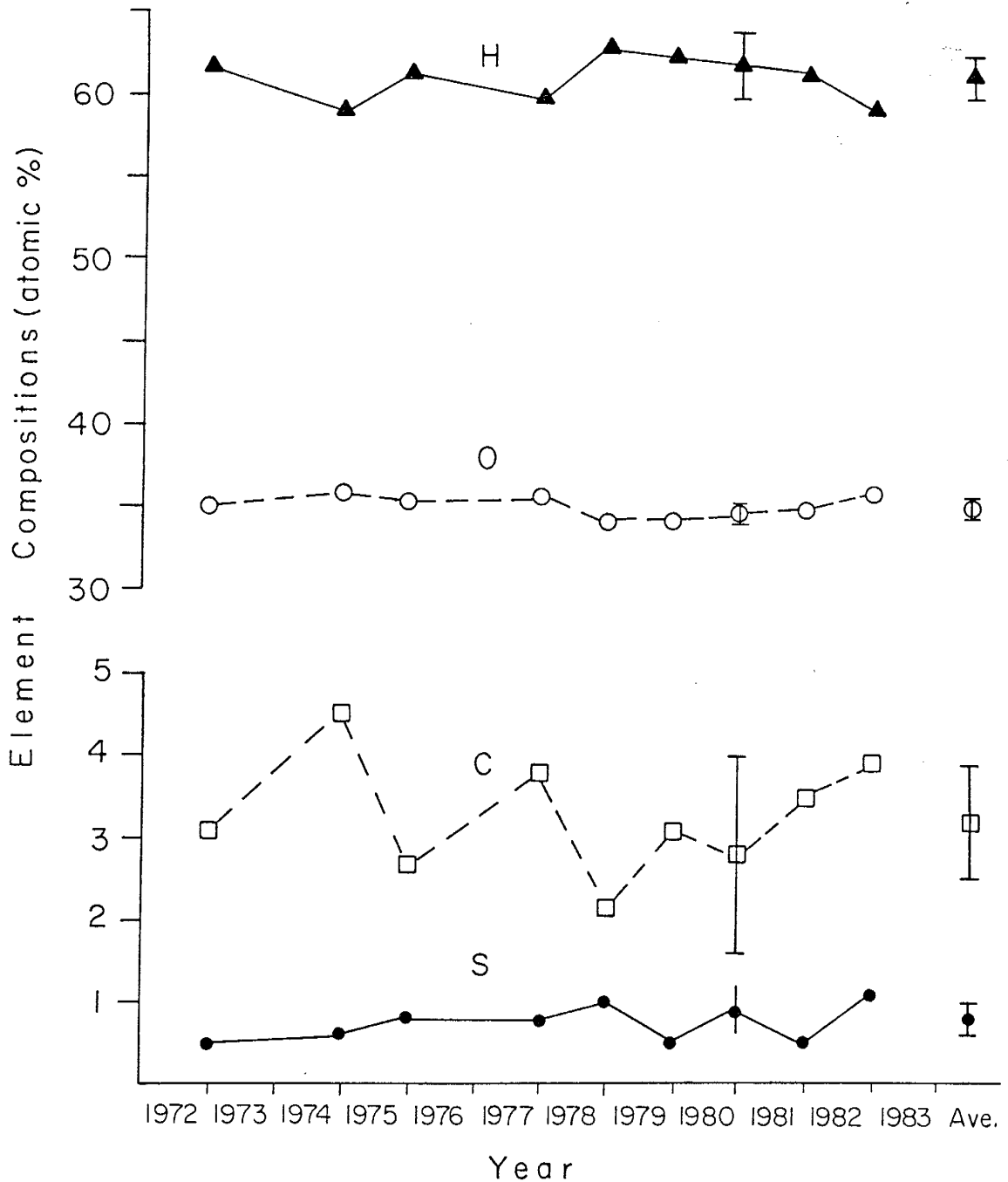


Fig. 6. Matrix Glass element (O, H, C, S) compositions, derived from gas compositions, 1972 to 1982.

Oxygen (O), ---^o---; Hydrogen (H), —▲—;
 Carbon (C), ---□---; Sulfur (S), —●—. Elements reported in atomic %.

Inclusion Glass

Concentrations of gases in inclusion glasses may represent primary melt volatile concentrations at the time of anorthoclase crystallization. The differences between matrix and inclusion glass concentrations should reflect the effects of melt degassing. The gas concentrations in inclusion glass were measured by analyzing whole anorthoclase phenocrysts which contained inclusions of glass and various minerals. The amount of glass trapped in the anorthoclase phenocrysts was estimated using the mass balancing procedure presented in Wright and Doherty (1970) and Wright (1974). The mass balance calculations (Appendix F) indicate that inclusion glass comprises $9^{+2}\%$ of the phenocryst by composition. The gas concentrations calculated from analyses of whole anorthoclase phenocrysts were assumed to have been derived mainly from inclusion glass. Sommer (1977) indicates that feldspar does not have significant volatile contents and that all the gas from a feldspar and inclusion glass sample can be attributed to the inclusion glass. However, analyses of nearly pure anorthoclase from Mount Erebus indicate that the anorthoclase contains significant quantities of gas (Table D1). This suggests that Sommer's assumption is not valid for this study. The total gas concentrations measured in whole anorthoclase samples could come from the anorthoclase and not from the glass inclusions. However, the analyses of

gas concentrations in anorthoclase are also suspect because glass and mineral contaminants could not be completely separated from the anorthoclase. Therefore, because there is an absence of conclusive evidence gas concentrations and compositions derived from analyses of whole anorthoclase samples are presented assuming that all evolved gases were derived from the glass inclusions.

The concentrations of gases in inclusion glasses from bombs collected in 1974, 1975, 1977 and 1980 (Table 7) are all similar within estimated analytical precision. The standard deviations of average gas concentrations in inclusion glass are similar to those of the replicate (n=7) analyses of matrix glass sample 81003. This indicates that the variations in gas concentrations from inclusion glass are due to analytical error. Oxygen, H, C and S concentrations recalculated to 100% (Table 7) also indicate that there are no significant differences in gas concentrations.

The average of the total gas concentrations in glass inclusions is greater than the average concentration in matrix glass. The average CO₂, SO₂ and H₂S concentrations in inclusion glass are significantly greater than concentrations in matrix glass whereas H₂O and CO concentrations are the same in inclusion and matrix glasses, within analytical error (Table 8).

TABLE 7

Gas concentrations (ppm) of inclusion glass in anorthoclase phenocrysts from recent bombs, Mount Erebus

Year	Year				AVE
	1974	1975	1977	1980	
n	1	1	1	1	4
Gas	5150	4600	3660	4030	4360(650)*
H ₂ O	3470	3310	2480	2720	2990(470)
H ₂	3	6	1	1	3(2)
CO ₂	743	544	541	450	570(124)
CO	413	119	209	229	243(123)
SO ₂	277	350	308	412	337(58)
H ₂ S	154	150	56	86	112(48)
COS	36	52	30	78	49(21)
CS ₂	33	22	17	21	23(7)
C ₂ H ₄	2	2	1	4	2(1)
CH ₄	14	44	6	8	18(18)
HCl	5	3	3	6	4(2)
N ₂	n.d.	n.d.	n.d.	n.d.	n.d.
Ar	tr	3	tr	1	1
He	tr	tr	tr	n.d.	tr

Element concentrations (ppm) recalculated to 100%.

O	3990	3593	2877	3118	3395(496)
H	399	394	282	312	347(59)
C	403	247	252	249	288(77)
S	330	371	237	347	321(59)

* = 1 Standard deviation

n = Number of analyses used to determine the listed average.

n.d. = not detected

tr = trace

TABLE 8

Average H₂O, CO₂, CO, SO₂ and H₂S concentrations (ppm) in matrix and inclusion glasses from recent bombs, Mount Erebus

	n	H ₂ O	CO ₂	CO	SO ₂	H ₂ S
MG	22	2920(590)	343(158)	240(61)	128(48)	56(13)
IG	4	2990(470)	570(124)	243(123)	337(58)	112(48)

* = 1 standard deviation

n = number of analyses

MG = Matrix glass

IG = Inclusion glass

An average S concentration in inclusion glass of 321 ppm, determined by mass spectrometry, is significantly less than the average S concentration of 440 ppm determined by electron microprobe analysis. The mass spectrometric analyses detected approximately 3 ppm of Cl in inclusion glasses whereas electron microprobe analyses measured an average concentration of 1600 ppm Cl.

Gas compositions in inclusion glass are assumed to represent the volatile composition of the melt at the time of anorthoclase crystallization. The gas compositions of the four inclusion glass analyses are similar (Table 9). Calculated standard deviations for average inclusion glass and sample 81003 compositions indicate that the observed variations in the inclusion glass compositions are within estimated analytical precision. The SO₂ and H₂S compositions seem to have complementary increasing and

TABLE 9

Gas compositions (mole %) of inclusion glass in anorthoclase phenocrysts from recent bombs, Mount Erebus

Year	1974	1975	1977	1980	AVE
n	1	1	1	1	4
H ₂ O	81.4	84.5	83.1	83.3	83.1(1.3)*
H ₂	0.59	1.33	0.34	0.34	0.65(0.47)
CO ₂	7.13	5.69	7.4	5.63	6.46(0.93)
CO	6.23	1.96	4.51	4.49	4.30(1.76)
SO ₂	1.83	2.62	2.89	3.55	2.79(0.71)
H ₂ S	1.92	2.03	0.99	1.38	1.58(0.49)
COS	0.26	0.40	0.31	0.71	0.43(0.20)
CS ₂	0.19	0.14	0.14	0.15	0.16(0.02)
C ₂ H ₄	0.03	0.02	0.03	0.07	0.04(0.02)
CH ₄	0.38	1.25	0.22	0.26	0.53(0.49)
HCl	0.06	0.03	0.05	0.09	0.06(0.03)
N ₂	n.d.	n.d.	n.d.	n.d.	n.d.
Ar	tr	0.03	tr	0.01	0.01(0.01)
He	tr	tr	tr	n.d.	tr

Element compositions (atomic%) recalculated to 100%.

O	36.0	34.5	36.8	36.1	35.9(1.0)
H	57.6	60.5	57.4	58.1	58.4(1.4)
C	4.9	3.2	4.3	3.8	4.0(0.7)
S	1.5	1.8	1.5	2.0	1.7(0.2)

* = 1 Standard deviation

n = Number of analyses used to determine the listed average.

n.d. = not detected

tr = trace

decreasing trends but elemental S compositions do not. This indicates that the apparent SO_2 and H_2S trends may be a result of the analytical procedures.

A comparison of inclusion and matrix glass compositions (Table 10) indicates that there are small but significant differences. The average mole percents of CO_2 , SO_2 and H_2S are enriched whereas the H_2O is depleted in inclusion glass compared to the matrix glass. The inclusion and matrix glass CO compositions are the same within analytical error. Average element compositions (Table 9) show that there is a clear difference between inclusion and matrix glass gas compositions. The C and S compositions are significantly greater in the inclusion glasses. Average H and O compositions are the same within analytical precision.

TABLE 10

Average H_2O , CO_2 , CO, SO_2 and H_2S compositions (mole %) of matrix and inclusion glasses from recent bombs, Mount Erebus

	H_2O	CO_2	CO	SO_2	H_2S
MG	87.2(2)*	4.1(41)	4.6(17)	1.13(39)	0.90(29)
IG	83.1(2)	6.5(14)	4.3(42)	2.79(25)	1.58(31)
81003	87.9(2)**	2.7(33)	5.1(31)	1.53(44)	0.90(32)

* = 1 standard deviation

MG = Matrix glass

IG = Inclusion glass

** = Coefficient of variation (standard deviation x100/mean)
based on 7 analyses of 81003

Volatile Elements

Whole Rock

Volatile element concentrations in whole rock samples from recently erupted bombs represent the total volatile content of the degassed magma. Whole rock S and Cl concentrations remain relatively constant, from 1972 to 1982 (Table 11), and average 260 ± 20 ppm S and 1110 ± 290 ppm Cl. Statistical analyses indicate that there are no significant S or Cl trends with time. There is very little variability in S concentrations except for a slight decrease during 1980 to 1981 (Figure 7). Chlorine concentrations in whole rock samples are not as consistent as the S concentrations. An increase in Cl during 1979 to 1981 compliments the slight decrease in S during these years. However, the erratic nature and unknown analytical precision of the Cl data obscures possible differences, if they exist.

TABLE 11

Whole rock S and Cl analyses (ppm) of recent bombs,
Mount Erebus

Year	1972	1975	1978	1979	1980	1981	1982	Ave.
n	1	1	1	1	1	2	2	9
S	280	280	270	230	245	245	270	260(20)*
Cl	1130	970	970	1500	1510	1080	895	1110(240)

* = 1 standard deviation

n = number of analyses

Analyst: J. Bodkin (Pennsylvania State University)

Matrix Glass

Volatile element concentrations in matrix glass represent the volatiles present in the magma at the time of quenching. These residual S, Cl and F concentrations were determined to detect concentration changes with time. Sulfur, Cl and F concentrations in matrix glasses generally remain constant within analytical error (Table 12). Statistical analyses indicate that there are no significant trends in the S, Cl or F concentrations from 1972 to 1982. Concentration fluctuations of these elements are within estimated analytical errors but seem to be complementary. The significance of these minor fluctuations, which can be attributed to analytical error, is difficult to assess because the analytical precision of the analyses is unknown.

Average S and Cl concentrations in matrix glass are significantly greater than whole rock concentrations (Table 13) due to the dilution affect of anorthoclase crystals in the whole rock samples. The S and Cl concentrations are greater in the matrix glass by approximately 27% and 41%, respectively.

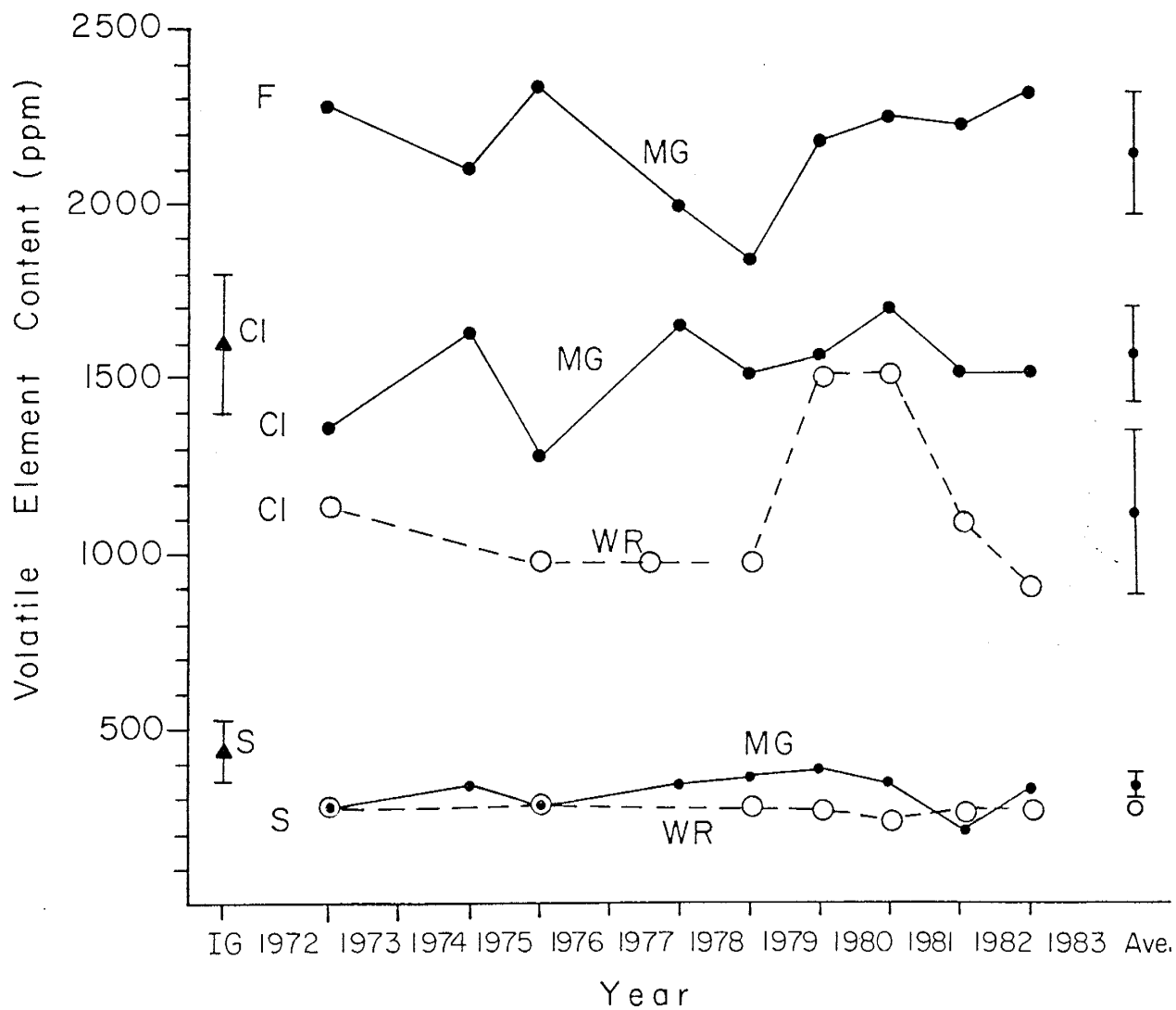


Fig. 7. Whole Rock (WR), Matrix Glass (MG) and Inclusion Glass (IG) volatile element (S, Cl, F) concentrations from 1972-1982.

WR, ---○---; MG, —●—; IG, ▲. All volatile elements reported in ppm.

TABLE 12

S, Cl and F analyses (ppm) of matrix glass from recent bombs, Mount Erebus

Year	72	74	75	77	78	79	80	81	82	Ave.
n	1	2	1	2	2	2	3	1	1	15
S	280	340	280	340	360	380	340	210	320	330(40)*
Cl	1360	1630	1280	1650	1510	1560	1700	1510	1510	1560(140)
F	2280	2100	2330	1990	1830	2180	2240	2220	2310	2140(180)

* = 1 standard deviation

n = number of analyses

Analyst: J. Bodkin (Pennsylvania State University)

Inclusion Glass

Volatile element analyses of glass inclusions in anorthoclase were made to determine pre-eruptive concentrations. The S and Cl concentrations are assumed to represent the concentration of these elements present in the melt at the time of anorthoclase crystallization. Inclusion glass S and Cl concentrations of 440^{+90} ppm S and 1600^{+200} ppm Cl are based on microprobe analyses of glass inclusions within one anorthoclase crystal. There is no indication that there is a difference in concentrations between different glass inclusions other than that caused by analytical error (Appendix D).

The average inclusion glass S and Cl concentrations are significantly greater than whole rock concentrations (Table 13) by 41% and 31% respectively. The Cl/S ratios indicate

that S is enriched relative to Cl in the inclusion glasses.

TABLE 13

Average S, Cl and F concentrations (ppm) of matrix and inclusion glass and whole rock samples from recent bombs, Mount Erebus

	WR	MG	IG
S	260(20)*	330(40)	440(90)
Cl	1110(240)	1560(140)	1600(200)
F	n.a.	2140(180)	n.a.
CL/S	4.3	4.7	3.6

* = 1 standard deviation

n.a. = not analyzed

WR = Whole rock

MG = Matrix glass

IG = Inclusion glass

Major Elements

Average major element analyses of whole rock samples, made by Dr. P. R. Kyle, can be used to determine if changes have occurred in the bulk composition of the Mount Erebus magma system. These analyses can be compared with analyses published by Kyle et al. (1982) and Goldich et al. (1975) to determine if there have been long-term changes in the anorthoclase phonolite composition.

Major element composition of bombs erupted between 1972 and 1978 have remained the same within analytical error (Table 14). Statistical tests indicate that the analyses do not have significant trends with respect to time. There is,

TABLE 14

Whole rock major element analyses of recent anorthoclase phonolite bombs, Mount Erebus

Year	1978	1977	1975	1974	1972
n	1	4	1	3	1
SiO ₂	56.51	56.21(0.45)**	55.96	56.32(0.12)	56.13
TiO ₂	0.92	0.96(0.04)	0.98	0.93(0.02)	0.95
Al ₂ O ₃	20.53	20.11(0.16)	19.92	20.18(0.04)	20.04
FeO*	4.57	4.76(0.23)	4.95	4.66(0.15)	4.83
MnO	0.21	0.22(0.01)	0.22	0.21(0.01)	0.21
MgO	0.88	0.86(0.04)	0.89	0.83(0.01)	0.84
CaO	2.71	2.62(0.07)	2.65	2.67(0.06)	2.68
Na ₂ O	8.80	8.66(0.07)	8.48	8.54(0.08)	8.41
K ₂ O	4.52	4.62(0.11)	4.57	4.54(0.06)	4.50
P ₂ O ₅	0.37	0.39(0.02)	0.42	0.38(0.01)	0.39
LOI	0.11	0.02	0.00	0.05	0.00
Sum	100.13	99.43	99.04	99.31	98.98

Sample	OB	CS	CR	CE
n	1	1	1	1
SiO ₂	55.16	55.70	56.20	55.10
TiO ₂	1.06	0.96	1.01	1.04
Al ₂ O ₃	19.72	19.92	19.90	19.50
FeO*	5.20	4.63	5.31	5.84
MnO	0.23	0.21	0.19	0.21
MgO	0.97	0.90	1.16	1.13
CaO	2.64	2.85	3.32	3.30
Na ₂ O	8.68	8.43	7.89	8.03
K ₂ O	4.70	4.42	4.24	4.68
P ₂ O ₅	0.44	0.41	0.46	0.42
LOI	0.19	0.10	0.21	0.40
Sum	98.99	98.53	99.89	99.65

* = Total Fe as FeO

** = 1 Standard deviation

n = number of analyses

OB = Old bomb of unknown age

CS = A bomb from the camp site of unknown age

All analyses were made by X-Ray fluorescence spectrometry by P. R. Kyle except for the Cape Royds(CR) and Cape Evans(CE) analyses which are from Goldich et al. (1975).

however, a possible fluctuation, within analytical error, in SiO_2 , Al_2O_3 and FeO concentrations with time (Figure 8). The SiO_2 and Al_2O_3 variations are complemented by an FeO variation. These variations could be caused by sample variability. Representative whole rock samples were difficult to obtain because the bombs are highly vesicular and phenocryst-rich.

Analyses of recent bombs are similar to those reported by Goldich et al., (1975) for a 0.68 my old (Treves, 1967) lava flow from Cape Royds and an undated flow from Cape Evans. There are slight compositional differences in CaO, FeO^* and MgO concentrations which are relatively depleted whereas Na_2O and to a lesser degree Al_2O_3 and SiO_2 concentrations are relatively enriched, in the recent rocks.

Major element analyses of matrix glasses, made by Dr. P. R. Kyle, were made to determine if mineral crystallization occurred during the last 10 years. Crystallization of the main mineral phase, anorthoclase, would cause a change in the melt (matrix glass) composition.

Major element compositions in the matrix glasses remained constant, within analytical error, from 1972 to 1982 (Table 15). Statistical analyses indicate that there are no significant composition trends with time (Figure 8).

TABLE 15

Major element analyses of matrix and inclusion glass from recent anorthoclase phonolite bombs, Mount Erebus

Year	1978	1977	1975	1974
n	42	27	11	36
SiO ₂	55.90(0.59) **	55.84(0.53)	55.76(0.45)	55.88(0.64)
TiO ₂	1.02(0.06)	1.01(0.05)	1.02(0.04)	1.02(0.06)
Al ₂ O ₃	19.86(0.28)	19.80(0.30)	20.00(0.20)	19.95(0.31)
FeO* ³	5.36(0.10)	5.36(0.11)	5.51(0.11)	5.38(0.13)
MnO	n.a.	n.a.	n.a.	n.a.
MgO	0.82(0.10)	0.82(0.06)	0.87(0.07)	0.85(0.07)
CaO	1.95(0.07)	1.92(0.08)	1.98(0.11)	1.96(0.08)
Na ₂ O	8.83(0.18)	9.07(0.15)	9.02(0.11)	9.10(0.13)
K ₂ O	5.56(0.17)	5.48(0.17)	5.51(0.10)	5.56(0.15)
P ₂ O ₅	0.22(0.04)	0.22(0.03)	0.25(0.03)	0.23(0.04)
Sum	99.52	99.52	99.92	99.93

Year/sample	1972	Mean	IG
n	11	5	9
SiO ₂	55.70(0.56)	55.81(0.08)	55.29
TiO ₂	1.03(0.04)	1.02(0.01)	0.99
Al ₂ O ₃	19.87(0.30)	19.90(0.08)	18.79
FeO* ³	5.41(0.12)	5.40(0.06)	5.11
MnO	n.a.	n.a.	0.26
MgO	0.87(0.07)	0.85(0.02)	0.80
CaO	1.95(0.07)	1.95(0.02)	1.72
Na ₂ O	9.00(0.12)	9.00(0.10)	9.14
K ₂ O	5.53(0.16)	5.53(0.03)	6.26
P ₂ O ₅	0.25(0.04)	0.23(0.02)	n.a.
	99.61	99.69	98.36

* = Total Fe as FeO

** = 1 Standard deviation

n = Number of analyses

n.a. = not analyzed

All analyses were made by electron microprobe by P. R. Kyle except for the inclusion glass (IG) analysis which is from Kyle (1977a).

The composition differences between matrix glass and whole rock compositions are due to the high anorthoclase phenocryst content of the whole rocks. The CaO and to a lesser degree SiO_2 and Al_2O_3 concentrations are depleted whereas Na_2O , K_2O and FeO^* are enriched in the matrix glasses. Instrumental neutron activation analyses (Table 16) on bulk samples (100 mg) of the matrix glass are very similar to the microprobe analyses (Table 15) for Na_2O whereas the FeO^* concentrations are significantly different. This difference is probably due to small amounts of contaminant olivine and/or pyroxene in the bulk matrix glass samples.

Trace and rare earth element analyses of matrix glasses (Table 16), which are more sensitive to composition changes than the major elements analyses, also remain constant from 1974 to 1980.

Analyses of glass inclusions in anorthoclase crystals are important because they may reflect the composition of the source magma, prior to significant anorthoclase crystallization. A comparison of inclusion glass, matrix glass and whole rock compositions also provides an insight into the evolution of the Mount Erebus magma system.

Major element analyses of glass inclusions (Table 15), made by Dr. P. R. Kyle are very similar and show a greater resemblance to the matrix glass than to the whole rock

TABLE 16

Trace and rare earth element analyses of matrix glass from recent bombs, Mount Erebus

Year	1974		1977		1978		1979		1980		OB	MEAN
	n	3	n	4	n	2	n	2	n	2		
FeO*	5.84	5.84	6.06	6.06	5.38	5.38	5.77	5.77	5.64	5.64	5.95	5.81(0.32)**
Na ₂ O	9.31	9.31	9.10	9.10	9.15	9.15	9.12	9.12	9.30	9.30	9.09	9.18(0.18)
Sc	3.69	3.69	3.52	3.52	3.06	3.06	3.53	3.53	3.15	3.15	3.64	3.52(0.36)
Cr	<10	<10	<10	<10	<10	<10	<10	<10	<10	<10	<10	<10
Co	2.9	2.9	3.2	3.2	2.2	2.2	2.6	2.6	2.4	2.4	2.8	2.7(0.6)
As	3.1	3.1	3.2	3.2	2.9	2.9	2.9	2.9	3.0	3.0	3.3	3.1(0.1)
Rb	124	124	126	126	121	121	120	120	123	123	122	123(2)
Sb	0.52	0.52	0.49	0.49	0.48	0.48	0.49	0.49	0.50	0.50	0.49	0.50(0.01)
Ba	574	574	569	569	580	580	566	566	623	623	595	580(19)
Cs	1.94	1.94	1.94	1.94	1.88	1.88	1.82	1.82	1.96	1.96	1.80	1.91(0.06)
La	163	163	162	162	157	157	160	160	159	159	162	161(4)
Ce	326	326	320	320	306	306	317	317	316	316	324	318(10)
Sm	19.6	19.6	19.3	19.3	18.3	18.3	19.2	19.2	19.0	19.0	19.3	19.2(0.7)
Nd	120	120	119	119	115	115	116	116	118	118	120	118(2)
Eu	4.04	4.04	4.03	4.03	3.77	3.77	3.96	3.96	4.00	4.00	4.11	3.99(0.09)
Tb	2.47	2.47	2.46	2.46	2.33	2.33	2.39	2.39	2.41	2.41	2.47	2.43(0.05)
Yb	7.90	7.90	7.75	7.75	7.78	7.78	7.52	7.52	7.67	7.67	7.59	7.73(0.13)
Lu	0.90	0.90	0.89	0.89	0.87	0.87	0.86	0.86	0.87	0.87	0.88	0.88(0.01)
Hf	30.6	30.6	30.0	30.0	30.2	30.2	29.9	29.9	30.2	30.2	30.2	30.2(0.3)
Ta	25.5	25.5	25.2	25.2	25.4	25.4	25.2	25.2	25.2	25.2	25.0	25.3(0.2)
Th	28.9	28.9	28.5	28.5	28.9	28.9	28.7	28.7	28.7	28.7	28.5	28.7(0.2)
U	7.5	7.5	7.7	7.7	7.9	7.9	7.4	7.4	8.0	8.0	7.8	7.7(0.2)

* = Total Fe as FeO

** = 1 Standard deviation

n = Number of analyses used to determine the listed average.

OB = Old bomb of unknown age

Analyzed by instrumental neutron activation by P. R. Kyle.

analyses. Kyle (1977a) states that some glass inclusions in anorthoclase phenocrysts represent progressively younger inclusions from core to rim. He also indicates that a variation in glass composition was observed between the core and rim, in one crystal, poorly observed in a second and not observed in a third. The variation observed in the first crystal was a small systematic decrease of FeO_T and an increase of Al_2O_3 from core to rim (Kyle, 1977a). This is opposite to that which would be expected if anorthoclase crystallization was the only factor controlling the inclusion glass chemistry.

The average inclusion glass compositions (Table 15) are relatively depleted in CaO and Al_2O_3 and are relatively enriched in K_2O and Na_2O compared to the whole rock and matrix glass analyses (Figure 8).

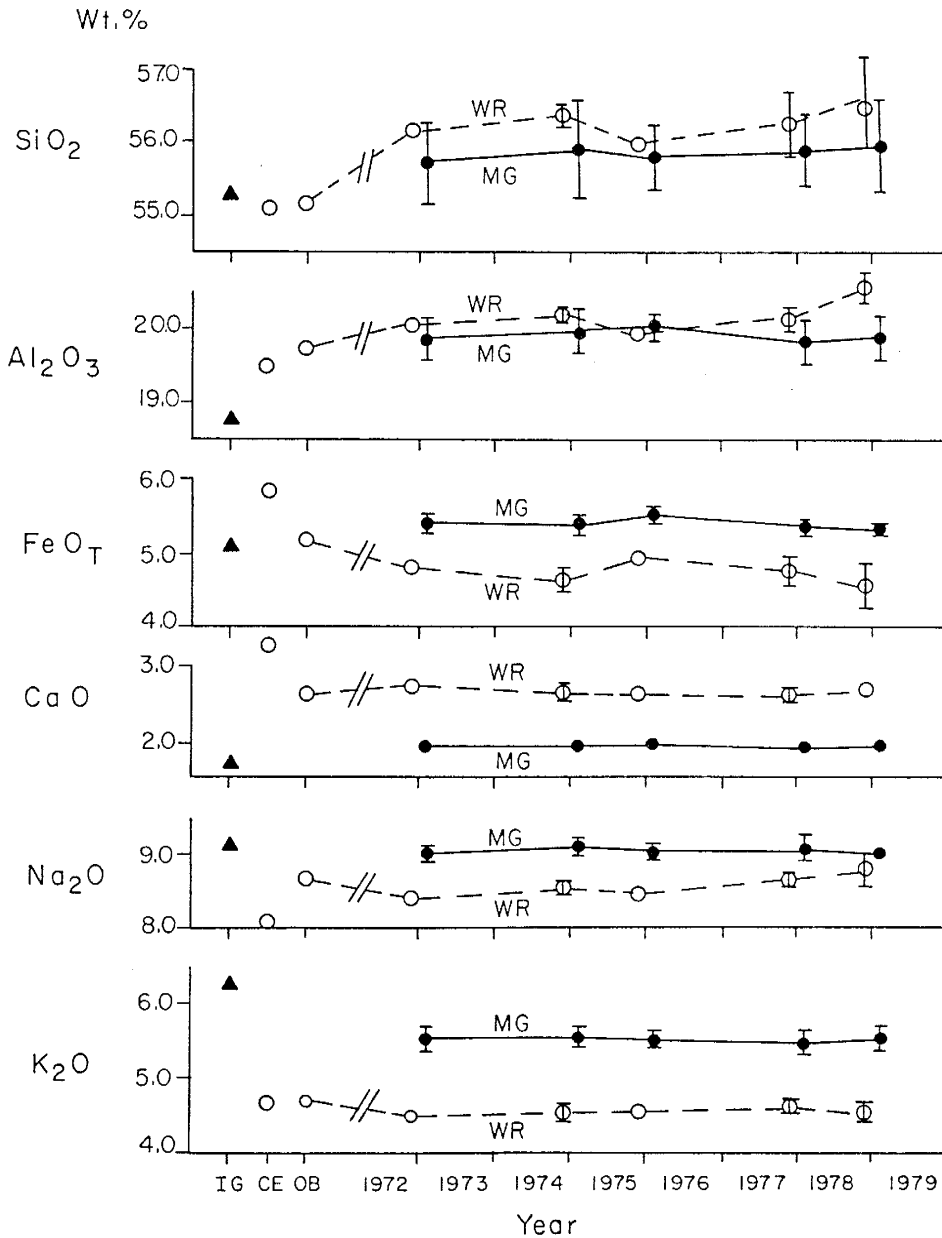


Fig. 8. Whole Rock (WR), Matrix Glass (MG) and Inclusion Glass (IG) oxide (SiO_2 , Al_2O_3 , FeO_T , CaO , Na_2O , K_2O) concentrations from old lava flows and recent bombs.

WR, ---○---; MG, —●—; IG, ▲; Old bomb (OB); Cape Evans (CE) from Goldich et al. (1975); Unknown length of time, //.
All oxides reported in wt. %.

Discussion

Assumptions

1) Gases evolved from glass samples in the laboratory are assumed to be representative of the magmatic volatile concentrations and compositions. For this assumption to be valid, volatiles bound in the glass by quenching must be liberated by thermal decrepitation such that the integrity of the original volatile concentration and composition is retained. It is unlikely, however, that the process of gaseous entrapment can be completely reversed while maintaining the integrity of volatile concentrations and compositions. Despite this problem, meaningful interpretations may be made if volatile concentrations and compositions are slightly altered but still reflective of the original components. The restoration procedures presented by Gerlach (1980d) may partially resolve this problem by eliminating the affects of alteration caused by gas reactions which take place during analysis.

2) Volatiles in inclusion and matrix glasses are generally believed to be representative of the melt concentrations and compositions (Watson, 1976; Sommer, 1977; Delaney et al., 1978; Anderson, 1979; Eichelberger and Westrich, 1981,1982,1983; Watson et al., 1982 and Harris and Anderson, 1983). However, the assumption that gas concentrations and compositions of Mount Erebus glasses are

reflective of the magma concentrations, is not totally valid.

It is assumed that matrix glass gas concentrations and compositions represent magma which has been degassed. The vesicularity (Eichelberger and Westrich, 1981) of the matrix glass indicates that its volatile concentration may be relatively depleted compared to the degassed magma which is recycled back to the magma chamber. Matrix glass gas analyses represent only structurally bound volatiles in the magma at the time of quenching, whereas the degassed magma which returns to the magma chamber retains an unknown quantity of insoluble vapor phase gases which are retained in the melt.

It is further assumed that volatile concentrations and compositions of inclusion glass represent the concentrations and compositions of the melt at the time of anorthoclase crystallization. Harris and Anderson (1983) indicate that if the glass inclusions are relatively large and if inclusion and matrix glass chemistries are very similar, the inclusion glasses are probably representative of the bulk magma. Glass inclusions in anorthoclase crystals from Mount Erebus meet these conditions (See Kyle, 1977a). The potential problem with this assumption is that diffusion rates of incompatible and compatible elements, with respect to the anorthoclase, will cause enrichment and depletion

gradients in the magma near the crystal-liquid interface (Albarede and Bottinga, 1972). The same principle may be applied to gas phases and dissociated gas forms in the magma.

Gases

Residual volatiles in the matrix glasses are structurally bound and probably reflect their solubility concentrations at 1 atm and 1000°C. However, matrix glass gas analyses indicate that there has been a slow consistent decline in magma H₂O and CO₂ concentrations over the last ten years. If the concentrations truly reflect solubilities, one of the parameters which control solubility must be changing. The main parameters which control the H₂O and CO₂ solubilities are magma composition, temperature, volatile species composition and pressure. It is unlikely that magma composition is causing the decline because major element analyses show that the magma composition has not changed. A slow decline in temperature can explain the decline in the CO₂ concentration but does not explain the similar decline in the H₂O concentration. Mysen (1976) states that CO₂ concentrations in NaAlSi₃O₈, NaAlSi₂O₆ and NaAlSiO₄ composition melts are positively correlated with temperature whereas the solubility of H₂O, in albite melts (Burnham and Jahns, 1962), decreases very slightly with increasing temperature. This suggests that a decline in

temperature would cause CO_2 to decrease at a greater rate than H_2O . However, Figure 6 shows that the H_2O and CO_2 concentrations are declining at approximately the same rate. The major volatiles other than H_2O and CO_2 do not have concentration changes with time and therefore should not affect the H_2O and CO_2 solubilities. A decline in H_2O concentration should cause a CO_2 concentration decline (see Volatile Solution Mechanisms and Species) but the relationship is not well understood. This leaves pressure as the only parameter which may cause the similar concentration declines. However, if the concentrations represent solubilities at 1 atm and 1000°C the equilibrium pressure is always the same and therefore can not account for the H_2O and CO_2 concentration declines. It is possible that the volatile concentrations in the matrix glass only approach equilibrium and are quenched before equilibrium is attained. Therefore, the H_2O and CO_2 concentration trends may reflect a slight decline in the bulk magma volatile content due to degassing. It seems probable that the structurally bound volatiles in the melt can not diffuse out of the melt quickly enough to attain equilibrium with the changing pressure, as the magma rises to the surface. However, it must be emphasized that very little is known about the volatile diffusion rates and the time available for diffusion to take place. In addition, it is unlikely that the decline is due to post-quenching diffusion. The

samples were stored for no longer than ten years and the diffusion rates of gases through the glass should not be significant for this period of time. Alternatively, the constant nature of the composition measurements indicate that the volatile compositions of the matrix glasses are reflective of volatile solubilities at 1 atm and 1000°C. The contradiction of the concentration and composition results, which indicate a decline in and constant H₂O and CO₂ with time, may be due to the manner in which the two calculations are made. However, the answer to this dilemma may also be that the H₂O and CO₂ concentration declines are a result of analytical error which is not accounted for.

The mass spectrometric analyses of S, Cl and F are lower than the concentrations determined by wet chemistry and specific ion electrode methods. This may be due to absorption of S, Cl and F onto the glass extraction line. However, some of the structurally bound S, Cl and F may not be released during heating of the samples because these elements may have high solubilities in the glass at 0.1 torr and 1000°C.

A comparison of present and pre-eruptive volatile concentrations requires a comparison of whole rock and inclusion glass volatile concentrations. The average gas concentration in matrix glass can be adjusted to account for the dilution effect caused by phenocrysts, and thus

approximate whole rock gas concentrations Table 13.

Table 17

Estimated whole rock gas concentrations (ppm) in matrix glass from recent bombs, Mount Erebus

H ₂ O	CO ₂	CO	SO ₂	H ₂ S
2313	291	190	120	49

The relatively consistent gas analyses of inclusion glasses in four phenocrysts indicates that the glass inclusions were trapped at or near the same time or that degassing was not occurring during anorthoclase crystallization. Measured inclusion glass and estimated whole rock gas concentrations indicate that 30% degassing of volatiles has occurred. Degassing of structurally bound volatiles probably occurred as the magma vesiculated during its rise from the magma chamber to the surface. The vapor phase gases are probably lost as the magma approaches the surface and before the bombs are quenched.

Volatile Elements

The uniformity of whole rock S and Cl concentrations indicate that the Mount Erebus magma convection system has remained closed from 1972 to 1982. The higher Cl and F concentrations, compared to S, may be caused by the greater solubility of Cl and F in the melt at 1 atm and 1000°C.

Fumarole emission analyses from other volcanoes (Gerlach, 1979; 1980a,b,c,d; 1981) seem to support this suggestion because they indicate that greater quantities of S, relative to Cl and F, are degassed (Table 15). Giggenbach (1975b) reports a C:S:Cl ratio of 70:29:1 for fumarolic gases at 800°C, from White Island, New Zealand, which contrasts with the Mount Erebus whole rock ratio of 10:17:73. However, the relatively low oxygen fugacity of the Mount Erebus magma indicates that S should be relatively soluble in the melt as sulfides (Gerlach, Private communication).

Constant concentrations of S, Cl and F in matrix glass indicates that solubility is controlling volatile concentrations in the glass. Sulfur, Cl and F are structurally bound in matrix glass and have probably approached equilibrium at 1 atm and 1000°C. There has been little change in the parameters which control solubilities, from 1972 to 1982, if the concentrations represent solubility concentrations. However, it is possible that 10 years is not a sufficient period of time to see changes in concentrations. The matrix glass concentrations are greater than the whole rock concentrations because S, Cl and F are incompatible in anorthoclase. The relatively greater amounts of Cl, 41%, than S, 27%, in matrix glass may be due to pyrrhotite (FeS_2) microphenocrysts in the anorthoclase. A comparison of average S and Cl concentrations, assuming no S or Cl in the anorthoclase, indicates that anorthoclase

phenocrysts comprise 21% and 29% of the bombs, respectively. These estimates are only approximate because pyrrhotite, which contains S, and apatite, which contains Cl, are commonly included in anorthoclase crystals.

Significantly greater S and Cl concentrations in the inclusion glass, with respect to whole rock concentrations, indicate that there has been a 41% loss of S and a 31% loss of Cl due to degassing. Rose et al., (1982) indicates that Cl is probably retained and S lost in magmas as they cool and evolve. Anderson (1974) also states that water-poor magmas lose very little Cl. The H₂O content of the Mount Erebus magma is probably sufficiently low to cause Cl to be more soluble than S. However, the H₂O concentration seems to be great enough to allow the highly concentrated Cl to degas in significant quantities. The high matrix glass F concentration may be explained by the same reasoning used for high Cl concentrations. Martini (1983) proposes that F is more soluble in melts than either S or Cl, and will be strongly partitioned into the melt. A F estimate of 1500 ppm, using the matrix glass F concentration and 30% phenocryst composition in whole rocks, may be an accurate estimate of the original and present day F concentrations. However, some F must also be lost because Keys (1980) indicates that Cl and F precipitate as salts around the Mount Erebus crater. Fumarolic gas analyses (Table 15) seem to support this reasoning because S, Cl and F are usually

measured. However, because the Mount Erebus magma is very reduced, an f_{O_2} of 10^{-12} at $1050^{\circ}C$, S is probably present mainly as sulfide and is therefore relatively soluble in the melt. The Mount Erebus data seems to indicate that Cl and possibly F are degassed in greater quantities than S, which agrees with Key's observations.

Watson et al., (1982) states that it is important to consider kinetic factors which may complicate interpretations of inclusion glass volatile concentrations, especially when the inclusions occur in dense well defined bands. Albarede and Bottinga (1972) proposed that incompatible constituents, with respect to the inclusion glass host, will be concentrated in the melt adjacent to a rapidly-growing phenocryst. Watson et al., (1982) states that the concentration which will occur is determined by crystal growth rate and diffusion rates of incompatible volatiles away from the crystal-melt interface. Very little is known about S and Cl diffusion rates in alkalic silica undersaturated melts at high temperatures and pressures. However, all available information indicates that S and Cl concentrations for Mount Erebus inclusion glasses are representative of the magma at the time of anorthoclase crystallization.

Major Elements

The constant whole rock major element compositions of recent anorthoclase phonolite bombs and their similarity to older phonolite compositions indicate that parental sources and processes of Mount Erebus magma formation, have remained the same or similar for at least the last 0.7 m.y. The results also suggest that the system supplying the magma to the lava lake and Active Vent has been closed for at least the last ten years, unless the new magma was identical in composition. The minor variations in recent whole rock major element chemistries are due to sample variability and analytical error. A preliminary mass balance calculation indicates that the difference between the Cape Evans anorthoclase phonolite and the recent anorthoclase phonolites may be attributed to 1% magnetite and 3% pyroxene fractional crystallization. Alternatively, the differences can be attributed to the different analytical techniques used to analyze the older lava samples and the recent bombs.

Constant matrix glass major element compositions indicate that no crystallization of the magma has occurred in the last ten years. Variations in major element compositions in matrix glass are probably due to minor sample variability and analytical error. Differences between whole rock and matrix glass major element compositions is due to anorthoclase crystallization

(Carmichael, 1964). Matrix glasses are relatively enriched in FeO^* , K_2O and Na_2O and relatively depleted in Al_2O_3 and CaO compared to whole rock concentrations. A comparison of the anorthoclase chemistries presented by Boudette and Ford (1966) and Kyle (1977a) and whole rock compositions (Table 14) indicate that the whole rock and matrix glass chemistry differences are compatible with anorthoclase crystallization.

Inclusion glass major element analyses presented by Kyle (1977a) corroborate the interpretation that the relatively enriched and depleted values for oxide concentrations can be accounted for by anorthoclase crystallization. Inclusion glasses are relatively depleted in CaO and Al_2O_3 and are relatively enriched in K_2O and Na_2O , with respect to matrix glass and whole rock compositions. However, the relatively enriched and depleted oxide concentrations of inclusion glasses, compared to matrix glasses, may be explained by either continued anorthoclase crystallization of the melt after entrapment or by diffusion affects. The anorthoclase phenocrysts exhibit characteristics of rapid growth, such as dense bands of inclusions, which indicate that depletion and enrichment gradients probably existed during anorthoclase crystallization.

Comparative Results

A comparison of the volatile element and gas analyses presented in this thesis with published analyses is difficult because the magma compositions, oxygen fugacities, methods of analysis and environments of magma quenching are different in each study. These differences must be considered when the following comparisons are made.

Volatile concentrations in phonolitic and andesitic matrix glasses may be compared because they have similar SiO_2 concentrations. The average matrix glass S concentration of 330 ppm is within the range of 50 to 400 ppm S which Anderson (1974) reports for vesicular andesitic and basaltic glasses whereas the average phonolitic matrix glass Cl concentration of 1560 ppm is much greater than the range of 100 to 600 ppm Cl reported by Anderson (Table 18). Russell-Robinson and Smith (1983) report ranges of 880 to 920 ppm Cl and 220 to 250 ppm F in dacitic air-fall pumice from Mount St. Helens. They report that Cl and F concentrations increased with time and suggested that during long periods of repose a volatile-rich phase accumulates at the top of the magma chamber. This indicates that the relatively low volatile element concentrations reported by Russell-Robinson and Smith (1983) may be due to the explosive activity of Mount St. Helens, which contrasts with the passive activity of Mount Erebus, in addition to the

differences caused by the magma compositions.

The H₂O concentration of 6000 ppm measured by Anderson (1979) in andesitic glass matrix glass is significantly greater than the average Mount Erebus matrix glass H₂O concentration of 2920 ppm (Table 18). This exemplifies the problem of comparing concentrations determined by different techniques. The H₂O concentrations presented in this thesis were determined by pressure measurements whereas Anderson used a microprobe measurement technique. A more reliable comparison of H₂O concentrations may be made between results reported here and those presented by Eichelberger and Westrich (1981,1982,1983) for rhyolitic glasses. The H₂O solubility concentration of 1600 ppm for rhyolite at 1 atm H₂O vapor pressure and 859°C presented by Eichelberger and Westrich (1983) is slightly smaller than the 2920 ppm determined for the Mount Erebus matrix glass. Solubility curves presented by Hamilton et al. (1964) indicate that solubilities for melts of different compositions will converge at low pressures. This indicates that the comparison of rhyolitic and phonolitic solubilities, at low pressures, is valid and that the Mount Erebus matrix glass H₂O concentration probably represents a 1 atm and 1000°C solubility concentration. In contrast, H₂O concentrations in basaltic pumice reported by Harris (1981) are significantly less than those of the Mount Erebus phonolite. The basaltic pumice would normally be expected to have a

TABLE 18

Selected gas and volatile element concentration analyses
(ppm) of volcanic glasses

	H ₂ O	CO ₂	CO	SO ₂	S	Cl	F
Analyses of subaerially quenched glasses							
1	-----	-----	-----	-----	50-400	100-600	-----
2	6000	-----	-----	-----	-----	-----	-----
3	970	-----	-----	-----	-----	-----	-----
4	1000-4000	-----	-----	-----	-----	-----	-----
5	2000	-----	-----	-----	-----	-----	-----
6	630	-----	-----	-----	-----	-----	-----
7	880	220	20	190	130	620	120
Analyses of subaqueously quenched glasses							
8	9400	1100	100	-----	-----	3400	900
9	5300	-----	-----	-----	800-1200	120-280	120-770
10	2300	250	-----	-----	710	-----	-----
11	9000	-----	-----	-----	-----	-----	-----
Average Mount Erebus matrix glass gas concentrations							
12	2920	343	240	128	130	2	n.d.
13	-----	---	---	---	330	1560	2140

n.d. = not detected

Source 1)Anderson (1974), 2)Anderson (1979), 3)Eichelberger and Westrich (1981), 4)Eichelberger and Westrich (1982), 5)Eichelberger and Westrich (1983), 6)Harris (1981), 7)Shepherd and Merwin (1927), 8)Byers et al. (1983), 9)Muenow et al. (1979), 10)Harris (1981), 11)Moore (1970), 12)This study- by mass spectrometric analysis, 13)This study- using wet chemistry methods

greater H₂O content (Hamilton et al., 1964). However, these comparisons indicate that basaltic pumices contain less structurally bound volatiles than the more sialic pumices.

A comparison between volatile concentrations in phonolitic matrix glass quenched at atmospheric pressure (low quenching pressure) and matrix glass from subaqueously extruded basalt (high quenching pressure) provides a helpful contrast. Byers et al. (1983) and Muenow et al. (1979) present volatile concentrations for andesitic and basaltic glasses which were quenched subaqueously (Table 18) at pressures of approximately 60 atm. The volatile results of Byers et al. (1983) and Muenow et al. (1979) are generally greater than concentrations measured in glasses quenched at low pressures, such as the matrix glasses in this report. The greater volatile concentrations of samples quenched under pressure are expected because solubilities generally increase with increasing pressure.

Analyses of fumarole gases are generally very similar to the Mount Erebus matrix glass analyses (Table 19). However, fumarole gas analyses which have been recalculated by Gerlach contain significantly greater concentrations of CO₂. A comparison of fumarole emissions and glass volatile concentrations would be highly informative if the bulk magma compositions of each volcano were similar. Volatile concentrations reported by Huntingdon (1973) and Giggenbach

TABLE 19

Selected gas composition analyses of rocks and fumarole emissions (mole %)

	H ₂ O	H ₂	CO ₂	CO	SO ₂	H ₂ S	S ₂	COS	HCl
Rock Analyses									
1	87.20	1.35	4.10	4.60	1.13	0.90	-----	0.21	0.03
2	93.66	0.41	2.07	0.62	-----	-----	0.88	-----	-----
Fumarole Analyses									
3	49.91	0.54	23.56	0.49	25.05	0.21	0.21	-----	-----
4	60.42	0.87	23.21	0.74	14.31	0.14	0.07	-----	0.21
5	71.28	2.09	19.42	1.17	4.91	0.82	0.28	0.015	-----
6	45.90	1.59	45.44	2.72	2.30	1.41	0.55	0.080	-----
7	81.98	2.77	9.79	0.71	3.15	0.64	0.13	-----	0.81
8	77.75	1.71	4.02	0.17	13.52	1.62	1.17	-----	-----
9	87.00	1.50	6.40	0.14	0.21	-----	-----	-----	-----
10	79.40	1.49	10.40	10.00	6.50	-----	3.40	0.009	0.42
11	86.16	4.70	6.47	0.36	1.84	-----	-----	-----	0.40
12	79.60	0.16	13.90	-----	4.82	1.51	-----	-----	0.11

Source

- 1) This study, 2) Shepherd (1938) sample 12, 3) Gerlach (1979),
 4) Gerlach (1980a) 5) Gerlach (1980b), 6) Gerlach (1980c), 7) Gerlach (1980d),
 8) Gerlach (1981), 9) LeGuern et al. (1982), 10) Giggenbach and LeGuern (1976),
 11) Sigvaldason and Elisson (1968), 12) Giggenbach (1975b).

and LeGuern (1976) are consistently depleted in H_2O by 10 mole% and enriched in CO_2 by 5 mole% compared to the phonolitic matrix glass averages. This suggests that fumarolic emissions are enriched in the less soluble gases, as expected. However, results presented by LeGuern et al. (1982) and Sigvaldason and Elisson (1968) are very similar to the phonolitic matrix glass results. The dilemma caused by these seemingly conflicting comparisons is partially resolved by plotting the matrix glass results on a diagram presented by Giggenbach (1975a,b). The average phonolitic matrix glass composition plots along the H_2O-CO_2, SO_2 mixing line (Figure 9) along with the results of 12 analyses of fumarolic gases. This comparison indicates that the analyses of Mount Erebus volcanic glasses provide representative volatile composition results. The CO_2 differences may be due to the type of activity and stage of degassing of the various volcanoes.

Mount Erebus inclusion glass volatile concentrations are similar to previously reported concentration results (Table 20). Anderson (1974) reports a range of 50 to 2800 ppm S and 100 to 2200 ppm Cl for basaltic and andesitic inclusion glasses. The inclusion glass concentrations presented in this report fall within these ranges. Anderson (1979) presents an adjusted H_2O concentration of 1.4~~1~~⁴ wt% for inclusion glass with an andesitic composition. However, the large error makes this comparison of little value.

Sommer (1977) reports concentrations and compositions for H_2O , CO_2 and CO using electron probe microanalysis and mass spectrometry. A comparison of the results from these two methods indicates that electron microprobe analyses give relatively higher and less accurate contents. However, rhyolitic inclusion glass volatile concentrations and compositions determined by mass spectrometry (Sommer, 1977) are also significantly greater than the phonolitic results (Table 20). The gas concentrations presented by Harris and Anderson (1983) for basaltic inclusion glasses are very similar to the phonolite results (Table 20) and were measured using a method similar the one used in this study. These inclusion glass concentration analyses indicate that the sialic magmas contain greater pre-eruptive volatile concentrations than the more mafic melts. The comparisons also indicate that the inclusion glass results presented in this report are probably representative of the volatiles in the magma chamber at the time of anorthoclase crystallization.

TABLE 20

Selected gas and volatile element concentration analyses
(ppm) of inclusion glasses

	H ₂ O	CO ₂	CO	SO ₂	S	Cl	F
1	-----	-----	-----	-----	100-2200	500-2800	-----
2	14000	-----	-----	-----	-----	-----	-----
3	33080	970	1730	-----	-----	-----	-----
4	2700	800	-----	-----	-----	-----	-----
5	2990	570	240	340	440*	1600*	-----

Source

- 1) Anderson (1974), Basalts and Andesites
- 2) Anderson (1979), Andesite
- 3) Sommer (1977), Rhyolite
- 4) Harris and Anderson (1983), Basalt
- 5) This study, Phonolite

* Concentrations determined by electron microprobe.

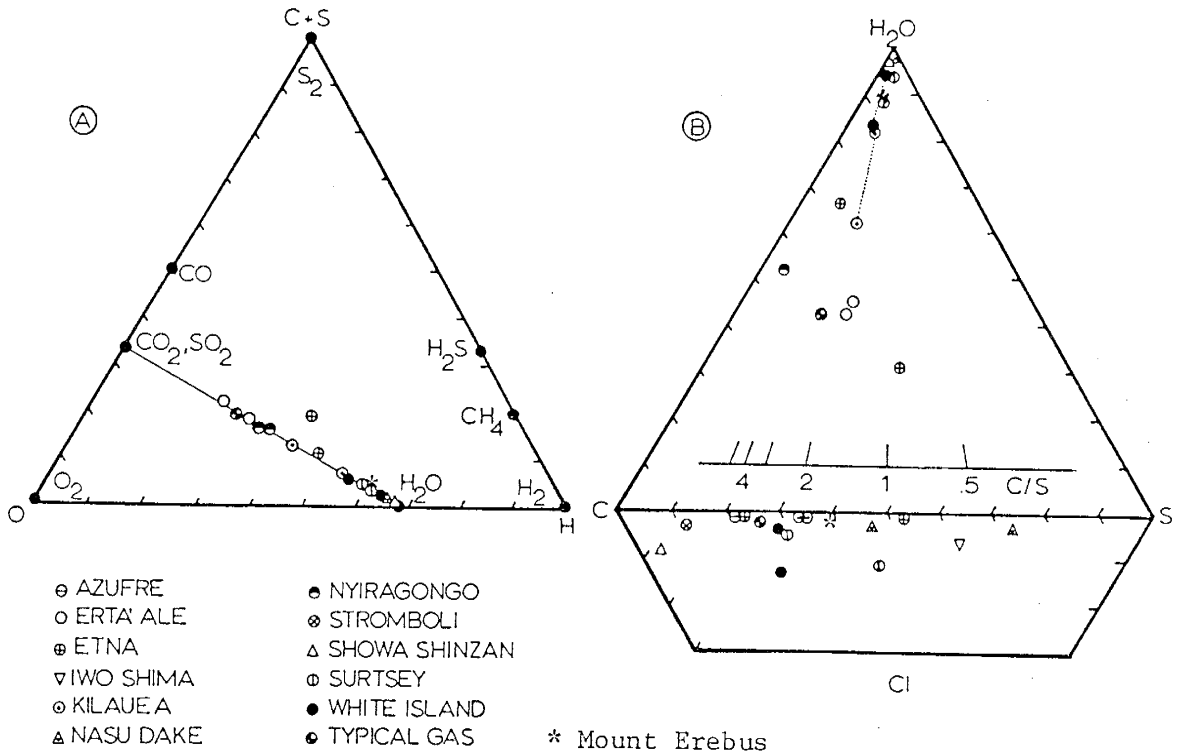


Fig. 9. A comparison of total O, H and (C+S) and C, S and H₂O from gas measurements taken at Mount Erebus and 12 other volcanoes. Ternary diagrams are from Giggenbach (1974a), plus averages from this report.

Magma Chamber Volume

The magma chamber volume was calculated using the method of Rose et al. (1982). The average inclusion glass S concentration of 440 ppm was used as the initial magma S concentration and the average whole rock S concentration of 260 ppm was used as the current bulk magma S concentration. The SO₂ flux of 230[±]90 tonnes per day, measured at Mount Erebus in November and December of 1983 (Kyle, private communication), was used in the calculations to represent the average flux over the time of degassing. This flux rate is significantly different from the 34.56 tonnes per day of SO₂ reported by Radke (1982). The following calculations provide minimum magma volumes which must be present to account for the observed SO₂ flux (Rose et al., 1982).

The density of the magma at 1 atm and 1000°C is probably near 2.5 or 2.6 g/cm³. A majority of the magma was assumed to be at a depth of 3 or 4 kms and therefore, a density of 2.7 g/cm³ was used. The presence of 20% anorthoclase phenocrysts may also increase the density. A period of 10 years was used as a minimum time of degassing because the Mount Erebus lava lake has been directly observed since 1972. Prior to 1972 the occasional observations indicate that passive degassing has been occurring since 1900. Alternatively, a minimum of 142 years of degassing may be assumed if constant degassing has

occurred since 1841 when Ross (1847) reported violent activity. The calculation assumes that no new magma or volatiles are introduced into the system.

The calculations in Table 21 indicate that the minimum volume of magma is about 1 km^3 if 10 years of degassing has occurred. Calculations indicate that for 20, 83 and 142 years of degassing, minimum volumes of 1.7, 7.2 and 12.2 km^3 , respectively, must be present to account for the observed SO_2 flux. Potential problems associated with these calculations are the initial and final S concentrations and the S flux rate. The initial S concentration of 440 ppm may be greater than the original bulk magma concentration due to diffusion problems (see Assumptions). The final S concentration of 260 ppm may be less than the final S concentration of degassed magma due to degassing of the bombs before quenching (see Assumptions). There are also problems associated with the use of data determined by different methods. The data used in the above calculation were determined by the following methods; initial S by electron microprobe analysis, final S by LECO titrimetric analysis and flux by remote correlation spectrometric analysis. Rose et al. (1982) indicates that these problems are minimized when S is used because S may be measured relatively accurately by various methods.

TABLE 21

Magma chamber volume calculations

Degassing of SO₂ at a constant rate of 230 tonnes/day was assumed for 10 years to calculate the sulfur produced by Mount Erebus.

$$\begin{aligned} \text{Sulfur produced } S_p &= (\text{Flux S}) \times (\text{Time}) \\ &= (4.2 \times 10^{10} \text{ g/y}) \times (10 \text{ y}) \\ &= 4.2 \times 10^{11} \text{ grams} \end{aligned}$$

$$\begin{aligned} \text{Using 440 and 260 ppm S as initial and final values;} \\ \text{Fraction of Degassing } D_f &= 1 - S_{\text{Final}}/S_{\text{Initial}} \\ &= 1 - 260/440 \\ &= 0.41 \end{aligned}$$

$$\begin{aligned} \text{Total S of the system is calculated using } S_p \text{ and } D_f; \\ \text{Total Sulfur } (S_t) &= (S_p)/(D_f) \\ &= 4.2 \times 10^{11} / 0.41 \\ &= 1.02 \times 10^{12} \text{ total grams S} \end{aligned}$$

$$\begin{aligned} \text{The weight of magma, with 440 ppm S, needed to produce } S_t \text{ is} \\ \text{calculated using } S_{\text{Initial}} \text{ and } S_t. \\ \text{Magma weight } M_w &= (S_t)/(S_{\text{Initial}}/1 \times 10^6) \\ &= 1.02 \times 10^{12} / (440/1 \times 10^6) \\ &= 2.32 \times 10^{15} \text{ grams} \end{aligned}$$

$$\begin{aligned} \text{The magma volume is calculated using } M_w \text{ and an estimated} \\ \text{density of } 2.7 \text{ g/cm}^3. \\ \text{Magma volume } (M_v) &= (M_w)/\text{density} \\ &= 1.62 \times 10^{15} / 2.7 \\ &= 8.6 \times 10^{14} \text{ cm}^3 = 0.9 \text{ km}^3 \end{aligned}$$

The 12.2 km³ volume estimate based on 142 years of degassing is considered an unrealistic volume. This indicates that the batch of magma that is presently degassing was emplaced less than 100 years ago. A volume of 2 km³ of magma, that is 41% degassed, is probably the best minimum estimate for a batch of magma, less than 100 years old, which has been degassing for a minimum of 20 years. Twenty years of degassing is used because a photograph taken in 1963, see Kyle et al. (1982), indicates that a lava lake was present 20 years ago. The 2 km³ volume represents totally degassed magma and therefore must be a minimum volume because the system is still degassing. Every additional year of degassing will increase the minimum volume by approximately 0.1 km³.

The calculation of total magma which convects through the feeder pipe (Table 22) indicates that approximately 1.24 km³ of magma moves through the feeder pipe in a year. This suggests that a magma volume of 2 km³ cycles through the system once every two years. A definitive volume estimate is not possible because the present bulk volatile content of the magma, structurally bound plus vapor phase volatiles, is not known. The structurally bound volatiles have been measured but there is no data which provides the concentrations of vapor phase volatiles in the magma which is recycled into the system after partially degassing.

Table 22

Total volume of magma convected through a 50m feeder pipe

The total volume of magma convected through an assumed 50 m diameter feeder pipe can be estimated using the calculated area of upwelling and an average convection rate. The average convection rate accounts for the difference of rates from the surface down to an axis point where the convection rate approaches 0.

The convection rate of the lava lake surface magma can be calculated using 3 time lapse photographs. Distances of movement were measured, from a reference point at 30 and 60 seconds.

<u>Time</u>	<u>Point 1</u>	<u>Point 2</u>
	<u>Movement</u>	
30 seconds=	4.0m	2.9m
60 seconds=	5.5m	5.0m

Convection Rate(CR)= 0.09 m/sec 0.08 m/sec

Convection Rate(CR)= 0.08 m/sec = 6912 m/day

The average convection rate is calculated from the surface convection rate by averaging the surface rate with a rate of zero. The zero convection rate represents the point in the feeder pipe where the rising magma starts moving downward after a negligible amount of horizontal movement.

$$\begin{aligned}
 \text{Average convection rate(ACR)} &= \text{CR}/2 \\
 &= 6912/2 \\
 &= 3456 \text{ m/day} \\
 &= 1.26 \times 10^6 \text{ m/year}
 \end{aligned}$$

The area of upwelling was calculated by assuming that half of the lava lake area is upwelling magma and the other half is downwelling.

$$\begin{aligned}
 \text{Area of Upwelling(AU)} &= \text{Area of Lava Lake}/2 \\
 &= \pi (25)^2/2 \\
 &= 982 \text{ m}^2
 \end{aligned}$$

Table 22 (continued)

The total volume of magma convected through the feeder pipe in a year is calculated using the average convection rate and the area of upwelling.

$$\begin{aligned} \text{Total Volume of Magma} &= (\text{AU}) \times (\text{ACR}) \\ &= (982)(1.26 \times 10^6) \\ &= 1.24 \times 10^9 \text{ m}^3/\text{year} \\ &= 1.24 \text{ km}^3/\text{year} \end{aligned}$$

This suggests that more than half of the total magma volume convects through the feeder pipe in one year.

Depth of Magma Chamber

The depth of the magma chamber may be approximately 3 to 4 km if the model for CO_2 in basalt, presented by Harris (1981) is valid for the Mount Erebus phonolite. Harris (1981b) presents apparent CO_2 solubility data for sea-floor quenched tholeiitic basalts and derives the equation $\text{CO}_2(\text{wt}\%) = 0.0005 + 0.059 P(\text{kb})$. Harris (1981b) states that the amount of CO_2 dissolved in H_2O -poor melt inclusions may be used to infer the minimum pressure at which individual phenocrysts have grown. Water and CO_2 concentrations of Mount Erebus inclusion glasses are very similar to those presented by Harris but the magma compositions are very different. Because the magma compositions are different the use of Harris's equation, to estimate the depth of phenocryst growth, is not totally valid.

Convection Models

The Mount Erebus lava lake is the only directly observable source of data from which the magmatic system may be modeled. Convection patterns indicate that the feeder pipe which supplies the lava lake and Active Vent may be larger than the Lava Lake itself. Geophysical data (Kienle et al., 1983) indicates that there is probably one feeder pipe, directly beneath the crater, which connects the lava lake and the magma chamber.

The simplest model, which explains the observations and data, is for volatile-rich magma to move from the magma chamber up a cylindrical feeder pipe to the lava lake where degassing and subsequent recycling occur. Fluid inclusion homogenization temperatures indicate that the melt is approximately 980 to 1030°C (Clocchiatti et al., 1976). The magma in the chamber is probably a homogeneous convecting body which is only heterogeneous in the sense that cool degassed magma returning to the magma chamber may not instantly mix with the hotter volatile-rich magma. Constant magma chemistries, volatile element concentrations and gas compositions combined with slowly declining gas concentrations indicate that the magma system is closed, homogeneous and slowly degassing.

Turner et al. (1983) proposes that high level low pressure environments, such as the Mount Erebus magma chamber, are the most likely systems to have stratified magma chambers. They propose that high temperature mafic magma injected into the magma chamber may be denser than the lower temperature differentiated magma. This results in a stratified system in which the two magmas co-exist with little or no chemical interaction (Turner et al., 1983). This model is compatible with the knowledge of Mount Erebus but there is no evidence that suggests that this model is more reasonable than the simpler model. However, Turner et al., (1983) indicate that cooling and volatile exsolution should eventually result in mixing and violent volatile release. If the Mount Erebus magma chamber is stratified one would expect that a violent eruption would occur in the near geologic future.

The feeder pipe is probably very similar to the pipe systems described by Carrigan (1983) who describes a magma-filled conduit which is kept open by forced convection of magma from a source chamber. The heat of the convecting magma must offset the heat loss to the wall rocks (Carrigan, 1983), and to the atmosphere in the Mount Erebus case, if the conduit is to remain open. Degassed magma moving downward will cool and possibly impair the convection system if the heat of the upward moving magma does not balance the heat loss (Carrigan, 1983). The persistent lava

lake at Mount Erebus indicates that there is a very large hot heat source suppling the Mount Erebus system, possibly a mantle plume.

The affects of bubble formation combined with heat differences probably drive the magma convection system by lowering the density of the relatively hot volatile-rich magma. Blackburn et al. (1976) indicates that CO₂ bubbles nucleate first, probably in the magma chamber or the lower portions of the feeder pipe, providing an easy site for exsolution of the more soluble volatiles as the magma rises and becomes saturated with the S gases then H₂O. Viscous drag of rising bubbles may contribute to convection at high pressures but Sparks (1978) indicates that the bubbles will eventually saturate the melt causing differential movement to be virtually impossible. The buoyant affect and the decreased density caused by the bubble formation plus the heat of the magma should continue the upward convection of the melt. As the magma rises, gases should continue to diffuse into the bubbles, even after growth has ceased due to the interference of neighboring bubbles, until equilibrium between the melt and vapor is attained (Sparks, 1978) or the magma is erupted. When the magma approaches the surface explosive decompression of large bubbles occurs (Sparks, 1978), resulting in the characteristic strombolian eruptions of the Mount Erebus lava lake. Scoriaceous bombs collected from the Mount

Erebus crater rim are very similar to the scoria described by Blackburn et al. (1976) as fragments of gas rich vesiculated magma which has been torn apart by the explosions of large bubbles. Scoriaceous bombs collected from the rim of the Mount Erebus crater are probably fragments of magma from the explosive decompression of large bubbles in the Active Vent. Confining pressures in the lava lake are probably only great enough to hurl magma fragments to the Main Crater floor.

The degassed magma is recycled back into the magma system. Calculations using a lava lake convection rate of 0.04 meters per second indicate that 25 km³ of magma has cycled through the feeder pipe in the last 20 years. It is difficult to quantify the number of times the magma has cycled but it is obvious that the system is convecting sufficiently to continuously mix and homogenize the magma. The uniform composition of ejecta and the possible decline in volatile concentrations of the magma, during the last 10 years, are easily explained by homogenization of the magma. The convection would also provide the mechanism needed to provide the heat to keep the feeder pipe and lava lake open and convecting for the last 10 years.

Conclusions

- 1) Matrix glass gas concentrations and compositions are residual volatiles which represent concentration and compositions very near those of solubility at 1 atm and 1000°C. The decreasing concentration trends, from 1972 to 1982, of H₂O and CO₂ in matrix glasses probably reflect an overall decline of volatiles in the magma chamber.
- 2) Inclusion glass gas compositions are representative of the volatiles in the melt at the time of anorthoclase crystallization. The compositions indicate that the pre-eruptive magma was CO₂ depleted or that the anorthoclase phenocrysts crystallized at a shallow depth in the feeder pipe.
- 3) The Mount Erebus magma system has been a closed convecting body of homogeneous magma, driven by a large hot heat source, from 1972 to 1982. The magma chamber is approximately 3 to 4 km deep and has a minimum volume of 2 km³. The magma is convecting at a rate sufficient to offset heat losses and therefore the lava lake remains open and active.

APPENDIX A

Equipment and Manufactures

Thermocouple Indicator DS-520	Doric
High Vacuum Teflon Valves with Vitron O-rings	Kontes Glass Co.
Ultra-Torr Fittings	Cajon
Glass/Metal Transition Tube (Stainless Steel)	Cajon
Nupro Needle Valve	Nuclear Products Co.
Gold Seal Ultra-High Vacuum Valves, Series 201	Varian
Flanges MDC MFG	Varian
Baratron 220 BHS-2Al-A-10 Pressure Transducer	MKS Instruments Inc.
LED Pressure Indicator	
Gauge Controllers, Series 260	Granville-Phillips
Hewlett Packard 85 Computer	Hewlett Packard
Inficon IQ200 Quadrupole with electron multiplier and Control Unit	Leybold-Heraeus Inc.
Oil Diffusion Pumps	
Duo-Seal Vacuum Pumps, Model 1400	The Welch Scientific Co.
Vac Ion Pump, Model 921-0015	Varian
Key Zeolite Traps	High Vacuum Prod. Inc.
Stable-Therm Gravity Oven	Blue m ELeetric Company
Jaw Crusher Model 150	Lemaire Instruments
Pulverizer Model 100	Progressive Expl. Prod.
Mechanical Agate Mortar and Pestle	Fisher Scientific

APPENDIX B

Mount Erebus

Geologic Setting

Mount Erebus (latitude $77^{\circ} 35'S$, longitude $167^{\circ} 10'E$) is the southern most active volcano in the world. It is the only active and the largest of four volcanoes which form Ross Island, Antarctica. Ross Island is located in McMurdo Sound just off the mainland along the Transantarctic Mountains (Figure 1). Mount Erebus is a 3794 m composite volcano which is capped with a slightly elliptical Main Crater which is approximately 600 meters in diameter. The Main Crater floor is from 100 to 160 meters below the crater rim. An Inner Crater is located at the north end of the Main Crater (Figures 2,3). The Inner Crater is approximately 250 meters in diameter and 100 meters deep and contains an active persistent convecting anorthoclase phonolite lava lake. The lava lake is at least 10 years old and may have been periodically present for the last 142 years (Kyle et al., 1982). Several high temperature fumaroles are on the Inner Crater floor adjacent to the lava lake.

Mount Erebus is composed predominantly of anorthoclase phonolite which sets it apart from the other three volcanoes which form Ross Island. Mounts Bird, Terra Nova and Terror

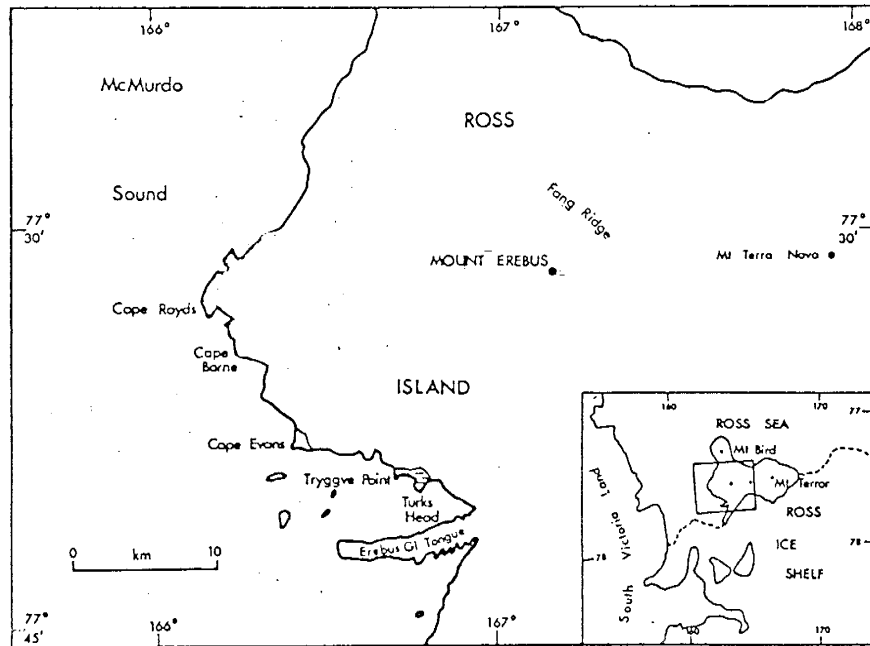
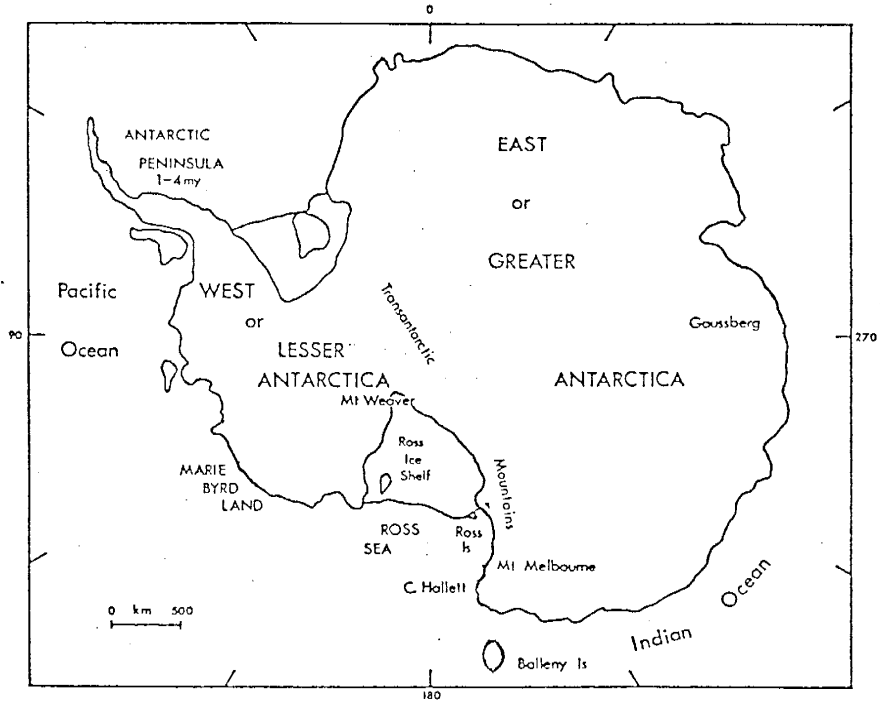


Fig. B1. Maps of Antarctica, Ross Island and Mount Erebus.

are predominately basanites with minor kaersutites and pyroxene phonolites (Kyle, 1976). The anorthoclase phonolite magma has been described by Kyle and Rankin (1976) and Sun and Hanson (1976) as a product of fractional crystallization of a mantle-derived basanitic melt. Phonolite is thought to be a 20 percent residual liquid of the basanitic melt which in turn is a 1 to 10 percent partial melt of a parental mantle garnet lherzolite. Mount Erebus is part of the Erebus volcanic province (Kyle and Cole, 1974) of the McMurdo Volcanic Group (Harrington, 1958; Nathan and Schulte, 1968). Radiometric dates suggest that Mount Erebus is approximately one million years old (Treves, 1967; Kyle, 1976 and Armstrong, 1978).

Previous Activity

Mount Erebus has been in a semi-constant state of activity since James Ross discovered it in 1841. The activity in 1841 was described by Ross (1847) as a major eruptive event. He reported great quantities of flame and smoke as well as possible streams of lava issuing from the summit. The subsequent activity of Mount Erebus is characterized by a persistent volcanic plume and occasional strombolian eruptions. Infrequent observations made between 1841 and 1956 indicate that activity has been at least periodic and possibly constant since 1841. In 1900, 1901 to 1904, 1908, 1912, 1915, and 1935 clouds of steam and gas

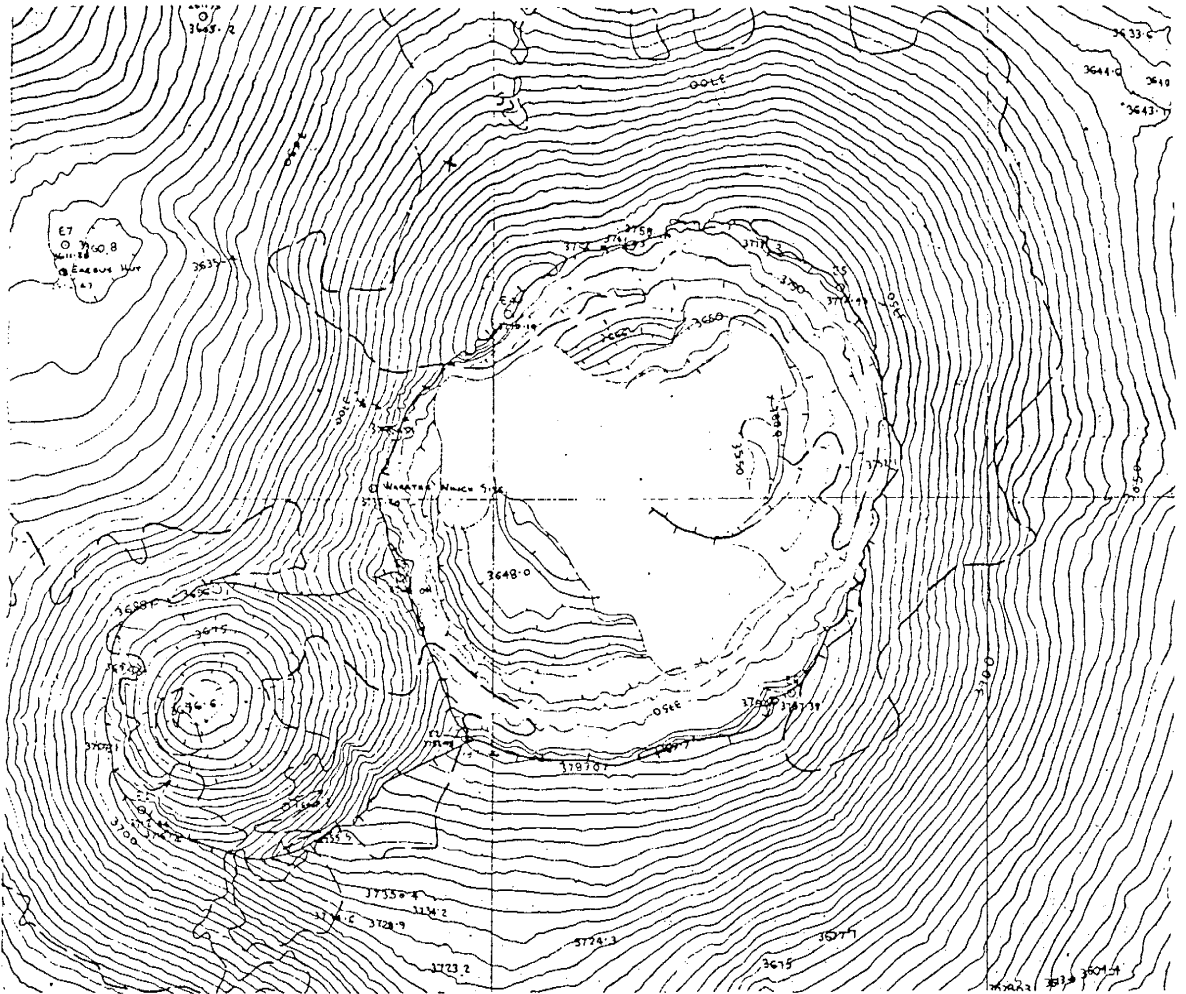


Fig. B2. Topographic map of Mount Erebus, 5 meter contours.

have been reported by Ferrar (1907), David and Priestley (1909), Priestley (1913), Shackleton (1919), Byrd (1935) and Scholes (1953). Descriptions of volcanic activity during 1908 (Shackleton, 1909 and Murray, 1909) and 1912 (Priestley, 1913) indicate that strombolian eruptions were occurring. Frequent observations of Mount Erebus made between 1956 and 1976 indicate that no significant changes in activity have occurred during this period of time (Kyle et al., 1982). Kyle et al. (1982) presents a more detailed review of reported observations between 1841 to 1974.

Present Activity

The lava lake, first observed in 1972 (Giggenbach et al., 1973), and the Active Vent are the focal points of volcanic activity at Mount Erebus. Before 1972 the history of the lava lake is not well known. Kyle et al. (1982) present an aerial photograph of the crater, taken in 1963, which suggests that the lava lake may have existed then. Development and activity of the lava lake from 1973 to 1976 has been described by Kyle et al. (1982) and Kienle et al. (In Press). The lava lake has grown from small hornitos in 1972 to approximately 50 meters in diameter in 1976. Since 1976 the size, shape and behavior of the lava lake has remained fairly constant.

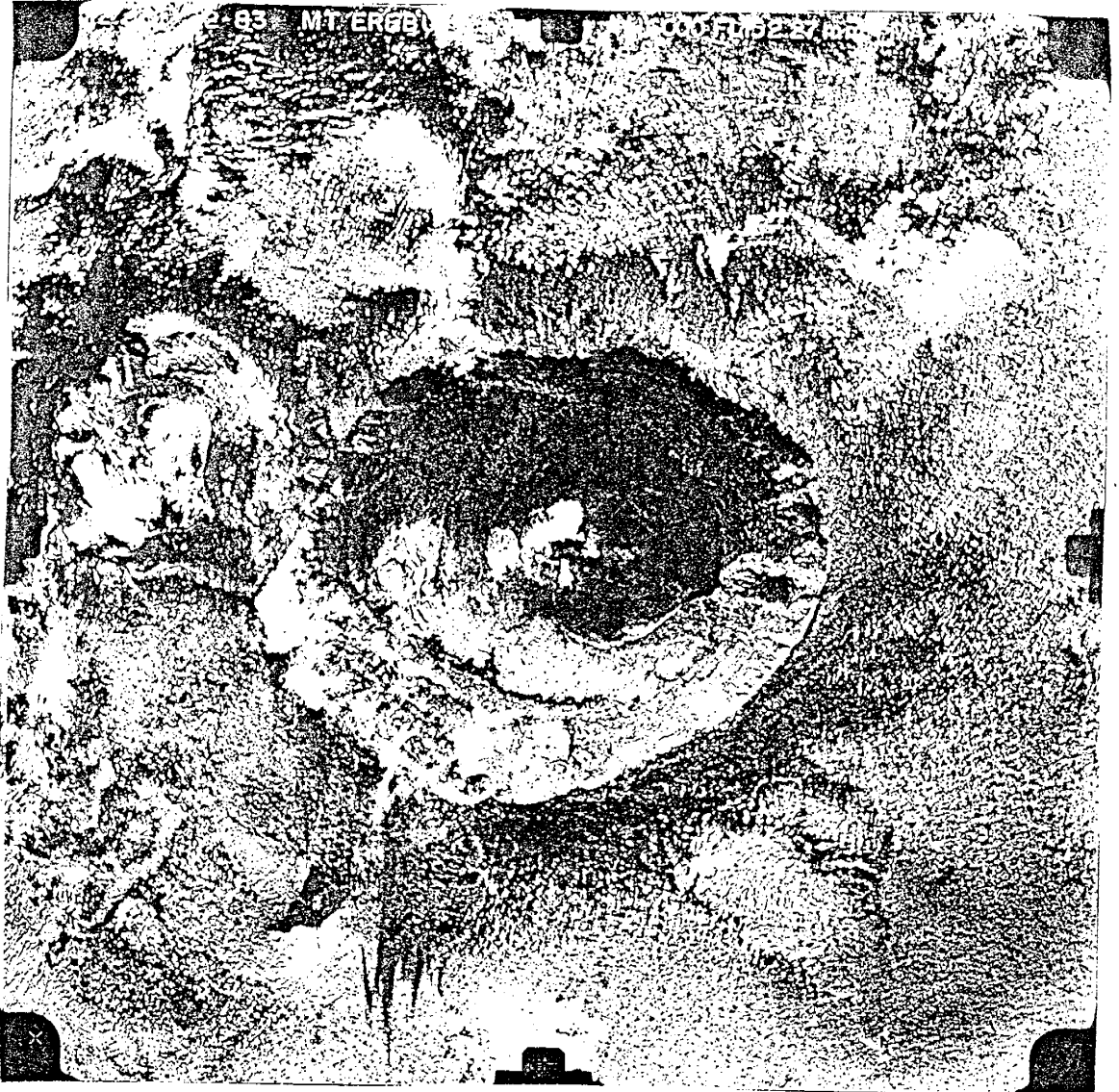


Fig. B3. Aerial photograph of Mount Erebus taken in December, 1983.

The following is a description of lava lake development and behavior as presented by Kyle et al. (1982). Private communication with Kyle has resulted in some minor modifications. In 1973-1974 the patches of lava described by Giggenbach et al. (1973) had developed into a lava lake 40 meters in diameter. Viscous lava was observed flowing from a small vent about 0.5 to 1 meter in diameter. A flow rate of about 0.01 to 0.03 meters per second was estimated for the 35 meter long, 5 meter wide flow. Observations in 1974-1975 indicate that the lava lake had increased to a size of 60 meters long and 15 to 20 meters wide. Two main sources of lava upwelling were reportedly located at the northern side of the lava lake. Magma flowed at an estimated rate of 0.04 meters per second along a curved path to a tunnel-like opening at the southern end of the lava lake. The moving surface was described as partly incandescent. Semicircular in outline, the lava lake was about 60 meters in diameter in 1975-1976. Kyle and Giggenbach (1976) reported that the lava lake filled the northern half of the Inner Crater. The partly solidified lava lake crust was reportedly broken by numerous disturbances which revealed incandescent material and most of the lava lake surface showed signs of vigorous random convection. In 1976 a lava lake temperature of 1000°C was measured using an optical pyrometer. The 1976-1977 observations indicate that the lava lake behavior and shape

had not changed significantly since 1975-1976. The only significant change observed in 1976-1977 was the obvious absence of explosive eruptions (Kyle and Giggenbach, 1976). An average of approximately 2 long drawn out whooshing explosions per day were heard.

During the years from 1976 to 1982 the lava lake was a stable convective system (Kyle, 1980). Observations of the lava lake in 1977-1978 described the lake as the same semicircular shape, 60 meters long, with an olive green crust (Kyle, 1977b). Kyle (1977b) reports little convective movement while Scott (1978) reported 2 zones of upwelling. Scott (1978) also reported 2 to 6 moderate strombolian eruptions per day. During the 1978-1979 field season observations made by Kyle (1978) indicate that the size and shape of the lava lake were the same while strombolian activity seemed to have decreased. However, two small congealed flows from a nearby vent were observed. Observations made by Kyle (1979) during a second trip to Mount Erebus in 1978-1979 indicate that an average of 1.6 eruptions per day occurred. In 1979-1980 Kyle (1980) reported that the lava lake was very similar to that of previous years except that it seemed to be lower. Kyle (1980) observed a small bench with 5 fumaroles on it. The bench indicates that the lava lake had dropped by 3 to 5 meters (Kyle, 1980). Convective upwelling about a third of the distance from both ends of the lava lake varied from

moderate and quiet to rapid and noisy (Kyle, 1980). About 2 explosive eruptions per day come from the nearby Active Vent (Kyle, 1980). Keys (1980) has described, in detail, the persistent plume associated with the eruptive activity. During the 1980-1981 field season the lava lake was the same as described in previous years except for an increase in activity (Kyle, 1981). Small strombolian eruptions averaged 2 to 6 per day (Kyle, 1981). Long drawn-out roars and occasional sharp explosions were associated with the eruptions (Kyle, 1981). Kyle (1982) describes the 1981-1982 lava lake as similar in size, shape and behavior as reported in previous years. Strombolian eruptions averaged 4 to 6 per day and probably originated from the Active Vent (Kyle, 1982). The number of fresh bombs found on the main crater rim indicate that the 1981-1982 eruptions were the strongest to occur in 3 years.

The Active Vent is probably the source of eruptions which have thrown most of the bombs to the crater rim. The Active Vent is first mentioned by Treves and Kyle (1973) as a vent from which a small ash eruption occurred on February 4, 1973. Kyle et al., (1982) indicates that the only volcanic ejecta observed in 1973 were around a small fumarole vent in the southwestern sector of the Inner Crater. During 1974 eruptions were closely observed and categorized as weak, medium and strong (Kyle et al., 1982). Weak to medium strombolian eruptions occurred in the lava

lake whereas medium to strong eruptions were believed to be typical of the Active Vent (Kyle et al., 1982). The vent observed in 1973 had become, what is now called the Active Vent. The Active Vent seems to have remained essentially the same from 1974 to 1982 with some variation in activity. Kyle and Giggenbach (1976) reported that there was very little activity during 1976. In 1979 Kyle (1980) reported that approximately 2 eruptions per day from the Active Vent. The activity of the Active Vent seems to have increased during 1981 as noted before by Kyle (1982).

Field Work

Observations of the lava lake and Active Vent at Mount Erebus were made in December, 1982 during the 1982-1983 austral summer. The lava lake and Active Vent were essentially the same as reported in preceding years. Lava was upwelling at the northern end of the lava lake and flowing to the southern end where it was being subducted beneath partly solidified crust. Small incandescent patches of magma were regularly observed as small bubbles disturbed the thinly crusted surface of the lava lake. Degassing was normally quiet as the small bubbles broke the surface. Keys (1980) attributes quiet degassing to slow convection. Louder roaring sounds typical of strombolian eruptions (Blackburn et al., 1976) were heard 1 to 4 times a day. These loud eruptions are believed to be associated with the

Active Vent or lava lake when unusually large bubbles degas. The duration of the loud roaring or whooshing would last from 3 to 20 seconds. Clouds of steam and gas were emitted in variable quantities, resulting in a persistent plume which varied from an occasional light blue or grey whisp to a more common thick white columnar cloud.

In December, 1982 fewer fresh bombs were thrown to the main crater rim compared to previous years. The scarcity of bombs supports the belief that Mount Erebus was relatively inactive during the 1982-1983 field season. However, many fresh bombs were observed on the Main Crater and Inner Crater floors. This seems to indicate a low intensity but average frequency of volcanic activity. The few fresh bombs which were found on the main crater rim probably came from the Active Vent. Fresh bombs were distinguished from older bombs by their dark color and resinous luster. The highly scoriaceous bombs were composed of dark olive green to black glass with rhombic anorthoclase phenocrysts. Fresh bombs were typically less than a meter in length and had an irregular slightly flattened shape. Older bombs, showing obvious signs of acidic alteration, varied in size and shape.

A majority of the samples were collected from the northeast to east sides of the main crater rim (Figure 3) because prevailing winds blew from the west. Bombs were

(100)

found at the very edge of the main crater rim to
approximately 30 meters down slope.

APPENDIX C

Previous Studies of Volcanic Volatiles

A variety of methods and techniques have been employed to identify and measure magmatic volatiles. Three major factors must be considered when comparisons of data are made; the method of sample acquisition, the method of analysis, and the physical and chemical properties of the magma.

Collection of volcanic gases from fumaroles and volcanic vents is one of the most direct methods of studying magmatic volatile compositions (Nordlie, 1971). However, these studies, which commonly utilize the evacuated bottle technique, are prone to contamination and other serious problems (Shepherd, 1938; Nordlie, 1971; Huntingdon, 1973; Giggenbach, 1975a; Graham, 1978; Graeber et al., 1979 and LeGuern et al., 1982). Another method which has been utilized in the attempt to obtain uncontaminated volatile samples, is the extraction of gases and volatile elements from rapidly quenched volcanic rocks. Eichelberger and Westrich (1981) state that the most direct means of determining magmatic volatile concentrations is to analyze rapidly quenched magmatic materials which have undergone very limited degassing. This method of measuring magmatic volatiles also has many potential problems which are described by Shepherd (1938), Roedder (1972), and Graham

(1978). The extraction and analysis of volatiles from rapidly quenched volcanic rocks by Moore (1965, 1979), Moore and Fabbi (1971), Muenow (1973), Killingley and Muenow (1975), Chaigneau et al. (1980), Eichelberger and Westrich (1981) and Byers et al. (1983), has provided volatile concentrations and compositions which reflect various stages of melt degassing. A likely source of relatively undegassed magmatic volatile concentrations and compositions is glass inclusions in phenocrysts and rocks. Studies of volatiles in inclusion and matrix glasses are described by Piperov and Penchev (1973), Anderson (1974), Watson (1976), Sommer (1977), Delaney et al. (1978), Garcia et al. (1979), Muenow et al. (1979, 1980), Harris (1981), LeGuern et al. (1982), and Harris et al. (1983). Anderson (1975) indicates that gases with low solubilities will dominate the vapor phase of the magma at high pressures, whereas vapor phases issuing from fumaroles at relatively low pressures are more representative of the original melt. Therefore, the gases in fluid inclusions, within glass inclusions, represent only the vapor phase volatiles which are insoluble in the high pressure environment of entrapment. An analysis of both fluid inclusion and structurally bound volatiles in glass inclusions, however, should provide volatile concentrations and compositions representative of the pre-eruptive magma.

A second variable which must be considered when contrasting analyses of magmatic volatiles is the method of analysis. Gas chromatography (Naughton et al., 1963; Graber et al., 1979; LeGuern et al., 1982 and Greenland, 1984), leachate (Stoiber et al., 1981), electron microprobe (Watson, 1976; Sommer, 1977 and Anderson, 1979) and mass spectrometer (Huntingdon, 1973; Muenow, 1973; Killingley and Muenow, 1975; Giggenbach and Leguern, 1976; Delaney et al., 1978; Graham, 1978; Garcia et al., 1979; Muenow et al., 1979, 1980; Chaigneau et al., 1980; Eichelberger and Westrich, 1981; Harris, 1981 and Palin, 1983) methods have been used to analyze volatiles. Harris (1981) has reported agreement when more than one method was used, but also points out inconsistencies and proposes explanations for the observed differences. Due to the multitude of variables involved in comparing analyses of magmatic volatiles, it is difficult to measure the comparability of methods. A critical comparison of these methods is beyond the scope of this study and will not be attempted.

The third complicating factor which must be considered is the chemical composition of the magmas. Magmas with different chemical compositions have different volatile solubilities and mechanisms of volatile retention. Volatile analyses of basaltic rocks and magma emissions are relatively numerous and have been presented by Shepherd (1938), Sigvaldason and Elisson (1968), Huntingdon (1973),

Muenow (1973), Killingley and Muenow (1975), Giggenbach and LeGuern (1976), Delaney et al. (1978), Graham (1978), Garcia et al. (1979), Graeber et al. (1979), Muenow et al. (1979, 1980), Chaigneau et al. (1980), Harris (1981), Byers et al. (1983) and Greenland (1984). In comparison, volatile analyses of andesitic (Shepherd and Merwin, 1927; Shepherd, 1938; LeGuern et al., 1982 and Byers et al., 1983) and rhyolitic (Shepherd, 1938; Sommer, 1977 and Eichelberger and Westrich, 1981, 1982, 1983) glasses and magma emissions are rare.

Data from a majority of these studies are in agreement that H_2O is the dominant volatile. The only other commonly abundant volatile is CO_2 . Other gas species which have been generally reported in minor quantities are CO , H_2 , He , Ar , N_2 , SO_2 , H_2S , CS_2 , HCl , HF and CH_4 . LeGuern et al. (1982) states that only a fraction of the several hundreds of published gas analyses are of sufficient quality to be applied to solving certain problems related to volcanic systems. Contamination, oxidation, condensation, reevaporation and chemical reaction are causes of inaccuracies (LeGuern et al., 1982). Giggenbach and LeGuern (1976) and Gerlach (1979; 1980a,b,c,d;1981) have shown that some analyses are amenable to recalculation and restoration to correct for the inaccuracies caused by the sampling and analytical problems. However, they qualify their results by stating that restored analyses are only more accurate

approximations. Gerlach (1980b) describes his restoration method as an iterative numerical procedure based on thermodynamic calculations to produce agreement between the adjusted analyses and equilibrium distributions in the collection temperature range. Several restored analyses are listed in Table 14. A significant result which has been elucidated and supported by Gerlach is that CO_2 is probably an important volatile in magmas prior to eruption. Studies on CO_2 solubility (Heald et al., 1963; Kadik and Lukanin, 1973 and Mysen et al., 1975, 1976) in magmas indicate that this hypothesis is plausible. This is especially true for alkali basaltic magmas and their derivatives. Mysen (1983) suggests that high CO_2 activity is important in the genesis of highly alkalic, silica-deficient magmas during partial melting of the mantle. This suggests that the Mount Erebus phonolitic magma, which is alkalic and silica-deficient, should have had a high preeruptive CO_2 content.

Chemical equilibria studies, of volatiles at magmatic temperatures, have also been presented in the literature. Ellis (1957) studied several hypothetical systems which he compared favorably to the data presented by Shepherd (1938). Matsuo (1962) also used data from Shepherd (1938) to examine chemical reactions of gases. Changes in equilibrium compositions of gases with temperature and pressure were modelled by Heald et al. (1963) and Gerlach and Nordlie

(1975a,b,c) using the C-S-H-O gaseous system. Heald et al. (1963) also calculated an equilibrium mixture of gases for a pre-eruptive magma but noted that the use of equilibrium data only allowed the attainment of a general volatile composition which only reflected what the real composition might be.

Volatile Solution Mechanisms

Introduction

Volatile components in silicious melts may be present in either a molecular or a dissociated form. Most of the information regarding mechanisms of solution come from solubility studies using thermodynamic modelling. It is important to understand the distinction between total, molecular and dissociated volatile components (Appendix A). Volatile concentrations and compositions reported in this study refer to total components regardless of their form in the glass or form of release. An understanding of the solution mechanisms and volatile solution species in silicious melts is helpful when interpreting volatile concentrations and composition data.

H₂O

The most important volatile, H₂O, is probably present in magma in both dissociated and molecular forms. Mysen (1977) states that H₂O appears to initially enter silicate melts by forming hydroxyl groups through interaction with bridging oxygens. Hamilton et al. (1964), Burnham (1967; 1975a,b; 1979a,b) and Watson (1978, 1981) also present evidence that H₂O molecules react with oxygen ions, that bridge adjacent (Al,Si)O₄ tetrahedra, to form hydroxyl ions. Additional H₂O in the melt may result in further decoupling of polymers and possibly the entry of molecular H₂O (Mysen, 1977). Burnham (1975a,b) postulates that adding water to melts with tetrahedrally coordinated trivalent ions, such as Al³⁺, involves the exchange of a proton between H₂O and a non-tetrahedrally coordinated cation that must be present to balance the net charge on the AlO₄ group. Stolper (1982) states that the thermodynamic modelling presented above successfully predicts some H₂O solubilities but that it is inconsistent with a considerable body of data that demonstrates that both hydroxyl groups and molecular H₂O are present in silicate glasses. Thermodynamic models by Stolper (1982) indicate that hydroxyl ions are the dominant form of H₂O in silicate melts with low H₂O concentrations while molecular H₂O is dominant when total H₂O concentrations are greater than 4.5 wt.%. Mysen (1983) again contends that water dissolves as hydroxyl groups. In

an attempt to resolve this disagreement McMillan et al. (1983) conducted a Raman spectra study and concluded that molecular water is present in glasses. Resolution of this dispute is not necessary for the purposes of this study because both models predict that hydroxyl ions are the dominant form of H₂O in Mount Erebus glasses.

H₂S, HCl and HF

The volatiles H₂S, HCl and HF are considered to be similar to H₂O in that they are hydrolyzed (Burnham, 1975b; 1979a,b) and are therefore present in silicious melts in a dissociated form. Ionic size determines their relative solubilities (Burnham, 1975b).

CO₂

The second most abundant volatile, CO₂, lacks the ability to hydrolyze with bridging oxygens (Burnham, 1975b; 1979a,b) and is present in melts as molecular CO₂ and CO₃²⁻ (Mysen, 1976 and Mysen et al., 1976). Molecular CO₂ enters vacancies in silicate melts while CO₃²⁻ formation is related to the degree of polymerization of the melt (Mysen, 1976). A relative increase in CO₃²⁻ abundance, with respect to molecular CO₂, occurs in the presence of H₂O, because H₂O will depolymerize a melt (Mysen, 1976). Total solubility of CO₂ is enhanced by the presence of H₂O (Burnham, 1979).

Mysen (1976) qualifies this statement by suggesting that CO_2 solubility increases and passes through a maximum when all bridging oxygens associated with exchangeable cations have been substituted with hydroxyl groups. A decrease in CO_2 solubility occurs after this maximum because increasing H_2O activity decreases the CO_2 activity (Mysen, 1976).

Molecular CO_2 appears to be the dominant form of CO_2 in silicious melts (Burnham, 1975b; Mysen, 1976 and Kadik et al., 1981) whereas CO_3^{2-} may be the dissolved form of CO_2 at high pressures and temperatures Mysen (1983).

Others

All volatiles which lack the ability to hydrolyze with the melt will probably be present mainly in the molecular form (Burnham, 1975b). The solubilities of these gases will be controlled by an inverse relationship with the degree of melt polymerization (Burnham, 1975b). The volatiles SO_2 (Burnham, 1979b), H_2 (Burnham, 1979b and Holloway, 1981), CO (Eggler et al., 1979) and CH_4 (Holloway, 1981) are probably dissolved in the melt as molecules.

APPENDIX D

List of Samples and Analyses

Sample Number	Year	GAS		CHEM.		VOL.ELE		WATER P
		MG	IG	MG	WR	MG	WR	
25726	Old Bomb	-	-	-	X	-	-	-
25724	1972-1973	X	-	X	X	X	X	-
25721	1974-1975	-	-	X	X	X	-	-
2E2	1974-1975	X	X	X	-	X	-	X
2E6	1974-1975	-	-	X	X	-	-	-
25723	1975-1976	X	X	X	X	X	X	-
77015	1977-1978	X	X	X	X	X	-	-
77016	1977-1978	-	-	X	X	-	-	-
78003	1977-1978	-	-	X	X	X	X	-
78004	1977-1978	-	-	X	X	-	-	-
78200	1978-1979	-	-	X	X	X	-	-
78325	1978-1979	X	-	X	X	X	X	X
78327	1978-1979	-	-	X	-	-	-	-
79301	1979-1980	X	-	X	-	X	X	X
79302	1979-1980	-	-	X	-	X	-	-
80300	1980-1981	-	-	X	-	-	-	-
81003	1980-1981	X	X	X	-	X	X	X
81005	1980-1981	-	-	X	-	X	-	-
81405	1981-1982	-	-	-	-	-	X	-
81410	1981-1982	X	-	-	-	X	X	-
82418	1982-1983	X	-	-	-	X	X	-
82420	1982-1983	-	-	-	-	-	X	-

WR-Whole Rock
 MG-Matrix Glass
 IG-Inclusion Glass
 P- Penfield method

X analysis
 - not analyzed

CHEM- Chemical analysis
 VOL.ELE- Volatile element

Gas Data

Table D1

Individual gas concentration analyses (ppm)

Sample	1	2	3	4	5	6	7
Gas	6260	4500	4000	3400	4780	4190	3990
H ₂ O	5130	3550	2950	2420	3820	3040	3410
H ₂	4	tr	5	6	3	6	3
CO ₂	557	383	595	633	423	604	515
CO	260	392	302	174	218	274	1998
SO ₂	194	72	58	46	207	183	146
H ₂ S	38	59	64	84	50	13	65
COS	44	n.d.	16	9	40	50	31
CS ₂	n.d.	3	7	6	n.d.	8	3
C ₂ H ₄	5	n.d.	4	4	5	3	4
CH ₄	25	22	2	7	11	16	12
HCl	2	n.d.	1	2	2	3	2
N ₂	n.d.	19	n.d.	n.d.	4	n.d.	5
Ar	tr	tr	tr	n.d.	tr	tr	tr
He	n.d.	tr	tr	tr	tr	tr	tr

Recalculated element concentrations (ppm)

O	5226	3686	3254	2741	3941	3400	3594
H	584	403	338	282	434	349	389
C	295	289	301	258	229	308	244
S	156	94	103	112	172	136	152

n.d. = not detected

tr = trace

#	Sample
1.	25724(125)
2.	25724(250)
3.	2E2(125)
4.	2E2(250)
5.	25723(125)
6.	77015(125)
7.	77015(250)

() = Grain size in mesh

Table D1 (continued)

Individual gas concentration analyses (ppm)

Sample	8	9	10	11	12	13	14
Gas	3530	3110	2760	5390	3030	2570	3130
H ₂ O	2920	2490	2210	4420	2420	2030	2490
H ₂	3	10	10	tr	tr	3	9
CO ₂	287	111	189	276	146	164	200
CO	122	179	184	579	255	170	164
SO ₂	45	231	83	n.d.	140	150	175
H ₂ S	104	49	38	99	37	38	44
COS	26	13	13	n.d.	14	2	25
CS ₂	8	8	5	n.d.	3	2	8
C ₂ H ₄	4	tr	1	1	1	1	3
CH ₄	4	7	11	8	8	9	14
HCl	1	2	2	7	1	1	2
N ₂	9	8	6	n.d.	7	n.d.	n.d.
Ar	tr	tr	tr	tr	tr	tr	n.d.
He	tr	tr	tr	tr	tr	tr	tr

Recalculated element concentrations (ppm)

O	2900	2512	2253	4457	2465	2102	2552
H	335	291	261	500	273	233	292
C	143	116	143	330	146	126	144
S	140	175	89	93	114	113	148

n.d. = not detected

tr = trace

#	Sample
8.	78325(125)
9.	78325(250)
10.	79301(125)
11.	79301(250)
12.	81003(125)
13.	81003(250)
14.	81003(125)

() = Grain size in mesh

Table D1 (continued)

Individual gas concentration analyses (ppm)

Sample	15	16	17	18	19	20	21
Gas	2930	3800	3050	3390	3470	2700	3260
H ₂ O	2330	3090	2470	2550	3220	2280	2370
H ₂	3	11	tr	2	1	13	5
CO ₂	117	136	227	292	682	138	438
CO	236	139	249	340	282	137	160
SO ₂	138	334	62	96	82	60	193
H ₂ S	49	77	24	75	65	21	69
COS	n.d.	n.d.	n.d.	24	29	9	11
CS ₂	25	n.d.	n.d.	10	2	6	5
C ₂ H ₄	4	3	1	tr	3	3	2
CH ₄	21	10	3	9	3	14	5
HCl	1	1	1	n.d.	2	2	2
N ₂	n.d.	n.d.	n.d.	n.d.	n.d.	17	n.d.
Ar	n.d.	tr	tr	tr	tr	tr	tr
He	tr	tr	tr	tr	tr	tr	tr

Recalculated element concentrations (ppm)

O	2360	3091	2542	2719	3567	2244	2622
H	271	361	278	291	364	272	275
C	155	107	172	238	318	112	195
S	136	239	54	140	120	60	172

n.d. = not detected

tr = trace

#	Sample
15.	81003(125)
16.	81003(125)
17.	81003(125)
18.	81003(250)
19.	81410(125)
20.	81410(250)
21.	82418(125)

() = Grain size in mesh

Table D1 (continued)

Individual gas concentration analyses (ppm)

Sample	22	23	24	25	26	27
Gas	3460	5150	4600	3660	4030	440
H ₂ O	2570	3470	3310	2480	2720	295
H ₂	2	3	6	1	1	tr
CO ₂	366	743	544	541	450	66
CO	264	413	119	209	229	43
SO ₂	116	277	350	308	412	25
H ₂ S	62	154	150	56	86	8
COS	54	36	52	30	78	tr
CS ₂	n.d.	33	22	17	21	tr
C ₂ H ₄	7	2	2	a	4	1
CH ₄	6	14	44	6	8	2
HCl	1	5	3	3	6	tr
N ₂	13	n.d.	n.d.	n.d.	n.d.	n.d.
Ar	tr	tr	3	tr	1	tr
He	tr	tr	tr	tr	tr	n.d.

Recalculated element concentrations (ppm)

O	2773	3990	3593	3118	3395	347
H	294	399	394	312	347	34
C	235	403	247	249	288	38
S	145	330	371	347	321	20

n.d. = not detected

tr = trace

#	Sample
22.	82418(250)
23.	2E2 IG
24.	25723 IG
25.	77015 IG
26.	81003 IG
27.	Anorthoclase

() = Grain size in mesh

Table D2

Individual gas composition analyses (mole %)

Sample	1	2	3	4	5	6	7
H ₂ O	90.34	87.65	84.32	83.09	89.33	84.17	87.84
H ₂	0.56	0.04	1.37	1.72	0.65	1.43	0.73
CO ₂	4.00	3.88	6.96	8.88	4.04	6.84	5.44
CO	2.94	6.23	5.56	3.83	3.28	4.88	3.28
SO ₂	0.96	0.50	0.46	0.44	1.36	1.42	1.05
H ₂ S	0.36	0.77	0.96	1.52	0.62	0.19	0.88
COS	0.23	n.d.	0.13	0.98	0.28	0.41	0.24
CS ₂	n.d.	0.02	0.05	0.05	n.d.	0.05	0.02
C ₂ H ₄	0.09	n.d.	0.07	0.08	0.07	0.05	0.06
CH ₄	0.50	0.60	0.08	0.26	0.28	0.51	0.34
HCl	0.02	n.d.	0.02	0.04	0.02	0.05	0.03
N ₂	n.d.	0.30	n.d.	n.d.	0.05	n.d.	0.09
Ar	tr	tr	tr	n.d.	n.d.	tr	tr
He	n.d.	tr	tr	tr	tr	tr	tr
Totals							
Wt.Sp	101.6	102.0	100.5	100.7	101.0	100.6	101.0
Wt.G	6.36	4.59	4.02	3.42	4.83	4.22	4.43
Ml.G	3.20	2.29	1.95	1.63	2.40	2.02	2.17

Wt.Sp = Weight of sample (milligrams)

Wt.G = Total grams of gas in (grams) $\times 10^{-4}$

Ml.G = Total moles of gas in (moles) $\times 10^{-5}$

n.d. = not detected

tr = trace

#	Sample
1.	25724(125)
2.	25724(250)
3.	2E2(125)
4.	2E2(250)
5.	25723(125)
6.	77015(125)
7.	77015(250)

() = Grain size in mesh

Table D2 (continued)

Individual gas composition analyses (mole%)

Sample	8	9	10	11	12	13	14
H ₂ O	90.27	87.38	86.31	88.87	88.70	87.96	87.21
H ₂	0.85	3.11	3.48	0.04	0.15	1.17	2.71
CO ₂	3.63	1.59	3.02	2.27	2.20	2.91	2.86
CO	2.44	4.04	4.61	7.49	6.04	4.72	3.69
SO ₂	0.40	2.28	0.91	n.d.	1.44	1.83	1.72
H ₂ S	1.70	0.90	0.79	1.05	0.72	0.86	0.81
CO ₂ S	0.24	0.13	0.15	n.d.	0.15	0.02	0.26
CS ₂	0.06	0.06	0.05	n.d.	0.03	0.02	0.06
C ₂ H ₄	0.07	0.01	0.03	0.02	0.03	0.03	0.06
CH ₄	0.14	0.27	0.47	0.18	0.35	0.44	0.56
HCl	0.02	0.03	0.03	0.07	0.01	0.02	0.04
N ₂	0.18	0.18	0.15	n.d.	n.d.	n.d.	n.d.
Ar	tr	tr	tr	tr	tr	tr	n.d.
He	tr	tr	tr	tr	tr	tr	tr
Totals							
Wt.Sp	100.0	100.7	101.2	104.1	101.4	99.9	101.9
Wt.G	3.53	3.13	2.79	5.61	3.07	2.57	3.19
ML.G	1.79	1.59	1.44	2.88	1.53	1.28	1.62

Wt.Sp = Weight of sample (milligrams)

Wt.G = Total grams of gas in (grams) $\times 10^{-4}$

ML.G = Total moles of gas in (moles) $\times 10^{-5}$

n.d. = not detected

tr = trace

#	Sample
8.	78325(125)
9.	78325(250)
10.	79301(125)
11.	79301(250)
12.	81003(125)
13.	81003(250)
14.	81003(125)

() = Grain size in mesh

Table D2 (continued)

Individual gas composition analyses (mole%)

Sample	15	16	17	18	19	20	21
H ₂ O	87.76	88.79	89.40	85.10	85.53	87.52	84.68
H ₂	1.11	2.78	0.18	0.67	0.28	4.56	1.61
CO ₂	1.80	1.60	3.36	4.01	7.41	2.16	6.38
CO	5.72	2.57	5.79	7.33	4.82	3.38	3.64
SO ₂	1.45	2.70	0.63	0.91	0.61	0.64	1.94
H ₂ S	0.97	1.17	0.46	1.33	0.91	0.43	1.31
COS	n.d.	n.d.	n.d.	0.24	0.23	0.11	0.12
CS ₂	0.23	n.d.	n.d.	0.08	0.01	0.05	0.05
C ₂ H ₄	0.08	0.04	0.03	tr	0.05	0.06	0.03
CH ₄	0.88	0.33	0.13	0.33	0.10	0.62	0.21
HCl	0.01	0.02	0.02	n.d.	0.03	0.04	0.03
N ₂	n.d.	n.d.	n.d.	n.d.	n.d.	0.43	n.d.
Ar	n.d.	n.d.	0.01	tr	tr	0.01	tr
He	tr	tr	tr	tr	tr	tr	tr
Totals							
Wt.Sp	101.7	103.2	100.7	103.7	101.2	100.7	100.3
Wt.G	2.98	3.92	3.07	3.52	4.42	2.72	3.27
Ml.G	1.50	1.99	1.55	1.72	2.12	1.46	1.56

Wt.Sp = Weight of sample (milligrams)

Wt.G = Total grams of gas in (grams)X10⁻⁴Ml.G = Total moles of gas in (moles)X10⁻⁵

n.d. = not detected

tr = trace

#	Sample
15.	81003(125)
16.	81003(125)
17.	81003(125)
18.	81003(250)
19.	81410(125)
20.	81410(250)
21.	82418(125)

() = Grain size in mesh

Table D2 (continued)

Individual gas composition analyses (mole%)

Sample	22	23	24	25	26	27	28
H ₂ O	85.39	81.36	84.48	83.11	83.29	80.82	92.54
H ₂	0.57	0.59	1.33	0.34	0.34	0.50	0.01
CO ₂	4.98	7.13	5.69	7.40	5.63	7.37	2.08
CO	5.64	6.23	1.96	4.51	4.49	7.52	2.80
SO ₂	1.08	1.83	2.62	2.89	3.55	1.90	n.d.
H ₂ S	1.09	1.92	2.03	0.99	1.38	1.17	n.d.
COS	0.53	0.26	0.40	0.31	0.71	tr	n.d.
CS ₂	n.d.	0.19	0.14	0.14	0.15	tr	n.d.
C ₂ H ₄	0.14	0.03	0.02	0.03	0.07	0.14	0.59
CH ₄	0.26	0.38	1.25	0.22	0.26	0.54	1.03
HCl	0.02	0.06	0.03	0.05	0.09	0.04	n.d.
N ₂	0.28	n.d.	n.d.	n.d.	n.d.	n.d.	0.97
Ar	tr	0.01	0.03	0.01	0.01	n.d.	0.02
He	tr	tr	tr	tr	n.d.	tr	tr
Totals							
Wt.Sp	99.9	378.8	526.1	496.6	498.5	155.0	0.0
Wt.G	3.46	1.56	2.42	1.82	1.81	0.68	0.34
Ml.G	1.67	0.72	1.14	0.83	0.82	0.32	0.18

Wt.Sp = Weight of sample (milligrams)

Wt.G = Total grams of gas in (grams) $\times 10^{-4}$

Ml.G = Total moles of gas in (moles) $\times 10^{-5}$

n.d. = not detected

tr = trace

Sample
 22. 82418(250)
 23. 2E2 IG
 24. 25723 IG
 25. 77015 IG
 26. 81003 IG
 27. Anorthoclase
 28. Blank

() = Grain size in mesh

Volatile Element Data

Table D3

Whole rock volatile element analyses (ppm) of recent bombs,
Mount Erebus

<u>Sample</u>	<u>S</u>	<u>Cl</u>
25724	280	1130
25723	280	970
78325	270	970
79301	260	1500
81003	230	1510
81405	240	1100
81410	250	1060
82418	260	870
<u>82420</u>	<u>280</u>	<u>920</u>
Ave.	260	1110
s	20	240
n	9	9
cv	8%	22%

n = number of analyses
s = 1 standard deviation
cv = coefficient of variation

Sulfur determinations were done by the LECO titrimetric method and Cl determinations were done by ion selective electrode, by J. B. Bodkin, Pennsylvania State University.

Table D4

Volatile element analyses (ppm) of matrix glass from recent bombs, Mount Erebus

Sample	S	F	Cl
25724	280	2280	1360
25721	340	2150	1660
2E2	340	2050	1590
25723	280	2330	1280
77015	370	1990	1590
78003	310	1990	1710
78200	350	1960	1550
78325	360	1700	1470
79301	380	2150	1510
79302	370	2210	1620
81003	330	2320	1870
81003	360	2090	1650
81005	320	2300	1570
81410	210	2220	1700
82418	320	2300	1510
Ave.	330	2140	1400
S	40	180	140
n	15	15	15
cv	12%	8%	10%

n = number of analyses
s = 1 Standard deviation
cv = coefficient of variation

Determinations were done by J. B. Bodkin, Pennsylvania State University, using the LECO titrimetric method for S, specific ion electrode followed fusion by lithium metaborate for F and Cl.

Table D5

S and Cl analyses (ppm) of glass inclusions in anorthoclase phenocrysts, Mount Erebus

Number	SO ₃	Cl
1	1200	2000
2	1000	1800
3	800	1600
4	----	1600
5	1400	1700
6	1000	1400
7	1400	1700
8	1000	1600
9	900	1800
10	1000	1800
12	1200	1500
13	900	1400
14	1000	1700
I	700	900
II	1300	1600
Ave.	1100	1600
S	200	200
n	15	16
cv	18%	13%

n = number of analyses

s = 1 Standard deviation

cv = coefficient of variation

Inclusion glass analyses were conducted by P. R. Kyle using electron microprobe analysis.

Major Element Data

Table D6

Individual whole rock major element analyses

Sample	25726	25724	25721	2E2	2E6	25723
SiO ₂	55.16	56.13	56.41	56.36	56.19	55.96
TiO ₂	1.06	0.95	0.91	0.93	0.95	0.98
Al ₂ O ₃ *	19.72	20.04	20.20	20.20	20.13	19.92
Fe ₂ O ₃	5.77	5.36	4.98	5.23	5.31	5.49
MnO	0.23	0.21	0.22	0.21	0.21	0.22
MgO	0.97	0.84	0.82	0.83	0.83	0.89
CaO	2.64	2.68	2.74	2.65	2.63	2.65
Na ₂ O	8.68	8.41	8.59	8.59	8.45	8.48
K ₂ O	4.70	4.50	4.47	4.57	4.59	4.57
P ₂ O ₅	0.44	0.39	0.38	0.38	0.39	0.42
LOI	0.19	0.00	0.07	0.07	0.01	0.00
Sum	99.55	99.51	99.77	100.02	99.69	99.58

n = number of analyses

* = Total Fe as Fe₂O₃

LOI = Loss on ignition at 1000°C

Analyzed by X-Ray fluorescence spectrometry
by P. R. Kyle.

Table D6 (continued)

Individual whole rock major element analyses

Sample	77015	77016	78003	78004	78200	78325
SiO ₂	55.59	56.64	56.18	56.43	56.84	56.01
TiO ₂	0.99	0.92	0.99	0.93	0.84	0.93
Al ₂ O ₃ *	19.89	20.26	20.14	20.15	19.67	19.98
Fe ₂ O ₃	5.56	5.08	5.42	5.07	4.81	5.31
MnO	0.22	0.21	0.22	0.21	0.29	0.33
MgO	0.91	0.83	0.82	0.87	0.87	1.00
CaO	2.55	2.68	2.57	2.69	2.67	2.66
Na ₂ O	8.68	8.57	8.67	8.73	7.95	8.28
K ₂ O	4.7	4.52	4.72	4.53	4.38	4.58
P ₂ O ₅	0.40	0.38	0.40	0.37	0.37	0.39
LOI ⁵	0.00	0.00	0.00	0.07	-0.15	-0.06
Sum	99.49	100.04	100.05	99.98	98.69	99.47

n = Number of analyses.

* = number of analyses

LOI = Loss on ignition at 1000°C

Analyzed by X-Ray fluorescence spectrometry
by P. R. Kyle.

Table D7

Individual major element analyses of matrix glass

Sample	25724	25721	2E2	2E6
n	11	13	10	13
SiO ₂	55.70(0.56) **	55.75(0.53)	56.09(0.91)	55.84(0.49)
TiO ₂	1.03(0.04)	1.01(0.06)	1.02(0.05)	1.03(0.06)
Al ₂ O ₃ *	19.87(0.30)	19.88(0.26)	20.08(0.41)	19.91(0.26)
Fe ₂ O ₃	5.41(0.12)	5.39(0.07)	5.38(0.15)	5.37(0.17)
MnO	n.a.	n.a.	n.a.	n.a.
MgO	0.87(0.07)	0.86(0.07)	0.86(0.05)	0.82(0.08)
CaO	1.95(0.07)	1.97(0.09)	1.99(0.09)	1.92(0.06)
Na ₂ O	9.00(0.12)	9.12(0.15)	9.20(0.11)	8.99(0.14)
K ₂ O	5.53(0.16)	5.48(0.15)	5.59(0.14)	5.61(0.15)
P ₂ O ₅	0.25(0.04)	0.23(0.04)	0.22(0.03)	0.25(0.04)
Sum	99.59	99.71	100.44	99.74

n = number of analyses

* = Total Fe as Fe₂O₃

** = 1 Standard deviation

n.a. = not analyzed

Mean chemical compositions of matrix (groundmass) glass in recent volcanic ejecta from Mount Erebus were analyzed by electron microprobe by P. R. Kyle.

Table D7 (continued)

Individual major element analyses of matrix glass

Sample	25723	77015	77016	78003
n	11	9	8	10
SiO ₂	55.76(0.45)**	55.81(0.62)	55.77(0.46)	55.93(0.48)
TiO ₂	1.02(0.04)	0.99(0.05)	1.02(0.05)	1.02(0.05)
Al ₂ O ₃ *	20.00(0.20)	19.80(0.38)	19.80(0.21)	19.80(0.21)
Fe ₂ O ₃	5.51(0.11)	5.38(0.09)	5.37(0.12)	5.32(0.12)
MnO	n.a.	n.a.	n.a.	n.a.
MgO	0.87(0.07)	0.80(0.04)	0.80(0.09)	0.85(0.06)
CaO	1.98(0.11)	1.92(0.07)	1.96(0.10)	1.89(0.07)
Na ₂ O	9.02(0.11)	9.09(0.16)	8.99(0.14)	9.12(0.14)
K ₂ O	5.51(0.10)	5.53(0.20)	5.40(0.17)	5.51(0.13)
P ₂ O ₅	0.25(0.03)	0.23(0.03)	0.22(0.03)	0.22(0.04)
Sum	99.92	99.55	99.32	99.66

n = number of analyses

* = Total Fe as Fe₂O₃

** = 1 Standard deviation

n.a. = not analyzed

Mean chemical compositions of matrix (groundmass) glass in recent volcanic ejecta from Mount Erebus were analyzed by electron microprobe by P. R. Kyle.

Table D7 (continued)

Individual major element analyses of matrix

Sample	78200	78325	78327
n	19	12	11
SiO ₂	56.04(0.61)**	55.75(0.62)	55.84(0.51)
TiO ₂	1.04(0.06)	1.02(0.06)	1.00(0.06)
Al ₂ O ₃ *	19.83(0.25)	19.92(0.32)	19.84(0.30)
Fe ₂ O ₃	5.40(0.07)	5.32(0.13)	5.33(0.10)
MnO	n.a.	n.a.	n.a.
MgO	0.80(0.11)	0.82(0.09)	0.86(0.09)
CaO	1.94(0.08)	1.97(0.07)	1.93(0.07)
Na ₂ O	8.56(0.16)	9.10(0.24)	8.99(0.11)
K ₂ O	5.65(0.19)	5.47(0.17)	5.49(0.15)
P ₂ O ₅	0.21(0.04)	0.22(0.04)	0.22(0.03)
Sum	99.47	99.59	99.48

n = number of analyses

* = Total Fe as Fe₂O₃

** = 1 Standard deviation

n.a. = not analyzed

Mean chemical compositions of matrix (groundmass) glass in recent volcanic ejecta from Mount Erebus were analyzed by electron microprobe by P. R. Kyle.

Table D8

Individual trace and rare earth element analyses of
matrix glass

Sample	25721	2E2	2E6	77015	77016
FeO*	5.97	5.68	5.86	5.53	6.33
Na ₂ O	9.34	9.30	9.28	9.32	8.83
Sc	3.72	3.74	3.60	3.16	4.05
Cr	<10	<10	<10	<10	<10
Co	2.7	2.9	3.1	2.1	3.6
As	3.1	2.9	3.2	3.2	3.1
Rb	126	121	124	127	118
Sb	0.54	0.53	0.49	0.50	0.48
Ba	602	623	496	563	566
Cs	2.02	1.86	1.94	1.96	1.77
La	169	161	159	162	167
Ce	337	322	318	322	335
Sm	20.4	19.3	19.1	18.8	20.4
Nd	124	119	117	120	126
Eu	4.17	4.07	3.89	3.93	4.26
Tb	2.51	2.45	2.46	2.45	2.58
Yb	7.97	7.86	7.86	7.98	7.87
Lu	0.92	0.88	0.89	0.91	0.86
Hf	30.9	30.4	30.4	31.3	29.2
Ta	25.8	25.4	25.4	26.1	24.3
Th	29.2	29.0	28.6	29.7	27.8
U	7.1	7.8	7.7	7.9	7.6

* = Total Fe as FeO

n = number of analyses

Analyzed by instrumental neutron activation
by P. R. Kyle.

Table D8 (continued)

Individual trace and rare earth element analyses of
matrix glass

Sample	78003	78004	78200	78325	79301
FeO*	5.92	6.47	5.40	5.35	5.74
Na ₂ O	9.34	8.92	9.14	9.16	8.94
Sc	3.51	3.35	3.06	3.06	3.35
Cr	<10	<10	<10	<10	<10
Co	3.0	4.0	2.1	2.3	2.6
As	3.6	2.9	3.1	2.6	2.6
Rb	122	135	120	121	117
Sb	0.52	0.47	0.48	0.48	0.47
Ba	586	561	583	577	568
Cs	1.83	2.19	1.92	1.85	1.81
La	163	156	157	157	157
Ce	319	303	307	304	309
Sm	19.5	18.5	18.2	18.4	18.6
Nd	119	112	116	113	112
Eu	3.99	3.92	3.77	3.76	3.93
Tb	2.43	2.39	2.31	2.34	2.36
Yb	7.66	7.47	7.74	7.81	7.34
Lu	0.90	0.88	0.87	0.87	0.81
Hf	30.3	29.3	30.3	30.0	29.1
Ta	25.3	25.0	25.3	25.4	24.6
Th	28.9	27.7	28.9	28.8	27.8
U	7.7	7.4	7.7	8.1	7.3

* = Total Fe as FeO

n = number of analyses

Analyzed by instrumental neutron activation
by P. R. Kyle.

Table D8 (continued)

Individual trace and rare earth element
analyses of matrix glass

Sample	79302	80300	81003	81005
FeO*	5.80	5.97	5.47	5.81
Na ₂ O	9.29	9.09	9.36	9.23
Sc	3.71	3.64	3.11	4.19
Cr	<10	<10	<10	<10
Co	2.5	2.8	2.1	2.7
As	3.3	3.3	3.2	2.7
Rb	122	122	128	118
Sb	0.51	0.49	0.50	0.50
Ba	564	595	618	627
Cs	1.82	1.80	1.98	1.94
La	164	162	158	160
Ce	325	324	317	315
Sm	19.7	19.3	18.6	19.4
Nd	119	120	118	118
Eu	3.98	4.11	3.98	4.01
Tb	2.42	2.47	2.38	2.44
Yb	7.70	7.59	7.76	7.57
Lu	0.91	0.88	0.87	0.86
Hf	30.7	30.2	30.8	29.6
Ta	25.8	25.0	25.7	24.7
Th	29.5	28.5	29.2	28.1
U	7.5	7.8	7.8	8.2

* = Total Fe as FeO

n = number of analyses

Analyzed by instrumental neutron activation
by P. R. Kyle.

APPENDIX E

Statistical Methods used to Test for Trend

The data reported in the chemistry and volatile sections of this report were tested for trends using the procedure "Testing Against Trend" presented by Lehmann (1975). The hypothesis tested was that gas compositions and concentrations of Mount Erebus glasses do not change with time. The level of test significance is $\alpha = 10\%$. A probability of 0.05 for an increasing or decreasing trend was used to determine the upper and lower critical values of D, using the appropriate sample size number (n). The formula used to determine D, $D = (T_1-1)^2 + (T_2-2)^2 + \dots + (T_N-N)^2$ is presented and discussed by Lehmann (1975) on page 291. The Test For Trend referred to in this text tests for trends instead of against trends as presented by Lehmann.

The computation of D is described by Lehmann in the following manner;

" The statistic D is an intuitively reasonable test statistic since under the alternatives large values of T_i will tend to occurred for large values of i and small values of T_i for small values of i , so that the differences $(T_i-i)^2$ will tend to be small."

The manner in which the test was used in this text tests for both very small and very large numbers of D. The value D is the test statistic which is calculated and compared to the

limit values D_L and D_U to determine if there is a trend to the data values. The value T_i is the rank of each individual data value with respect to the other data values. The data was always ranked with the lowest value receiving the rank of 1 and the largest value receiving the highest rank, n . This method of ranking is the same as described by Lehmann for an increasing trend test. Whole rock and matrix glass major element analyses, whole rock and matrix glass volatile element analyses and matrix and inclusion glass gas analyses D values are listed in Tables D1 and D2.

Example: Whole rock SiO_2 calculations.

Year	1978	1977	1975	1974	1972	OB
SiO ₂	56.51	56.21	55.96	56.32	56.13	55.16
Rank	6	4	2	5	3	1
D =	$(6-1)^2 + (4-2)^2 + (2-3)^2 + (5-4)^2 + (3-5)^2 + (1-6)^2$					
D =	60					

For a sample size (n) of 6 the lower and upper limits (D_L and D_U) are 7 and 64 respectively. Therefore, the calculated D_{SiO_2} value is within the range of values which do not define a trend, with a 10% chance for error.

TABLE E1

Major element D values

	WR	MG
SiO ₂	60	34
Al ₂ O ₃	60	10
FeO _T	10	6.5*
CaO	42	13.5*
Na ₂ O	46	14
K ₂ O	28	18.5*
<u>n</u>	<u>6</u>	<u>5</u>
D _L	7	3
D _U	64	37
<u>CL(%)</u>	<u>10</u>	<u>10</u>

Volatile element D values

	WR	MG
S	86.5*	115.5*
Cl	64.5*	92
F	n.a.	108
<u>n</u>	<u>7</u>	<u>9</u>
D _L	17	49
D _U	95	191
<u>CL(%)</u>	<u>10</u>	<u>10</u>

See Table E2 for descriptions.

TABLE E2

Gas and element D values

	MG Cp	MG Ct	IG Cp	IG Ct
H ₂ O	158	194	6	18
CO ₂	136*	198	14	6
CO	107*	180	14	12
SO ₂	74	120	0	2
H ₂ S	86	129.5*	16	18
O	127*	212	4	18
H	116	196.5*	10	18
C	110.5*	202*	14	14
S	74.5*	124	3.5*	10
n	9	9	4	4
D _L	49	49	0	0
D _U	191	191	20	20
CL(%)	10	10	8.5	8.5

n - number of test values

CL- confidence level

WR-Whole Rock

MG- Matrix Glass

IG- Inclusion Glass

Cp- composition

Ct- concentration.

D_L and D_U - lower and upper probability limits, respectively, determined from Lehmann (1975)

* - An error correction for ties was applied to the limits for these values

APPENDIX F

Introduction

The weight percent of glass inclusions in anorthoclase phenocrysts was determined using the least-squares calculations similar to those presented by Wright and Doherty (1970) and Wright (1974). Anorthoclase (FELD), inclusion glass (GLAS), pyroxene (PYRX), apatite (APAT), olivine (OLIV) and magnetite (MAGN), the major mineral components of anorthoclase phenocrysts (Kyle, 1977a), and major element compositions were used to estimate the whole anorthoclase phenocryst composition. The least-square calculations used these component's and the measured whole phenocryst major element compositions to estimate percentages of each component. The differences between the measured whole phenocryst and the estimated whole phenocryst major element compositions, listed as % Differences (DIFF), indicate how accurately the component percentages (SOLUTIONS) fit the component major element compositions to the measured whole phenocryst composition (Tables E1, E2, E3 and E4).

Mass Balance models

TABLE F1

Mass balance calculation of inclusion glass content in
anorthoclase, sample 2E2

	Weight	FEGL	+ GLAS	+ FELD	+ PYRX	+ APAT	+ OLIV	+ MAGN
SiO ₂	1.0	61.78	55.13	63.65	50.40	0.00	34.70	0.00
TiO ₂	1.0	0.20	0.93	0.13	1.32	0.00	0.04	25.30
Al ₂ O ₃	1.0	21.99	19.67	22.35	2.80	0.00	0.00	2.33
FeO	1.0	0.99	5.55	0.18	9.75	0.00	38.45	65.50
MnO	1.0	0.04	0.26	0.00	0.65	0.00	2.43	1.80
MgO	1.0	0.10	0.69	0.00	12.20	0.00	24.00	2.94
CaO	1.0	3.71	2.01	3.28	21.10	51.00	0.50	0.00
Na ₂ O	1.0	7.41	9.06	7.44	1.07	0.00	0.00	0.00
K ₂ O	1.0	3.05	5.53	3.36	0.00	0.00	0.00	0.00
P ₂ O ₅	1.0	0.14	0.32	0.00	0.00	43.30	0.00	0.00
Total		99.41	99.15	100.39	99.29	94.30	100.12	97.87
Sum=0.9999, Sol.=		0.0753	0.9099	0.0063	0.0056	0.0018	0.0010	

	CALC	DIFF	FEGL	GLAS	FELD	PYRX	APAT	OLIV	MAGN
SiO ₂	62.26	0.2%	62.15	55.60	63.40	50.76	0.00	34.66	0.00
TiO ₂	0.22	10.8%	0.20	0.94	0.13	1.33	0.00	0.04	25.85
Al ₂ O ₃	21.77	-1.6%	22.12	19.84	22.26	2.82	0.00	0.00	2.38
FeO	0.78	-21.3%	1.00	5.60	0.18	9.82	0.00	38.40	66.93
MnO	0.03	-25.1%	0.04	0.26	0.00	0.65	0.00	2.43	1.84
MgO	0.18	75.3%	0.10	0.70	0.00	12.29	0.00	23.97	3.00
CaO	3.56	-4.5%	3.73	2.03	3.27	21.25	54.08	0.50	0.00
Na ₂ O	7.44	-0.2%	7.45	9.14	7.41	1.08	0.00	0.00	0.00
K ₂ O	3.47	13.0%	3.07	5.58	3.35	0.00	0.00	0.00	0.00
P ₂ O ₅	0.28	100.1%	0.14	0.32	0.00	0.00	45.92	0.00	0.00

Solutions are
Sensitivity

7.53% 91.00% 0.63% 0.56% 0.18% 0.1%
0.37 0.47 0.33 0.45 0.28 0.23

TABLE F2

Mass balance calculation of inclusion glass content in
anorthoclase, sample 25723

	Weight	FEGL +	GLAS +	FELD +	PYRX +	APAT +	OLIV +	MAGN
SiO ₂	1.0	61.74	54.90	63.65	50.40	0.00	34.70	0.00
TiO ₂	1.0	0.23	0.94	0.13	1.32	0.00	0.04	25.30
Al ₂ O ₃	1.0	21.91	19.52	22.35	2.80	0.00	0.00	2.33
FeO	1.0	1.15	5.46	0.18	9.75	0.00	38.45	65.50
MnO	1.0	0.04	0.26	0.00	0.65	0.00	2.43	1.80
MgO	1.0	0.11	0.67	0.00	12.20	0.00	24.00	2.94
CaO	1.0	3.56	2.03	3.28	21.10	51.00	0.50	0.00
Na ₂ O	1.0	7.48	9.03	7.44	1.07	0.00	0.00	0.00
K ₂ O	1.0	3.13	5.43	3.36	0.00	0.00	0.00	0.00
P ₂ O ₅	1.0	0.16	0.34	0.00	0.00	43.30	0.00	0.00

Total	99.51	98.58	100.39	99.29	94.30	100.12	97.87
-------	-------	-------	--------	-------	-------	--------	-------

Sum=1.0004, Sol.=	0.1035	0.8837	0.0047	0.0046	0.0027	0.0011
-------------------	--------	--------	--------	--------	--------	--------

	CALC	DIFF	FEGL	GLAS	FELD	PYRX	APAT	OLIV	MAGN
SiO ₂	62.11	0.1%	62.04	55.69	63.40	50.76	0.00	34.66	0.00
TiO ₂	0.25	7.0%	0.23	0.95	0.13	1.33	0.00	0.04	25.85
Al ₂ O ₃	21.73	-1.3%	22.02	19.80	22.26	2.82	0.00	0.00	2.38
FeO	0.95	-17.4%	1.16	5.54	0.18	9.82	0.00	38.40	66.93
MnO	0.04	-3.1%	0.04	0.26	0.00	0.65	0.00	2.43	1.84
MgO	0.20	78.1%	0.11	0.68	0.00	12.29	0.00	23.97	3.00
CaO	3.45	-3.6%	3.58	2.06	3.27	21.25	54.08	0.50	0.00
Na ₂ O	7.50	-0.2%	7.52	9.16	7.41	1.08	0.00	0.00	0.00
K ₂ O	3.53	12.1%	3.15	5.51	3.35	0.00	0.00	0.00	0.00
P ₂ O ₅	0.25	53.5%	0.16	0.34	0.00	0.00	45.92	0.00	0.00

Solutions are
Sensitivity

10.35%	88.34%	0.47%	0.46%	0.27%	0.11
0.33	0.43	0.30	0.44	0.25	0.25

TABLE F3

Mass balance calculation of inclusion glass content in
anorthoclase, sample 77015

	Weight	FEGL +	GLAS +	FELD +	PYRX +	APAT +	OLIV +	MAGN
SiO ₂	1.0	61.60	54.05	63.65	50.40	0.00	34.70	0.00
TiO ₂	1.0	0.23	0.93	0.13	1.32	0.00	0.04	25.30
Al ₂ O ₃	1.0	21.10	19.23	22.35	2.80	0.00	0.00	2.33
FeO	1.0	1.11	5.50	0.18	9.75	0.00	38.45	65.50
MnO	1.0	0.04	0.26	0.00	0.65	0.00	2.43	1.80
MgO	1.0	0.07	0.69	0.00	12.20	0.00	24.00	2.94
CaO	1.0	3.62	2.00	3.28	21.10	51.00	0.50	0.00
Na ₂ O	1.0	7.53	9.14	7.44	1.07	0.00	0.00	0.00
K ₂ O	1.0	3.08	5.42	3.36	0.00	0.00	0.00	0.00
P ₂ O ₅	1.0	0.18	0.36	0.00	0.00	43.30	0.00	0.00
Total		98.56	97.58	100.39	99.29	94.30	100.12	97.87
Sum=1.0050, Sol.=		0.1017	0.8768	0.0234	0.0024	0.0006	0.0001	

	CALC	DIFF	FEGL	GLAS	FELD	PYRX	APAT	OLIV	MAGN
SiO ₂	62.12	-0.6%	62.50	55.39	63.40	50.76	0.00	34.66	0.00
TiO ₂	0.24	3.9%	0.23	0.95	0.13	1.33	0.00	0.04	25.85
Al ₂ O ₃	21.48	0.3%	21.41	19.71	22.26	2.82	0.00	0.00	2.38
FeO	0.99	-12.5%	1.13	5.64	0.18	9.82	0.00	38.40	66.93
MnO	0.04	8.2%	0.04	0.27	0.00	0.65	0.00	2.43	1.84
MgO	0.37	425.7%	0.07	0.71	0.00	12.29	0.00	23.97	3.00
CaO	3.68	0.2%	3.67	2.05	3.27	21.25	54.08	0.50	0.00
Na ₂ O	7.44	-2.6%	7.64	9.37	7.41	1.08	0.00	0.00	0.00
K ₂ O	3.48	11.4%	3.13	5.55	3.35	0.00	0.00	0.00	0.00
P ₂ O ₅	0.15	-20.1%	0.18	0.37	0.00	0.00	45.92	0.00	0.00
Solutions are				10.12%	87.24%	2.33%	0.24%	0.06%	0.01
Sensitivity				-0.03	0.01	-0.00	0.48	0.10	0.35

TABLE F4

Mass balance calculation of inclusion glass content in
anorthoclase, sample 81003

	Weight	FEGL	GLAS	FELD	PYRX	APAT	OLIV	MAGN
SiO ₂	1.0	61.78	55.01	63.65	50.40	0.00	34.70	0.00
TiO ₂	1.0	0.26	0.92	0.13	1.32	0.00	0.04	25.30
Al ₂ O ₃	1.0	22.05	19.67	22.35	2.80	0.00	0.00	2.33
FeO	1.0	1.09	5.59	0.18	9.75	0.00	38.45	65.50
MnO	1.0	0.04	0.26	0.00	0.65	0.00	2.43	1.80
MgO	1.0	0.05	0.66	0.00	12.20	0.00	24.00	2.94
CaO	1.0	3.57	2.02	3.28	21.10	51.00	0.50	0.00
Na ₂ O	1.0	7.47	9.03	7.44	1.07	0.00	0.00	0.00
K ₂ O	1.0	3.06	5.49	3.36	0.00	0.00	0.00	0.00
P ₂ O ₅	1.0	0.13	0.32	0.00	0.00	43.30	0.00	0.00

Total 99.50 98.57 100.39 99.29 94.30 100.12 97.87

Sum=1.0001, Sol.= 0.0923 0.8975 0.0012 0.0051 0.0030 0.0010

	CALC	DIFF	FEGL	GLAS	FELD	PYRX	APAT	OLIV	MAGN
SiO ₂	62.19	0.2%	62.09	55.58	63.40	50.76	0.00	34.66	0.00
TiO ₂	0.23	-12.4%	0.26	0.93	0.13	1.33	0.00	0.04	25.85
Al ₂ O ₃	21.82	-1.5%	22.16	19.87	22.26	2.82	0.00	0.00	2.38
FeO	0.87	-20.2%	1.10	5.65	0.18	9.82	0.00	38.40	66.93
MnO	0.03	-15.2%	0.04	0.26	0.00	0.65	0.00	2.43	1.84
MgO	0.15	200.3%	0.05	0.67	0.00	12.29	0.00	23.97	3.00
CaO	3.42	-4.5%	3.59	2.04	3.27	21.25	54.08	0.50	0.00
Na ₂ O	7.49	-0.2%	7.51	9.12	7.41	1.08	0.00	0.00	0.00
K ₂ O	3.52	14.3%	3.08	5.55	3.35	0.00	0.00	0.00	0.00
P ₂ O ₅	0.27	103.5%	0.13	0.32	0.00	0.00	45.92	0.00	0.00

Solutions are

Sensitivity

9.22% 89.75% 0.12% 0.51% 0.30% 0.10
0.36 0.45 0.32 0.45 0.27 0.19

(INSERTS)-----

REFERENCES

- Abbey, S., 1981. The search for "best values" - a study of three Canadian rocks. *Geostandards Newsletter*, 5: 13-26.
- Albarede, F. and Bottinga, Y., 1972. Kinetic disequilibrium in trace element partitioning between phenocrysts and host lava. *Geochimica et Cosmochimica Acta*, 36: 141-156.
- Anderson, A. T., 1974. Chlorine, sulfur, and water in magmas and oceans. *Geological Society of America Bulletin*, 85: 1485-1492.
- Anderson, A. T., 1975. Some basaltic and andesitic gases. *Reviews of Geophysics and Space Physics*, 13: 32-55.
- Anderson, A. T., 1979. Water in some hypersthenic magmas. *Journal of Geology*, 87: 509-531.
- Armstrong, R. L., 1978. K-Ar dating: Late Cenozoic McMurdo Volcanic Group and dry valley glacial history, Victoria Land, Antarctica. *New Zealand Journal of Geology and Geophysics*, 21: 685-698.
- Berresheim, H. and Jaesehke, W., 1983. The contribution of volcanoes to the global atmospheric sulfur budget. *Journal of Geophysical Research*, 88: 3732-3740.
- Blackburn, E. A., Wilson, L. and Sparks, R. S. J., 1976. Mechanisms and dynamics of strombolian activity. *Journal of the Geological Society of London*, 132: 429-440.
- Boudette, E. L., and Ford, A. B., 1966. Physical properties of anorthoclase from Antarctica. *The American Mineralogist* 51: 1374-1387.
- Burnham, C. W., 1967. Hydrothermal fluids at the magmatic stage, in *Geochemistry of Hydrothermal Ore Deposits*, edited by H. L. Barnes, pages 34-74, Holt, Rinehart and Winston, New York.
- Burnham, C. W., 1975a. Water and magmas; a mixing model. *Geochimica et Cosmochimica Acta*, 39: 1077-1084.
- Burnham, C. W., 1975b. Thermodynamics of melting in experimental silicate-volatile systems. *Fortschr. Miner.*, 52: 101-118.

- Burnham, C. W., 1979a. The importance of volatile constituents, in *The Evolution of Igneous Rocks, Fiftieth Anniversary Perspectives*, edited by H. S. Yoder, Jr., Chap. 16, Princeton University Press, Princeton, N.J.
- Burnham, C. W., 1979b. Magmas and hydrothermal fluids, in *Geochemistry of Hydrothermal Ore Deposits*, 2nd ed., John Wiley and Sons, New York.
- Byers, C. D., Muenow, D. W. and Garcia, M. O., 1983. Volatiles in basalts and andesites from the Galapagos. *Geochimica et Cosmochimica Acta*, 47: 1551-1558.
- Byrd, R. E., 1935. *Discovery*. New York, Putnam's, 405 pp.
- Carmichael, I. S. E., 1964. Natural liquids and the phonolite minimum. *Geological Journal*, 4: 55-60.
- Carrigan, C. R., 1983. A heat pipe model for vertical, magma-filled conduits. *Journal of Volcanology and Geothermal Research*. 16: 279-298.
- Chaigneau, M., Hekinian, R., and Cheminee, J. L., 1980. Magmatic gases extracted and analysed from ocean floor volcanics. *Bulletin Volcanologique*, 43: 241-253.
- Clocchiatti, R., Desnoyers, C., Sabroux, J., Tazieff, H. and Wilhelm, S., 1976. Relations entre les anorthoses de l'Erebus et leurs inclusions vitreuses. *Bulletin de la Societe francaise de Mineralogie et de Cristallographie*, 99: 98-110.
- David, T. W. E. and Priestley, R. E. 1909. Notes in regard to Mount Erebus. In: E. H. Shackleton, *The Heart of the Antarctic, Being the Story of the British Antarctic Expedition, 1907-09*, 2. Heinemann, London, pp. 308-309.
- Delaney, J. R., Muenow, D. W. and Graham, D. G., 1978. Abundance and distribution of water, carbon and sulfur in the glassy rims of submarine pillow basalts. *Geochimica et Cosmochimica Acta*, 42: 581-594.
- Eggler, D. H., Mysen, B. O., Hoerning, T. C. and Holloway, J. R., 1979. The solubility of carbon monoxide in silicate melts at high pressures and its effect on silicate phase relations. *Earth and Planetary Science Letter*, 43: 321-330.
- Eichelberger, J. C. and Westrich, H. R., 1981. Magmatic volatiles in explosive rhyolitic eruptions. *Geophysical Research Letter*, 8: 757-760.

- Eichelberger, J. C. and Westrich, H. R., 1982. Water in obsidian and in magmas (Abstract). EOS, 63: 1131.
- Eichelberger, J. C. and Westrich, H. R., 1983. Behavior of water in rhyolitic magma at shallow depth (Abstract). EOS, 64: 338.
- Ellis, A. J., 1957. Chemical equilibrium in magmatic gases. American Journal of Science, 255: 416-431.
- Ferrar, H. T., 1907. Report on the field geology of the region explored during the "Discovery" Antarctic Expedition, 1901-4. Nat. Antarctic Expd., 1901-1904, Natural History, 1: 1-100.
- Garcia, M. O., Liu, N. W. K. and Muenow, D. W., 1979. Volatiles in submarine volcanic rocks from the Mariana Island arc and trough. Geochimica et Cosmochimica Acta, 43: 305-312.
- Gerlach, T. M., 1979. Evaluation and restoration of the 1970 volcanic gas analyses from Mount Etna, Sicily. Journal of Volcanology and Geothermal Research, 6: 165-178.
- Gerlach, T. M., 1980a. Evaluation of volcanic gas analyses from Surtsey volcano, Iceland, 1964-1967. Journal of Volcanology and Geothermal Research, 8: 191-198.
- Gerlach, T. M., 1980b. Chemical characteristics of the volcanic gases from Nyiragongo lava lake and the generation of CH₄ rich fluid inclusions in alkaline rocks. Journal of Volcanology and Geothermal Research, 8: 177-189.
- Gerlach, T. M., 1980c. Evaluation of volcanic gas analyses from Kilauea Volcano. Journal of Volcanology and Geothermal Research, 7: 295-317.
- Gerlach, T. M., 1980d. Investigation of volcanic gas analyses and magma outgassing from Erta'Ale Lava Lake, Afar, Ethiopia. Journal of Volcanology and Geothermal Research, 7: 415-441.
- Gerlach, T. M., 1981. Restoration of new volcanic gas analyses from basalts of the Afar Region: further evidence of CO₂-degassing trends. Journal of Volcanology and Geothermal Research, 10: 83-91.
- Gerlach, T. M. and Nordlie, B. E., 1975. The C-O-H-S gaseous system, Part I: composition limits and trends in basaltic gases. American Journal of Science, 275: 353-376.

- Gerlach, T. M. and Nordlie, B. E., 1975. The C-O-H-S gaseous system, Part II: temperature, atomic composition, and molecular equilibria in volcanic gases. *American Journal of Science*, 275: 377-394.
- Gerlach, T. M. and Nordlie, B. E., 1975. The C-O-H-S gaseous system, Part III: magmatic gases compatible with oxides and sulfides in basaltic magmas. *American Journal of Science*, 275: 395-410.
- Giggenbach, W. F., 1975a. A simple method for the collection and analysis of volcanic gas samples. *Bulletin Volcanologique*, 39: 132-145.
- Giggenbach, W. F., 1975b. Variations in the carbon, sulfur, and chlorine contents of volcanic gas discharges from White Island, New Zealand. *Bulletin Volcanologique*, 39: 15-27.
- Giggenbach, W. F. and LeGuern, F., 1976. The chemistry of magmatic gases from Erta'Ale, Ethiopia. *Geochimica et Cosmochimica Acta*, 40: 25-30.
- Giggenbach, W. F., Kyle, P. R. and Lyon, G. L., 1973. Present volcanic activity on Mount Erebus, Ross Island, Antarctica. *Geology*, 1: 135-136.
- Goldich, S. S., Treves, S. B., Suhr, N. H. and Stuckless, J. S., 1975. Geochemistry of the Cenozoic volcanic rocks of Ross Island and vicinity, Antarctica. *Journal of Geology*, 83: 415-435.
- Graeber, E. J., Modreski, P. J. and Gerlach, T. M., 1979. Compositions of gases collected during the 1977 east rift eruption, Kilauea Hawaii. *Journal of Volcanology and Geothermal Research*, 5: 337-344.
- Graham, D. G., 1978. A mass spectrometric investigation of the volatile content of deep submarine basalts. University of Hawaii, Ph.D. Dissertation, 176 pp.
- Greenland, L. P., 1984. Gas composition of the January 1983 eruption of Kilauea Volcano, Hawaii. *Geochimica et Cosmochimica Acta*, 48: 193-195.
- Hamilton, D. L., Burnham, C. W. and Osborn, E. F., 1964. The solubility of water and effects of oxygen fugacity and water content on crystallization in mafic magmas. *Journal of Petrology*, 5: 21-39.

- Harrington, H. J., 1958. Nomenclature of rock units in the Ross Sea region, Antarctica. *Nature*, 182: 290.
- Harris, D. M., 1981a. The microdetermination of H₂O, CO₂, and SO₂ in glass using a 1280°C microscope vacuum heating stage, cryopumping, and vapor pressure measurements from 77 to 273 K. *Geochimica et Cosmochimica Acta*, 45: 2023-2036.
- Harris, D. M., 1981b. The concentration of CO₂ in submarine tholeiitic basalts. *Journal of Geology*, 89: 689-701.
- Harris, D. M. and Anderson, A. T. Jr., 1983. Concentrations, sources, and losses of H₂O, CO₂, and S in Kilauean basalt. *Geochimica et Cosmochimica Acta*, 47: 1139-1150.
- Heald, E. F. and Naughton, J. J., 1962. Calculation of chemical equilibria in volcanic systems by means of computers. *Nature*, 193: 642-644.
- Heald, E. F., Naughton, J. J. and Barnes, I. L. Jr., 1963. The chemistry of volcanic gases, 2. Use of equilibrium calculations in the interpretation of volcanic gas samples. *Journal of Geophysical Research*, 68: 545-557.
- Holloway, J. R., 1981. Volatile interactions in magmas. In: R.C. Newton, A. Navrotsky and B. J. Wood (Editors), *Advances in Physical Geochemistry. 1, Thermodynamics of Minerals and Melts*, Springer-Verlag, New York, pp. 273-293.
- Huntingdon, A. T., 1973. The collection and analysis of volcanic gas from Mount Etna. *Philosophical Transactions of the Royal Society of London*, A274: 119-128.
- Kadik, A. A. and Lukanin, O. A., 1973. The solubility-dependent behavior of water and carbon dioxide in magmatic processes. *Geochemistry International*, 10: 115-129.
- Kadik, A. A., Shilobreyeva, S. N., Akhmanova, M. V., Slutshiy, A. B. and Korobkov, V. I., 1981. Solubility of CO₂ in melts of acid composition for the case of the albite--silica system (65:35). *Geochemistry International*, 18: 42-48.
- Keys, J. R., 1980. Salts and their distribution in the McMurdo Region, Antarctica. Ph.D. Thesis, Victoria University of Wellington, 332 pp.

- Kienle, J., Kyle, P. R., Kaminuma, K., Marshall, D. L. and Dibble, R. R., 1983. Volcanic activity and seismicity of Mt. Erebus, 1982-1983. *Antarctic Journal of the U.S.* (In Press)
- Killingley, J. S. and Muenow, D. W., 1975. Volatiles from Hawaiian submarine basalts determined by dynamic high temperature mass spectrometry. *Geochimica et Cosmochimica Acta*, 39: 1467-1473.
- Kyle, P. R., 1976. Geology, mineralogy and geochemistry of the Late Cenozoic McMurdo Volcanic Group, Victoria Land, Antarctica. Unpublished Ph.D. Thesis, Victoria University of Wellington, 444 pp.
- Kyle, P. R., 1977a. Mineralogy and glass chemistry of recent volcanic ejecta from Mt. Erebus, Ross Island, Antarctica. *New Zealand Journal of Geology and Geophysics*, 20(6): 1123-1146.
- Kyle, P. R., 1977b. Mount Erebus Volcano. *Natural Science Event Bulletin*, 2(12): 1-2.
- Kyle, P. R., 1978. Mount Erebus Volcano. *SEAN Bulletin*, 3(10): 2-3.
- Kyle, P. R., 1979. Mount Erebus Volcano. *SEAN Bulletin*, 4(5): 7-10.
- Kyle, P. R., 1980. Mount Erebus Volcano. *SEAN Bulletin*, 5(3): 8.
- Kyle, P. R., 1981. Mount Erebus Volcano. *SEAN Bulletin*, 6(2): 7.
- Kyle, P. R., 1982. Mount Erebus Volcano. *SEAN Bulletin*, 7(3): 12.
- Kyle, P. R. and Cole, J. W., 1974. Structural control of volcanism in the McMurdo Volcanic Group, Antarctica. *Bulletin Volcanologique*, 38: 16-25.
- Kyle, P. R., Dibble, R. R., Giggenbach, W. F. and Keys, J., 1982. Volcanic activity associated with the anorthoclase phonolite lava lake, Mount Erebus, Antarctica. In: C.C. Craddock (editor), *Antarctic Geoscience*, University of Wisconsin Press, pp. 735-745.
- Kyle P. R. and Giggenbach, W. F., 1976. Mount Erebus Volcano. *Natural Science Event Bulletin*, 1(6): 1-2.

- Kyle, P. R. and Rankin, P. C., 1976. Rare earth element geochemistry of Late Cenozoic alkaline lavas of the McMurdo Volcanic Group, Antarctica. *Geochimica et Cosmochimica Acta*, 40: 1497-1507.
- LeGuern, F., Gerlach, T. M. and Nohl, A., 1982. Field gas chromatograph analyses of gases from a glowing dome at Merapi Volcano, Java, Indonesia, 1977, 1978, 1979. *Journal of Volcanology and Geothermal Research*, 14: 223-245.
- Lehmann, E. L., 1975. *Nonparametrics*. Holder Day Inc., San Francisco.
- Martini, M., 1983. On the behavior of fluorine in volcanic processes (Abstract). XVIII General Assembly of the International Association of Volcanology and Chemistry of the Earth's Interior, 18: 55.
- Matsuo, S., 1962. Establishment of chemical equilibrium in the volcanic gas obtained from the lava lake of Kilauea, Hawaii. *Bulletin Volcanologique*, 24: 59-71.
- McMillan, P. F., Jakobsson, S., Holloway, J. R. and Silver, L. A., 1983. A note on the Raman spectra of water-bearing albite glasses. *Geochimica et Cosmochimica Acta*, 47: 1937-1943.
- Moore, J. G., 1965. Petrology of deep-sea basalt near Hawaii. *American Journal of Science*, 263: 40-52.
- Moore, J. G., 1979. Vesicularity and CO₂ in mid-ocean ridge basalt. *Nature*, 282: 250-253.
- Moore, J. G. and Fabbi, B. P., 1971. An estimate of the juvenile sulfur content of basalt. *Contributions to Mineralogy and Petrology*, 33: 118-127.
- Muenow, D. W., 1973. High temperature mass spectrometric gas-release studies of Hawaiian volcanic glass: Pele's Tears. *Geochimica et Cosmochimica Acta*, 37: 1551-1561.
- Muenow, D. W., Graham, D. G., Liu, N. W. K. and Delaney, J. R., 1979. The abundance of volatiles in Hawaiian tholeiitic submarine basalts. *Earth and Planetary Science Letters*, 42: 71-76.
- Muenow, D. W., Liu, N. W. K., Garcia, M. O. and Saunders, A. D., 1980. Volatiles in submarine volcanic rocks from the spreading axis of the East Scotia Sea Back-arc Basin. *Earth and Planetary Science Letters*, 47: 272-278.

- Murray, J., 1909. Additional notes on eruptions. In: E. H. Shackleton, *The Heart of the Antarctic, Being the Story of the British Antarctic Expedition, 1907-09*, 2. Heinemann, London, pp. 310-315.
- Mysen, B. O., 1976. The role of volatiles in silicate melts: solubility of carbon dioxide and water in feldspar, pyroxene and feldspathoid melts of 30 kbar and 1625 degrees C. *American Journal of Science*, 276: 969-996.
- Mysen, B. O., 1977. The solubility of H₂O and CO₂ under predicted magma genesis conditions and some petrological and geophysical implications. *Reviews of Geophysics and Space Physics*, 15: 351-361.
- Mysen, B. O., 1983. The solubility mechanisms of volatiles in silicate melts and their relations to crystal-andesite liquid equilibria. *Journal of Volcanology and Geothermal Research*, 18: 361-385.
- Mysen, B. O., Arculus, R. J. and Eggler D. H., 1975. Solubility of carbon dioxide in melts of andesite, tholeiite and olivine nephelinite composition to 30 kbar pressure. *Contributions to Mineralogy and Petrology*, 53: 227-239.
- Mysen, B. O., Eggler, D. H., Seitz, M. G. and Holloway, J. R., 1976. Carbon dioxide in silicate melts and crystals: I. Solubility measurements. *American Journal of Science*, 276: 455-479.
- Nathan, S. and Schulte, F. J., 1968. Geology and petrology of the Campbell-Aviator Divide, Northern Victoria Land, Antarctica. Part 1-Post Paleozoic rocks. *New Zealand Journal of Geology and Geophysics*, 11: 940-975.
- Naughton, J. J., Heald, E. F. and Barns, I. L., Jr., 1963. The chemistry of volcanic gases, 1, collection and analysis of equilibrium mixtures by gas chromatography. *Journal of Geophysical Research*, 68: 539-544.
- Noguchi, K. and Kamiya, H., 1963. Prediction of volcanic eruption by measuring the chemical composition and amounts of gases. *Bulletin Volcanologique*, 26: 367-378.
- Nordlie, B. E., 1971. The composition of the magmatic gas of Kilauea and it's behavior in the near surface environment. *American Journal of Science*, 271: 417-463.
- Piperov, N. B. and Penchev, N. P., 1973. A study on gas inclusions in minerals. analysis of the gases from micro-inclusions in allanite. *Geochimica et Cosmochimica Acta*, 37: 2075-2097.

- Price, W. F., Huntingdon, A. T. and Bailey, D. K., 1977. The effect of crushing on the release of volatile components from heated obsidian. *Mineralogical Magazine*, 41: 551-553.
- Priestley, R. E., 1913. The ascent of Erebus, December 1912. In: R. F. Scott, *Scott's Last Expedition*. 2. Smith and Elder, London, pp. 278.
- Radke, L. F., 1982. Sulphur and sulphate from Mt Erebus. *Nature*, 299: 710-712.
- Roedder, E., 1972. Composition of fluid inclusions, in *Data of Geochemistry*, 6th Edition, Chapter JJ, 164pp. USGS Prof. Paper, 440-JJ.
- Ross, J., 1847. *Voyage to the Southern Seas*. 1. John Murray, London, 366 pp.
- Rose, W. I., Jr., Stoiber, R. E. and Malinconico, L. L., 1982. Eruptive gas compositions and fluxes of explosive volcanoes: budget of S and Cl emitted from Fuego Volcano, Guatemala. in *Andesites*, Thorpe, R. S. ed., John Wiley and Sons.
- Russell-Robinson, S. L. and Smith, R. L., 1983. Mount St. Helens: minor-element variation of pumices and dome rocks from 1980 to 1982 (Abstract). *EOS Transactions, American Geophysical Union*, 64: 336.
- Scholes, A., 1953. *Seventh Continent*. George Allen and Unwin, London, 226 pp.
- Scott, B. J., 1978. Mount Erebus Volcano. *SEAN Bulletin*, 3(5): 2-3.
- Shackleton, E. H., 1909. *The Heart of the Antarctic, Being the Story of the British Antarctic Expedition, 1907-09*. 1. Heinemann, London, 372 pp.
- Shackleton, E. H., 1919. *South, The Story of Shackleton's 1914-1917 Expedition*. Heinemann, London, 376 pp.
- Shepherd, E. S., 1938. The gases in rocks and some related problems. *American Journal of Science*, 35(A): 311-351.
- Shepherd, E. S. and Merwin, H. E., 1927. Gases of the Mt. Pelee lavas of 1902. *Journal of Geology*, 35: 97-116.
- Sigvaldason, G. E. and Elisson, G., 1968. Collection and analysis of volcanic gases at Surtsey, Iceland. *Geochimica et Cosmochimica Acta*, 32: 797-805.

- Sommer, M. A., 1977. Volatiles H₂O, CO₂ and CO in silicate melt inclusions in quartz phenocrysts from the rhyolitic Bandelier air-fall and ash-flow tuff, New Mexico. *Journal of Geology*, 85: 423-432.
- Sparks, R. S. J., 1978. The dynamics of bubble formation and growth in magmas: a review and analysis. *Journal of Volcanology and Geothermal Research*, 3: 1-37.
- Stoiber, R.E., Williams, S. N., Malinconico, L. L., Johnston, P. A., Jr. and Casadevall, T. J., 1981. Mt. St. Helens: evidence of increased magmatic gas component. *Journal of Volcanology and Geothermal Research*, 11: 203-212.
- Stolper, E., 1982. The speciation of water in silicate melts. *Geochimica et Cosmochimica Acta*, 46: 2609-2620.
- Sun, S. and Hanson, G. N., 1976. Rare earth element evidence for differentiation of McMurdo Volcanics, Ross Island, Antarctica. *Contributions to Mineralogy and Petrology*, 54: 139-155.
- Treves, S. B., 1967. Volcanic rocks from the Ross Island, Marguerite Bay, and Mt. Weaver areas, Antarctica. In: T. Nagata, (Editor), *Proceedings of the Symposium on Pacific-Antarctic Sciences*. JARE Science Report, Special Issue, 1: 136-149.
- Treves, S. B. and Kyle, P. R., 1973. Renewed volcanic activity of Mount Erebus, Antarctica. *Antarctic Journal of the U.S.*, 8: 156.
- Turner, J. S., Huppert, H. E. and Sparks, R. S. J., 1983. An experimental investigation of volatile exsolution in evolving magma chambers. *Journal of Volcanology and Geothermal Research*, 16: 263-277.
- Watson, E. B., 1981. Diffusion in magmas at depth in the earth: the effects of pressure and dissolved H₂O. *Earth and Planetary Science Letter*, 52: 291-301.
- Watson, E. B., 1976. Glass inclusions as samples of early magmatic liquid: determinative method and application to a South Atlantic basalt. *Journal of Volcanology and Geothermal Research*, 1: 73-84.
- Watson, E. B., Sneeringer, M. A. and Ross, A., 1982. Diffusion of dissolved carbonate in magmas: experimental results and applications. *Earth and Planetary Science Letters*, 61: 346-358.

Wright, T. L., 1974. Presentation and interpretation of chemical data for igneous rocks. Contributions to Mineralogy and Petrology, 48: 233-248.

Wright, T. L. and Doherty, P. C., 1970. A linear programming and least squares computer method for solving petrologic mixing problems. Geological Society of America Bulletin, 81: 1995-2008.